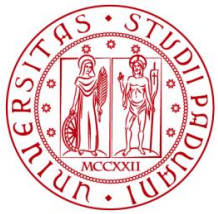

UNIVERSITÀ DEGLI STUDI DI PADOVA

University of Padova
Department of Information Engineering

Ph.D. School in Information Engineering
Section: Bioengineering
Series: XXVI

MODELING THE EFFECT OF PHYSICAL ACTIVITY ON POSTPRANDIAL GLUCOSE TURNOVER

School director: *Ch.mo Prof. Matteo Bertocco*

Coordinator: *Prof. Giovanni Sparacino*

Advisor: *Ing. Chiara Dalla Man*

Ph.D. Candidate: *Ing. Michele Schiavon*

2014

Contents

Abstract

English

In healthy subjects, glucose regulation relies on a complex control system that keeps blood glucose level within a narrow range around its basal value. A common element that offers a net benefit for most individuals with and without diabetes is regular physical activity, which is known to enhance insulin sensitivity, improve glycemic control and reduce the risk of cardiovascular mortality.
Nowadays numerous studies have demonstrated increased rate of glucose uptake (R_d) and rate of endogenous glucose production (EGP) during physical activity in individuals with and without diabetes in the postabsorptive state, while very few have examined the effects of exercise in the postprandial state although many people, with and without diabetes, exercise a few hours after a meal. A method for the quantification of the effect and effect size of exercise on insulin sensitivity and a physiological model quantitatively describing the effect of exercise on glucose turnover in the postprandial state have never been developed. This represents a significant knowledge gap, especially in type 1 diabetes, because this information could be incorporated into currently available artificial pancreas control algorithms, thus extending their applicability to treat people with type 1 diabetes. However, such tools will need to be developed and tested in healthy subjects before validating in those with diabetes.

In this work data of 12 healthy individuals who underwent a triple-tracer mixed-meal and a moderate-intensity exercise session 2 hours after meal ingestion for 75 minutes have been used. The tracer-to-tracee clamp method was used to accurately estimate postprandial glucose turnover continuously after the meal, during and after exercise by clamping tracer-to-tracee ratios in order to minimize non-steady-state errors. Since it is almost impossible to realize a "perfect" clamp of the plasma tracer-to-tracee ratio, the use of models, to compensate the non-steady-state errors, is needed. Use of models requires the estimation of derivatives both for tracer-to-tracee ratio and glucose signals and, due to ill-conditioning, this issue is generally solved via regularized deconvolution. However, an implicit assumption of standard regularized deconvolution is that, in a Bayesian embedding, expectations on smoothness of the unknown input can be formalized by describing it a priori as the multiple integration of a stationary white noise process but, because of physical activity, signals represented marked nonstationarity. We solved the problem by resorting to an improved stochastic deconvolution method, in order to account for nonstationarity introduced by exercise.
Fluxes analysis showed that during exercise session EGP rose, which can be explained by both falling insulin and rising glucagon concentrations, while glucose concentrations fell and R_d plateaued, which can be explained by increasing muscle uptake by both insulin-independent and -dependent mechanisms.

In order to quantify the effect and effect size of exercise on net insulin sensitivity (S_I), i.e. the ability of insulin to stimulate glucose disposal and suppress endogenous glucose production, we developed a method able to calculate net insulin sensitivity and evaluate the relative contribution of liver and disposal insulin sensitivity based on glucose fluxes data. S_I was estimated first using data of first 2 hours after the meal, i.e. in absence of physical activity, and then using the data of the whole experiment, i.e. in presence of physical activity. We found that net S_I increases by almost 75% during moderate-intensity exercise and that this increase is associated to insulin-dependent glucose disposal. Furthermore, we validated these results by cal-

culating an index of net insulin sensitivity, both in absence and presence of physical activity, based on an integral formula using glucose and insulin concentration data. We found a strong correlation between net S_I indices calculated with the two methods.
The results on effect size of physical activity on S_I have been incorporated into the UVA/Padova T1DM simulator in order to suggest the best strategy that could be adopted during artificial pancreas clinical trials that involves a session of moderate physical activity. We showed that, in order to prevent hypoglycemia during and after exercise, any control algorithm would benefit by knowing in advance of upcoming physical activity and, if patient-specific basal insulin reduction pattern is not available, an optimal basal reduction strategy has been proposed.

However, the method for the quantification of the effect size of exercise on insulin sensitivity was not able to tease out the insulin-independent effect of exercise on glucose uptake. Therefore, to discriminate the effect of exercise on insulin-dependent and -independent glucose turnover, the development of a mathematical model to assess the effect of physical activity on glucose kinetics has been approached. A set of models of increasing complexity have been developed and selection was tackled using standard criteria (e.g. ability to describe the data, precision of parameter estimates, model parsimony, residual independence). The models proposed well fitted the data and allowed the estimation of physiologically interpretable parameters quantifying the effect of physical activity on glucose turnover.

Italiano

In soggetti sani, il controllo della glicemia si basa su un complesso sistema di regolazione che permette di mantenere il livello di glucosio nel sangue all'interno di un range ristretto che oscilla attorno al suo valore basale. Ben noti sono i netti benefici offerti dall'attività fisica per la maggior parte degli individui, sia sani che diabetici, come, per esempio, l'aumento della sensibilità insulinica, il miglioramento del controllo glicemico e la riduzione del rischio di mortalità cardiovascolare. Oggigiorno in molti studi è stato dimostrato che, sia in soggetti sani che diabetici, durante lo stato post-assorbitivo vi è un aumento dell'utilizzazione (R_d) e della produzione endogena di glucosio (EGP), mentre in pochissimi studi sono stati analizzati gli effetti dell'attività fisica durante lo stato post-prandiale, sebbene moltissime persone, sane e diabetiche, siano solite praticare attività fisica poche ore dopo un pasto. Fino ad ora, comunque, non sono ancora stati sviluppati né un metodo per la quantificazione dell'effetto dell'attività fisica sulla sensibilità insulinica né un modello che descrivi quantitativamente l'effetto dell'attività fisica sull'utilizzazione del glucosio, soprattutto durante lo stato post-prandiale. Ciò rappresenta un importante gap dal punto di vista conoscitivo soprattutto per soggetti diabetici di tipo 1 in quanto, l'utilizzazione di questa informazione permetterebbe di estendere i range di applicabilità degli algoritmi di controllo oggigiorno utilizzati per la realizzazione del pancreas artificiale anche in queste particolari condizioni sperimentali. Tuttavia, questi metodi devono ovviamente essere sviluppati e testati in soggetti sani prima di poterli validare in soggetti affetti da diabete.

In questo lavoro sono stati utilizzati dati provenienti da 12 soggetti sani sottoposti ad un protocollo di triplo tracciante con pasto misto ed una sessione di esercizio fisico di moderata intensità, 2 ore dopo il pasto, della durata di 75 minuti. Al fine di stimare accuratamente ed in maniera continua il turnover post-prandiale del glucosio durante tutto l'esperimento è stata utilizzata la tenica del clamp del rapporto tracciante-tracciato il cui obiettivo consiste nel minimizzare gli errori di stato non stazionario clampando i rap-

porti tracciante-tracciato ottenuti. Tuttavia, siccome a livello pratico è quasi impossibile realizzare il clamp "perfetto" del rapporto tracciante-tracciato nel plasma, si rende necessario l'impiego di modelli al fine di compensare gli errori di stato non stazionario. A sua volta, l'utilizzo di modelli necessita della stima delle derivate sia dei rapporti tracciante-tracciato che del segnale glicemico e, generalmente, questo problema viene approcciato mediante la tecnica di deconvoluzione regolarizzata. Tuttavia, in un contesto bayesiano, la tecnica di deconvoluzione regolarizzata standard assume implicitamente che l'informazione sulla regolarità del segnale incognito in ingresso possa essere descritta a priori mediante un processo di rumore bianco stazionario plurintegrato ma tuttavia, a causa dell'esercizio fisico, i segnali utilizzati presentano forti non stazionarietà. Al fine di tener conto dell'effetto di non stazionarietà introdotto dall'esercizio fisico, questo problema è stato approcciato utilizzando un metodo di deconvoluzione stocastica migliorata.
Infine, nei risultati così ottenuti, è stato possibile osservare, durante l'attività fisica, un forte aumento dell'EGP, probabilmente dovuto ad una contemporanea riduzione dell'insulina ed un aumento della concentrazione di glucagone nel plasma, mentre vi è una riduzione della concentrazione di glucosio con il raggiungimento di un plateau da parte di R_d, che potrebbe essere associato ad un aumento dell'utilizzazione del glucosio mediante meccanismi insulino-dipendenti ed -indipendenti.

Al fine di poter quantificare l'effetto dell'esercizio fisico sulla sensibilità insulinica (S_I), ossia la capacità dell'insulina di stimolare l'utilizzazione del glucosio ed inibirne la produzione endogena, è stato sviluppato un metodo, basato sui flussi post-prandiali di glucosio, per stimare tale effetto sulla sensibilità insulinica totale e valutarne il relativo contributo esercitato sulla sensibilità insulinica epatica e tessutale. Tale metodo prevede di stimare due valori di S_I: uno sfruttando solo i dati delle prime 2 ore dopo il pasto, ossia in assenza di attività fisica, e l'altro sfruttando i dati dell'intero esperimento, ossia in presenza di attività fisica. I risultati ottenuti hanno dimostrato un aumento di circa il 75% della sensibilità insulinica totale dovuto all'effetto esercitato dall'attività fisica e che questo effetto era principalmente associ-

ato ad un aumento della sensibilità insulinica tessutale. Questi risultati, inoltre, sono stati validati calcolando un indice di sensibilità insulinica applicando sempre lo stesso razionale, ossia in assenza e presenza di attività fisica, basato su una formula integrale precedentemente pubblicata che utilizza dati di glucosio ed insulina plasmatica. Gli indici di sensibilità insulinica ottenuti con i due metodi si sono dimostrati fortemente correlati tra loro, validando così il nuovo indice proposto di sensibilità insulinica basato sui flussi postprandiali di glucosio.
Questi risultati sono stati inoltre implementati nel simulatore UVA/Padova del diabete di tipo 1 (T1DM) al fine di poter individuare una strategia di ottimizzazione della terapia insulinica durante i trials clinici per la realizzazione del pancreas artificiale in cui fosse prevista una sessione di esercizio fisico. Con questo studio di simulazione è stato possibile dimostrare che, al fine di prevenire fenomeni di ipoglicemia, un qualsiasi algoritmo di controllo trarrebbe beneficio dal conoscere in anticipo eventuali sessioni di attività fisica futura e, in caso di una mancanza di informazioni a priori sulla terapia standard paziente-specifica, è stata proposta una strategia ottima di riduzione di infusione di insulina basale durante l'attività fisica che si è rivelata essere sicura ed efficace durante gli studi di simulazione.

Il metodo proposto per la quantificazione dell'effetto dell'esercizio fisico sulla sensibilità insulinica, tuttavia, non permette di discriminare il contributo dell'esercizio fisico sull'utilizzazione insulino-indipendente del glucosio. Per questo motivo, al fine di caratterizzare l'effetto dell'esercizio fisico sull'utilizzazione del glucosio insulino-dipendente ed -indipendente, è stato sviluppato un modello matematico per quantificare l'effetto dell'esercizio fisico sulla cinetica del glucosio. Sono stati sviluppati ed implementati una serie di modelli di diversa complessità e la selezione del modello ottimo è stata affrontata confrontando le prestazioni dei modelli sulla base di criteri standard (capacità di descrivere i dati, precisione della stima dei parametri, parsimonia, casualità dei residui). Infine i modelli proposti hanno dimostrato di descrivere correttamente i dati sperimentali e di permettere un'interpretazione fisiologica dei parametri stimati caratterizzanti la quanti-

ficazione dell'effetto dell'esercizio fisico sulla cinetica del glucosio.

Glossary

T1DM	Type 1 Diabetes Mellitus
T2DM	Type 2 Diabetes Mellitus
CLC	Closed-Loop Control
CRU	Clinical Research Unit
R_a	Rate of total glucose appearance
$R_{a\ meal}$	Rate of meal glucose appearance
EGP	Endogenous glucose production
R_d	Rate of glucose disposal
SA	Specific activity
TTR	Tracer-to-tracee ratio
WRSS	Weighted Residuals Sum of Squares
WESS	Weighted Estimated Sum of Squares
S_I	Insulin Sensitivity
GE	Glucose Effectiveness
IVGTT	Intravenous Glucose Tolerance Test
OGTT	Oral Glucose Tolerance Test
MTT	Meal Tolerance Test
BG	Blood Glucose
CGM	Continuous Glucose Monitoring
CSII	Continuous Subcutaneous Insulin Infusion
AP	Artificial Pancreas
CVGA	Control-Variability Grid Analysis
PA	Physical Activity
CV	Coefficient of Variation
BIC	Bayesian Criterion Information

1 Introduction

1.1 Background

In healthy subjects, glucose regulation relies on a complex control system that keeps blood glucose level within a narrow range around its basal value. The target blood glucose range is usually considered between 70 and 180 mg/dL. Hypoglycemia is identified when plasma glucose concentration falls below 70 mg/dL, while hyperglycemia when glucose concentration raises over 180 mg/dL [132] and both conditions are dangerous in the short and long term, respectively. It is crucial that plasma glucose level does not decrease under 70 mg/dL since this can cause complications, and in particular of the brain, given that glucose is the predominant metabolic fuel. Hypoglycemia can also alter cardiac conduction abnormalities leading to cardiac arrhythmias. Thus, the prevention of hypoglycemia is critical to survival. On the other hand, the chronic hyperglycemia leads to micro-vascular and macro-vascular complications which include limb loss, blindness, ischemic heart disease, and end-stage renal disease [132–134].
Comprehension of the mechanisms that regulate plasma glucose have greatly evolved since the discovery in the 1920s of the peptide hormone insulin, which was considered the principal actor of glucose homeostasis. Insulin is secreted by β-cells in response to high levels of plasma glucose, promoting glucose utilization by tissues and inhibiting endogenous glucose production by the

liver and kidney. In the 1950s, pancreatic α-cells hormone glucagon was discovered. It is secreted in response to a fall in plasma glucose concentration below the hypoglycemic threshold, and acts by stimulating hepatic glycogenolysis and ultimately gluconeogenesis, thus raising EGP and consequently increasing plasma glucose concentration. All these elements lead to a bihormonal view of glucose regulation, where insulin was the key regulatory hormone of glucose disappearance and glucagon the major regulator of glucose appearance.

Impairment of the glucose regulatory system is the cause of several metabolic disorders, such as diabetes. Diabetes is a chronic disease, characterized by the inability of the body to control the concentration of glucose (glycaemia) in blood. In particular, deficiency in the secretion and action of insulin represents the main cause of impaired glucose control, although such impairments can have very different genesis. Two major pathologies are usually considered: type 1 and type 2 diabetes (T1DM and T2DM, respectively).

Type 1 diabetes is the result of immune-mediated destruction of the pancreatic β-cells in the islets of Langerhans, i.e. the site of insulin production and secretion. In general, the disease occurs in childhood and adolescence (although it can occur at all ages) and is characterized by absolute insulin deficiency. Consequently, affected individuals require exogenous insulin injections to compensate the lack of secretion from the pancreas and sustain life. As a rule, obesity does not play a part in the pathogenesis of T1DM, although obesity in T1DM is associated with the development of cardiovascular complications.

Type 2 diabetes occurs because insulin secretion is inadequate and cannot overcome the prevailing defects in insulin action, resulting in hyperglycemia. Excess caloric intake, inactivity and obesity all play parts in the pathogenesis of T2DM. In general, it is a disease that occurs with increasing frequency with increasing age and is uncommon before age 40 (although there are important exceptions). In addition, people with T2DM are more likely to have associated adverse cardiovascular risk factors such as dyslipidemia

and hypertension and are major components of health care spending [113]. Conventional therapy for T2DM consists of a combination of diet, regular physical activity and drugs such as oral hypoglycemic agents, sulfonylureas and insulin.
The prevalence of diabetes mellitus is increasing dramatically all over the world and its global incidence has been increasing steadily in the past several years. Ninety percent of the world population with diabetes is type 2, with type 1 diabetes comprising between 5%-10%. Over time, uncontrolled diabetes leads to complications, in particular: diabetic retinopathy, which leads to blindness; diabetic neuropathy, which increases the risk of foot ulceration and limb loss; and diabetic nephropathy leading to kidney failure. In addition, there is an increased risk of heart disease and stroke, with 50% of people with diabetes dying for them. Finally, the overall risk of dying among people with diabetes is at least double the risk of their peers without diabetes.

A common element that offers a net benefit for most individuals with and without diabetes is regular physical activity, which can include structured exercise in a variety of forms. Regular physical activity is known to enhance insulin sensitivity, increase cardiorespiratory fitness, improve glycemic control, reduce the risk of cardiovascular mortality, decrease fatty mass, arterial pressure and incidence of the T2DM [72, 106, 126]. It is well established that exercise increases rates of glucose uptake (R_d) and that rates of endogenous glucose production (EGP) must increases to meet the increased metabolic demands of the exercising muscle to prevent hypoglycemia [28, 43, 121, 125]. These changes in glucose fluxes are facilitated by falling insulin and rising glucagon and catecholamine levels during exercise in healthy individuals [131]. Numerous factors determine the rate of glucose uptake during and after exercise. During exercise, one of the most important regulatory responses is an increase in blood flow to the contracting skeletal muscles [2, 92]. The increase in blood flow provides ample substrate to the working muscles, and thus, glucose availability is usually not the rate-limiting factor for glucose utilization when exercise is performed under normal physiological conditions. The principal mechanisms by which exercise increases glucose uptake in skeletal muscle is

through the translocation of a glucose transporter protein, i.e. GLUT-4 isoform, from an intracellular compartment to the surface cell [48, 49, 114, 128] and increasing its transcription [39, 95], and that this is independent of insulin [88, 91, 97, 123]. In addition to the acute effects of exercise to increase muscle glucose uptake, the postexercise period is characterized by muscle being more sensitive to the action of insulin [51, 52], even if the mechanisms are still under investigation.
The therapeutic effects of exercise in the treatment of diabetes have been clearly recognized, including decreased insulin requirements, improved cardiovascular fitness and blood lipid profiles. However, in some cases, the increase in glucose uptake due to exercise can lead to hypoglycemic episodes in insulin-treated diabetic people and may exacerbate hyperglycemia and promote ketosis in poorly metabolic-controlled patients [5]. In some studies on T1DM subjects it was showed that exercise training improve insulin sensitivity but not glucose control [122, 127]. However, the lack of improvement in glucose control is mainly due to to the fear of hypoglycemia leading to overcompensation with additional carbohydrate intake or excessive insulin infusion reduction and/or counterregulatory hormones response.

Although numerous studies have demonstrated increased R_d and EGP during physical activity in individuals with and without diabetes [46, 64] in the postabsorptive state, very few have examined the effects of exercise in the postprandial state in individuals with and without type 2 diabetes [17, 18, 58, 65, 74, 75] and none in individuals with type 1 diabetes. Furthermore, very few studies [27] have used methods that minimize fluctuations in tracer-to-tracee specific activity to enable accurate continuous (every 10 min) measurement of glucose turnover and during the transition from rest to exercise in nondiabetic subjects.
Models of insulin action and secretion in response to physiological perturbations (e.g., oral glucose or mixed-meal challenges) have been developed and validated in humans with and without type 2 diabetes. However, none of these methods have been tested or validated when these perturbations are further challenged by exercise. This is an important practical issue related

to the model that needs to be tested since many people, with and without diabetes, exercise a few hours after a meal. Furthermore, lack of development and validation of such physiological models of whole-body insulin sensitivity during exercise, especially in the postprandial state, precludes quantification of the effect size of exercise on insulin sensitivity. This represents a significant knowledge gap that would be important to supply, because accurate quantification of exercise effect on insulin sensitivity, especially in people with type 1 diabetes, could perhaps be incorporated into currently available artificial pancreas control algorithms, thus extending their applicability and wider use to treat people with type 1 diabetes. However, such models will first need to be developed and tested in healthy subjects before validating in those with diabetes.

1.2 Aim

The general aim of this thesis is to develop a methodology to accurately quantifying the effect of moderate-intensity physical activity on postprandial glucose turnover in healthy subjects. The aim of this work can be divided into the following tasks:

- To establish a novel method for the estimation of postprandial glucose turnover during physical activity with the state-of-the-art techniques.
- To propose a method for the quantification of the effect size of exercise on insulin sensitivity when exercise is part of the postprandial period.
- To propose a whole-body mathematical model describing the effect of physical activity on glucose-insulin system.

1.3 Outline of the thesis

The thesis is articulated as follows:
Chapter 2 presents a brief overview on some aspects of exercise physiology

useful for the comprehension of the results throughout the work.
Chapter 3 describes the experimental protocol used for the estimation of postprandial glucose fluxes, quantification of insulin sensitivity and modeling glucose kinetics during physical activity in healthy subjects.
Chapter 4 describes the triple-tracer technique and presents the methods used for an accurate estimation of postprandial glucose fluxes during physical activity.
Chapter 5 presents a method for the quantification of the effect size of physical activity on insulin sensitivity based on postprandial glucose fluxes and which is also validated with a well-established method based on glucose and insulin data. Moreover, the obtained results are used in a simulation study for the optimization of insulin therapy in T1DM patients during exercise.
Chapter 6 presents a whole-body mathematical model to assess the effect of physical activity on glucose kinetics.
The results obtained in this work as well as emerged open questions and future direction of research are discussed in *Conclusions*.

2 Exercise Physiology

2.1 Introduction

In this Chapter a brief overview on some aspects of exercise physiology that are useful for the comprehension of the results throughout the work is presented. The main mechanisms of the complex glucose regulation system during exercise are first described, then particular attention is focused on describing the effect of exercise in increasing muscle glucose uptake and insulin sensitivity. In the end, a brief introduction on the role of physical activity in diabetes is presented.

2.2 Glucose regulation during exercise

Exercise is known to increase muscle glucose uptake from blood. The maintenance of nearly "normal-resting" blood glucose level is always of primary importance, in particular for the brain given that glucose is the predominant metabolic fuel, at variance with the muscle which can recur to alternative substrates. The coordinated physiological response to maintain blood glucose homeostasis during exercise is governed by chemical mediators released by both the autonomic nervous and hormonal systems to help in maintaining an adequate blood glucose level. When blood glucose falls during exercise,

powerful conterregulatory controls come into play to increase glucose production and maintain circulating glucose concentration in two ways. The first one is via the increased release into the blood of glucose from the liver, kidneys and gut. The second approach is to raise the circulating levels of alternative substances to glucose and deliver these to active tissues in order to slow glucose and glycogen utilization, thereby delaying fatigue during exercise. However, at the start of exercise and during moderate to hard intensity exercise, "feed-forward" mechanisms operate to maintain or raise blood glucose concentration. Conversely, if blood glucose concentration falls during prolonged submaximal exercise, powerful feedback responses are elicited to maintain blood glucose level [12].

All these mechanisms are governed by a complex system of redundant con-

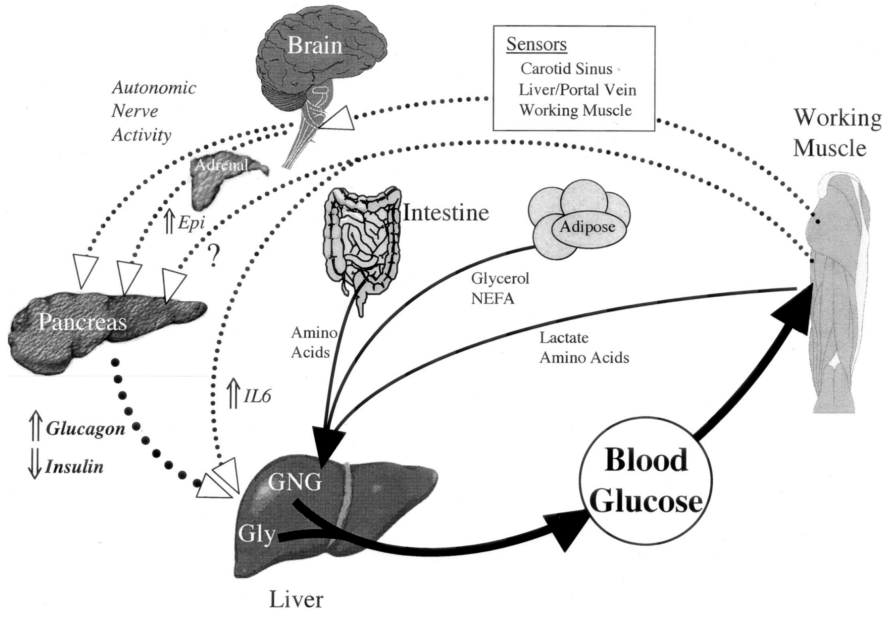

Figure 2.1: Substrates and signals implicated in control of glucose fluxes to working muscle during euglycemic exercise. This scheme illustrates the complex metabolic, neural and endocrine responses that normally prevent hypoglycemia, despite the increase in glucose associated with exercise. Broken lines represent controlling signals, and solid lines represents substrates fluxes. Certain aspects of the scheme, such as Sensors, still remain speculative. The scheme is largely based on studies of the dog engaged in moderate-intensity treadmill exercise. Adapted from [14].

trols (Figure 2.1), mainly regulated by chemical mediators secreted by the hormonal (feedback control), such as insulin and its antagonist glucagon, and autonomic nervous system (feed-forward control), such as catecholamines. Among the glucoregulatory hormones in resting people, insulin is the most important since it stimulates glucose uptake and inhibit glucose production, thus its action during exercise is fundamental to avoid hypoglycemic episodes. Whereas insulin is secreted when blood glucose levels are high, e.g. after a meal, glucagon is secreted when blood glucose levels are low, enhancing glycogenolysis and increasing gluconeogenesis. In terms of the antagonistic effects of insulin and glucagon, possibly the best way to conceive of differing effects is to focus on their ratio (I/G): during prolonged exercise, the ratio I/G is lower due to an increase in blood glucagon and a decrease in insulin levels thus stimulating glucose production. At exercise onset, feed-foward regulation involves catecholamines, e.g. norepinephrine and epinephrine, stimulating muscle and liver glycogenolysis, lipolysis in adipose tissue and suppressing insulin secretion, causing a fall in insulin concentration even if glucose rises. Furthermore, other important hormones exert their actions on maintaining blood glucose level such as cortisol, helping the glucagon in the gluconeogenic function by stimulating proteolysis in muscle, and growth hormone, stimulating the release of fatty acids from adipose tissue as alternative fuels and postponing the time when glucose and glycogen stores become critical.

2.3 Exercise effect on glucose transport and insulin sensitivity

In the exercising muscle, the increased need for metabolic fuel is met partially through an increase in the utilization and uptake of glucose. To meet this increased need, there is a significant elevation in the rate of glycogenolysis and an “insulin-like effect” to increase the uptake of glucose from circulation in the contracting muscles. In addition to the acute effects of exercise, the period after exercise is characterized by the muscle being more

sensitive to the action of insulin, an effect that facilitates the resynthesis of muscle glycogen stores [50, 57, 60, 99, 101]. Initially it was thought that the increase in glucose transport process in skeletal muscle induced by exercise requires the presence of insulin [96]. In earlier study in perfused rat hindlimb [45], it was found that the enhancement of glucose uptake after exercise occurs in two phases: the first is independent of added insulin, and, as this increase in glucose transport reverses, it is replaced by an increase in insulin sensitivity [45, 60]. Subsequent studies have established that contractions stimulate glucose transport in the complete absence of insulin [91, 123], and that maximal effects of contractions and insulin are additive [59, 124] stimulating glucose transport by separate pathways [80].

When exercise is performed under normal physiological conditions, one of the most important regulatory responses is an increase in blood flow [2, 92], which provides ample substrate to the working muscles, while glucose transport is considered to be the rate-limiting factor in glucose utilization. Glucose transport in skeletal muscle occurs primarily by facilitated diffusion, utilizing carrier proteins for transport of the substrate across the membrane. GLUT-4 is the major isoform present in both human and rat skeletal muscle, whereas the GLUT-1 and GLUT-5 isoforms are expressed at a much lower abundance [67]. Exercise and insulin are the major mediators of glucose transport activity in muscle: it follows a saturation kinetics and most reports have shown that exercise and insulin increase glucose transport through an increase in the maximal velocity ($V_{\max}$) without an appreciable change in the substrate concentration at which glucose transport is half maximal (K_{m}) [8].

There is substantial evidence that exercise increases glucose uptake in skeletal muscle through the translocation of GLUT-4 isoform from an intracellular compartment to the surface of the cell [48, 49, 114, 128] and increasing its transcription [39, 95], while a single bout of exercise does not alter the abundance of the other plasma membrane proteins [48, 49, 71]. Similar to the effect of exercise, insulin is known to cause GLUT-4 translocation in skeletal muscle [47, 49]. However, even if blood flow is increased during exercise and thus this could lead to an increased delivery of insulin to the working muscle, the exercise-induced recruitment of GLUT-4 to the plasma membrane has been

demonstrated to be independent of insulin [47, 88, 91, 123]. Thus, contraction in the absence of insulin, as well as insulin alone, can independently result in the movement of glucose transporters to the plasma membrane (Figure 2.2).

The increase in muscle glucose transport with the combination of a maximal

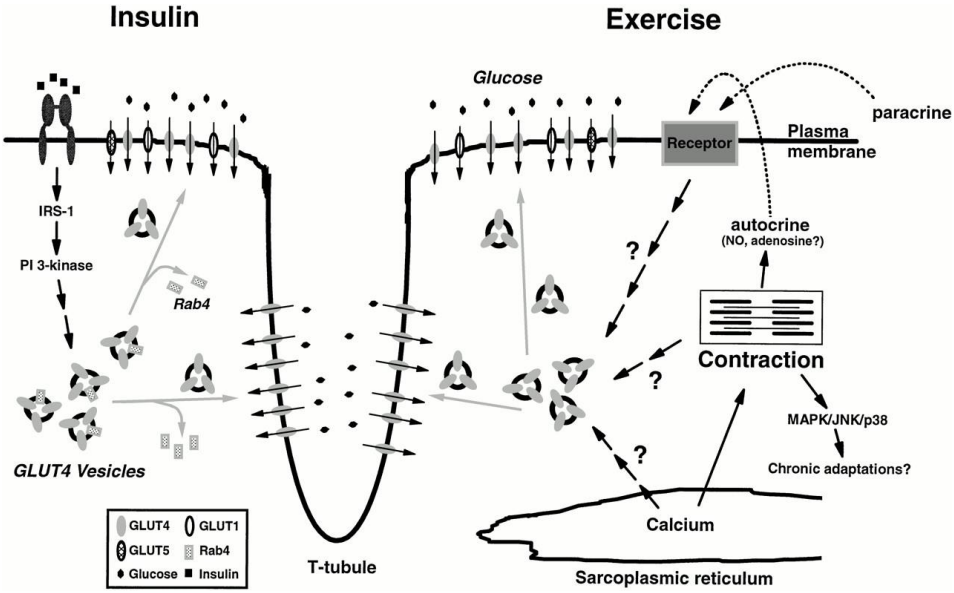

Figure 2.2: GLUT-4 translocation in skeletal muscle. Muscle contractions and insulin cause translocation of GLUT-4 glucose transporter proteins to plasma membrane and transverse tubules (T-tubules). GLUT-1 and GLUT-5 are present in plasma membrane. The subcellular origin of GLUT-4-containing vesicles is not clear, but exercise and insulin appear to recruit distinct GLUT-4-containing vesicles and/or mobilize different "pools" of GLUT-4 proteins. Adapted from [50, 57].

contraction stimulus and a maximal insulin stimulus is greater than the effect of either contraction or insulin alone [45, 124]. Thus the combination of contraction and insulin can have additive or partially additive effect on glucose transport, which may be associated with an additive effect on GLUT-4 recruitment on plasma membrane, and these findings support the hypothesis that the two stimuli can act independently with different mechanisms. In fact, there is evidence that there are two distinct intracellular locations or pools of glucose transporters in skeletal muscle, one that responds to exercise and one to insulin [40]. However, as recently reviewed [111], studies of adipose cells suggest that there is a low rate of continuous recycling of GLUT-4 in

the basal state, and that insulin acts primarily through increasing transporter exocytosis. In skeletal muscle, it is not known if the exercise-induced recruitment of GLUT-4 occurs through the regulation of vesicular exocytosis or other mechanisms.

Increased insulin sensitivity in skeletal muscle glucose uptake is usually observed after a single bout of exercise [96] and this effect can persist for several hours following the cessation of exercise [45, 60]. However, one-legged exercise models in humans have demonstrated that the exercise-induced increase in insulin sensitivity for glucose uptake is a local phenomenon restricted to the exercised muscle [98].
The molecular basis for this phenomenon has not been completely elucidated but appears to be dependent on multiple factors. The rate that glucose is stored or metabolized in the postexercise period may be involved in the reversal of the increased insulin sensitivity of muscle glucose uptake and may partially explain the different durations of this effect [86, 96]. While insulin clearance rates and insulin binding to its receptor seem to not change after exercise [98, 118], another possible mechanism which can contribute to this effect comes from studies in which the postexercise period is not characterized by increased insulin sensitivity, i.e. when intact muscles are isolated, washed and then contracted in vitro [16]. This work and the subsequent report [44] have suggested that a serum factor is required for the effects of contraction to enhance insulin sensitivity. However, the effect of exercise on increasing sensitivity is not only limited to insulin, in fact the effect of hypoxia on glucose transport is also markedly amplified after exercise [16]. Thus, there may be multiple factors that regulate the enhanced muscle insulin sensitivity for glucose uptake in the postexercise period, in fact this phenomenon may be regulated by a combination of humoral factors, autocrine/paracrine mechanisms and muscle glycogen concentrations.

2.4 Role of exercise in diabetes

Regular physical activity is known to have several potential benefits that apply to both diabetic and nondiabetic individuals. In addition to lowering blood glucose due to exercise-induced glucose uptake and increasing insulin sensitivity, regular exercise improves several risk factors for cardiovascular disease. Psychological benefits of exercise, such as an increased sense of well-being, improved self-esteem and enhanced quality of life may also be important for those with either type 1 and type 2 diabetes [61].
Although persons with diabetes may derive many benefits from regular physical activity, there are also a number of hazards that make exercise difficult to manage if not properly addressed. In T1DM individuals, risks of hypoglycemia during or after exercise, in case of hyperinsulinemic state, or of worsening metabolic control, in case of insulin-deficient state, have been recognized. In T2DM individuals, treated by diet alone, exercise usually results in a decrease in glucose concentration toward normal levels and it can be used safely as an adjunct to diet to achieve weight loss and improved insulin sensitivity, while, in individuals treated with sulfonylureas or insulin, an increased risk of developing hypoglycemia during or following exercise has been recognized.

Exercise in type 1 diabetes

Shortly after the introduction of insulin, exercise has been demonstrated to strengthen the hypoglycemic effect of injected insulin [76] thus leading to decreased insulin requirements to overcome the increased risk of hypoglycemic reactions in T1DM patients.
One major problem for the T1DM patient is that plasma insulin concentrations do not decrease during exercise as in normal subjects and may even increase when insulin injection is administered in a short time interval from the onset of exercise, particularly if the injection site is in an exercising part of the body [68]. The major effect of sustained insulin levels is related to the inhibition of both glycogenolysis and gluconeogenesis [138], even though

counterregulatory hormone responses may be excessive, causing blood glucose concentration to fall.

Whereas the decrease in blood glucose concentrations may be considered a beneficial effect during mild to moderate exercise of short duration, during more vigorous or prolonged exercise, if no insulin-reduction dosage and/or supplemental carbohydrate feedings before and during exercise are considered, hypoglycemia may occur. In fact, it is a well-established clinical reality that physical activity influences glucose concentrations in T1DM patients not only during exercise but also several hours postexercise leading to late evening and nocturnal hypoglycemia [63, 83]. Different types of exercise (resistance vs. aerobic) have contrasting effects on the duration and severity of acute [137] and delayed [135] postexercise hypoglycemia. A recent review [9] has identified the importance of exercise as a major hurdle in the current standard closed-loop control (CLC) efforts. While there is sufficient evidence to recommend physical activity in the management of T1DM [22], the duration, intensity and form of exercise that should be recommended and whether such interventions would translate to better outcomes are presently unclear. A recent meta-analysis [117] suggests benefits of regular aerobic training, interspersed with brief bouts of sprinting on glycated haemoglobin concentrations and incidence of delayed hypoglycemia in T1DM.

In contrast, opposite effects on glucose regulation during exercise in T1DM subjects may also occur when exercise is undertaken during an insulin-deficient state exacerbating hyperglycemia and promoting ketosis [5].

In general T1DM patients, in order to avoid hyperglycemic and hypoglycemic events, are recommended to take some precautions when exercise is performed: if blood glucose is greater than 250 mg/dL and ketones are present in urine or blood, exercise should be postponed and the individual should take supplemental insulin to reestablish good metabolic control; likewise, if blood glucose is lower than 100 mg/dL and the individual has taken insulin within the past $60 - 90$ min, supplemental feedings should be taken before and during exercise to avoid hypoglycemia. However, recently, research have been focused on the therapeutic approaches to mitigate hypoglycemia during and after physical activity in T1DM [41, 100, 102, 136].

Exercise in type 2 diabetes

Type 2 diabetes is characterized by insulin resistance and impaired insulin secretion, thus the major aim of T2DM therapy is to compensate these states through an appropriate use of drugs, diet and exercise.
Exercise has long been advocated as beneficial in T2DM, partially because, even in the face of insulin resistance, it can stimulate glucose uptake thus resulting in a lower glycosylated haemoglobin concentrations and maybe an improved insulin sensitivity. In fact, with onset of exercise, peripheral glucose utilization increases normally, but plasma insulin concentrations fail to decline inducing blood glucose concentrations to fall toward normal but not to hypoglycemic levels [87]. Thus, the risk of exercise-induced hypoglycemia is prevented during mild to moderate exercise in T2DM who are not being treated with insulin or sulfonylureas. In fact, these treatments can cause a higher than normal insulin concentration during exercise which may sufficiently inhibit hepatic glucose production to result in hypoglycemia.
In general, a regular exercise program can be an important part of a treatment regimen for T2DM potentiating the effects of diet or drugs therapy to lower glucose levels and improve insulin sensitivity [73].

3 Database & Protocol

3.1 Introduction

In this Chapter the experimental protocol used for the estimation of postprandial glucose fluxes, quantification of insulin sensitivity and modeling glucose kinetics during physical activity in healthy subjects is described in detail. The triple tracer approach, a validated technique able to minimize fluctuations in tracer-to-tracee ratio enabling accurate measurement of glucose turnover, is here used to assess postprandial glucose fluxes during a session of physical activity. Moreover, plasma glucose and insulin concentration data and glucose fluxes are used to quantify the effect size of physical activity on insulin sensitivity and to model its effect on glucose-insulin dynamics.

3.2 Research Design and Methods

3.2.1 Subjects

The study cohort is composed of 12 healthy individuals, 5 males and 7 females, age 37.1 $\pm$ 3.1 yr, body mass index 24.1 $\pm$ 1.1 kg/m^2, fat-free mass 50.9 $\pm$ 3.9 kg with normal fasting glucose and standard 75 grams oral

glucose tolerance test (OGTT), and normal gastric emptying to solids and liquids. Exclusion criteria were significant gastrointestinal symptoms by questionnaire, documented recent upper gastrointestinal disorder, medications affecting gastric motility (e.g., erythromycin), pregnancy or breast feeding, or other comorbidities precluding participation. Medications (except stable thyroid hormone or hormone replacement therapy) that could influence glucose tolerance, history of diabetes in first degree family members or prior history of diabetes were also exclusionary. Subjects did not engage in vigorous physical activities for 72 h prior to screen and study visits. Each subject underwent two screen visits.

3.2.2 Screening visits

Visit 1

Subjects reported in the morning after an overnight fast to the Clinical Research Unit (CRU) of the Mayo Center for Translational Science Activities for a history, physical examination, screening laboratory tests, a 75-gram standard OGTT, standard urinalysis and resting ECG. All women of childbearing potential had a negative pregnancy test within 24 h of study visit. A dietary history was taken to ensure adherence to a weight-maintaining diet consisting of at least 200 grams of carbohydrates/day and that diet met American Diabetes Association guidelines for protein, fat and carbohydrates. Body composition was also measured using dual-energy X-ray absorptiometry [103]. After completion of the OGTT, participants performed a graded exercise test on a treadmill to determine $\dot{V}O_{2max}$ according to guidelines (American College of Sports Medicine Guidelines for Exercise Testing and Prescription, 7^{th} Edition) and ensure stable cardiac status. Expired gases were collected and analyzed using indirect calorimetry. $\dot{V}O_{2max}$ was determined when at least two of three criteria were met: 1) Participant too tired to continue exercise, 2) respiratory exchange ratio exceeded 1.0; 3) a plateau was reached in oxygen consumption with increasing workload. The purpose of this test was to use individual $\dot{V}O_{2max}$ data to determine workload during the moderate intensity ($\sim$50% of $\dot{V}O_{2max}$) protocol during the study

day.

Visit 2

Using established scintigraphic techniques (5), gastric emptying of solids and liquids were assessed in all subjects who were eligible after the first screening visit; results were summarized as the time required for 50% of solids and separately liquids to empty. Thereafter, subjects who had normal gastric emptying for solids and liquids proceeded to the inpatient study visit within 3 wk of the second screening visit.

3.2.3 Experimental design

All subjects spent ∼40 h in the CRU.

Day 1

Subjects were admitted to the CRU at ∼1600. A point-of-care urine pregnancy test was performed where appropriate to ensure that the test was negative before proceeding any further. Thereafter two Dexcom 7 plus continuous glucose monitors (CGM) and a Modular Signal Recorder (MSR) accelerometer (MSR Electronics GmbH, Seuzach, Switzerland) were placed and maintained for the rest of the study period. They were then provided a standard 10 kcal/kg meal (55% carbohydrate, 15% protein, and 30% fat) consumed between 1700 and 1730. No additional food was provided until the next morning. A heart rate monitor was also attached to capture heart rate during the study. Intravenous cannula was inserted into a forearm vein at ∼2000 for tracer infusion and periodic blood draws during the study day the following morning.

Day 2

At ∼0400 (t = *-180*) a primed continuous infusion of [6,6 $-^2$ H_2]glucose was started. At ∼0600, an intravenous cannula was inserted retrogradely into a hand vein for periodic blood draws. The hand was placed in a heated (55°C) plexiglass box to enable drawing of arterialized-venous blood for glucose, glucose tracer and hormone analyses. At ∼0700 ($time$ = *0*) a triple tracer

mixed meal study was performed [4]. A mixed meal containing 75 grams of glucose labeled with [1 $-^{13}$ C]glucose (Jell-O) was consumed within 15 min along with the rest of the mixed meal of egss and ham/steak. Simultaneously, an intravenous infusion of [6 $-^{3}$ H]glucose was started and continued for the next 6 h (t = *360*) at a variable rate to mimic the anticipated rate of appearance of the ingested [1 $-^{13}$ C]glucose contained within the meal. Concurrently, the [6,6 $-^{2}$ H_2]glucose infusion rate was varied to mimic the anticipated rate of endogenous glucose production (EGP). The meal provided ∼33% of daily estimated calorie intake. Two hours (t = *120*) following the first bite, subjects stepped on a treadmill to exercise at moderate intensity activity (∼50% of $\dot{V}O_{2max}$): i.e., four bouts of walking at 3-4 miles/h for 15 min with rest periods of 5 min between each walking bout: total duration 75 min. The workload during physical activity was continuously monitored by heart rate responses and measurements of $\dot{V}O_2$ during exercise to maintain target $\dot{V}O_{2max}$ ∼50% exercise intensity. The [6,6 $-^{2}$ H_2]glucose infusion rate was modified from the start of physical activity at t = *120* for the next 3 h to mimic the anticipated changes in EGP during physical activity. To determine the optimal [6,6 $-^{2}$ H_2]glucose infusion rate necessary to minimize changes in tracer/tracee concentration for determination of postprandial EGP, we analyzed data from the first 2 subjects and modified the tracer infusion rates accordingly to minimize changes in tracer/tracee ratios. This procedure was adopted to also optimize the [6$-^{3}$H]glucose infusion rate to minimize changes in [6 $-^{3}$ H]glucose/[1 $-^{13}$ C]glucose concentrations to enable accurate estimation of meal glucose appearance. Blood was sampled at periodic intervals for measurement of glucose, insulin, glucagon and C-peptide (Figure 3.1) and tracers molar ratios and counts (Figure 3.2); while tracer/tracee concentrations were calculated by the ratio between [6 $-^{3}$ H]glucose/[1 $-^{13}$ C]glucose and [6,6 $-^{2}$ H_2]glucose/endogenous glucose, respectively. CGM and accelerometer recordings were collected throughout the study period to monitor interstitial fluid glucose and quantitate activity levels, respectively, as part of another study. Following the last blood draw, all tracer infusions were stopped and the hand vein cannula removed. Lunch at 1300 and dinner at 1900 were provided, each meal contributing 33% of daily estimated caloric

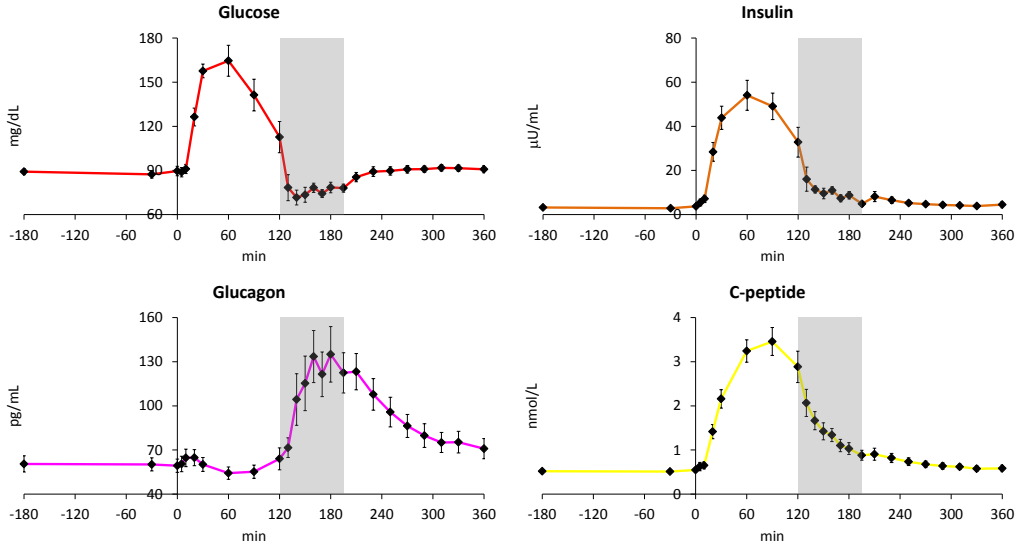

Figure 3.1: Glucose (top-left), insulin (top-right), glucagon (bottom-left) and C-peptide (bottom-right) concentrations obtained from t = *-180* to t = *360* min. Shaded box between t = *120* and t = *195* min represents the exercise period at 50% $\dot{V}O_{2max}$.

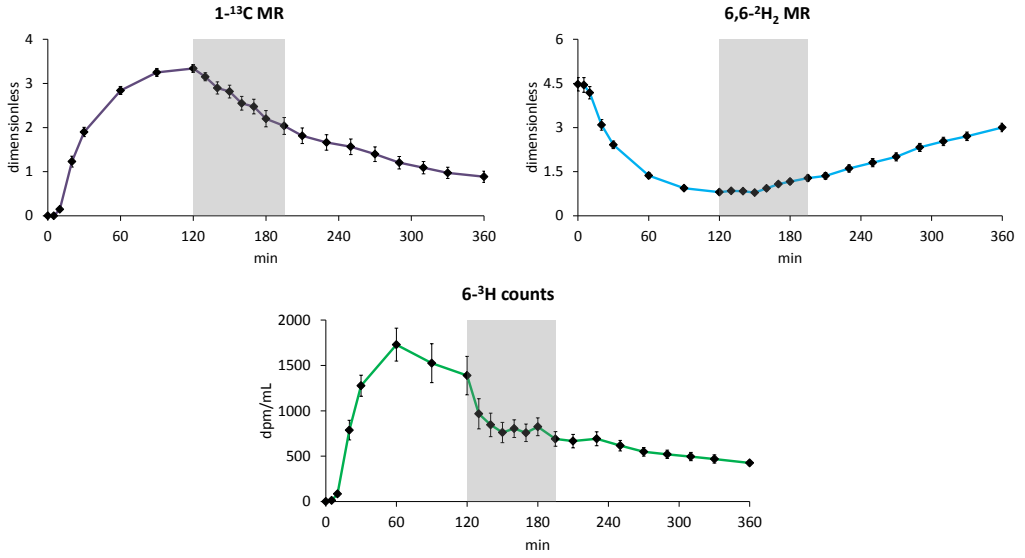

Figure 3.2: Above naural ratio of $[1-^{13}\text{C}]$glucose to $[1-^{12}\text{C}]$glucose in plasma (MR_{13_C}, top-left), ratio of $[6,6-^{2}\text{H}_2]$glucose to $[6,6-^{1}\text{H}_2]$glucose in plasma (MR_{2_H}, top-right) molar ratios, $[6-^{3}\text{H}]$glucose counts (bottom) obtained from t = *0* and t = *360* min.

intake and having similar macronutrient composition as the breakfast meal. From 1500 until 2200, subjects were asked to walk at 1.2 miles/h on the treadmill for 26.5 min in 1 h, ie., 26.5 min on, 33.5 min off with time off during dinner at 1900. This activity represents low grade activity levels that mimic activities of daily living (ADL) [82]. The continuation of the study for the rest of the day and overnight, including use of the CGM and accelerometer data, was part of additional investigation that is being currently analyzed for future reporting.

Day 3

Basal resting metabolic rate ws measured at ∼0630. After completion of the study at 0800, all cannulas were removed, and subjects were dismissed from the CRU.

3.2.4 Analytical techniques

Hormone analyses

C-Peptide was measured on the Cobas e411 (Roche Diagnostics, Indianapolis, IN) using a 2-site electrochemiluminescence immunometric assay. Insulin was measured by a two-site immunoenzymatic assay performed on the DxI automated system (Beckman Instruments, Chaska, MN) and Glucagon by a direct, double antibody radioimmunoassay (Linco Research, St. Charles, MO) [103].

Glucose tracers

Plasma samples were placed on ice, centrifuged at 4°C, separated, and stored at 80°C until assay. Plasma glucose concentration was measured using a glucose oxidase method (YSI, Inc., Yellow Springs, OH). Plasma $[6-^{3}\mathrm{H}]$glucose specific activity was measured by liquid scintillation counting. Plasma enrichment of $[1-^{13}\mathrm{C}]$glucose and $[6,6-^{2}\mathrm{H}_2]$glucose were measured using GCMS (Thermoquest, San Jose, CA) to simultaneously quantitate C-1 to C-2 and C-3 to C-6 fragments [103].

4 Estimation of Postprandial Glucose Fluxes

4.1 Introduction

In this Chapter the triple-tracer technique for the estimation of postprandial glucose fluxes is introduced. The method allows to estimate postprandial glucose fluxes in a "model-independent" way by infusing tracers in order to minimize fluctuations in tracer-to-tracee ratio (TTR). However, since it is almost impossible to realize a "perfect" clamp of the plasma TTR, the use of models is necessary to compensate the non-steady-state errors. This requires the estimation of derivatives both for TTR and glucose signals and, due to ill-conditioning, derivatives calculation is generally solved via regularized deconvolution.

4.2 The triple-tracer approach

The ability of an individual to dispose an oral glucose load is the result of three different processes: appearance in plasma of ingested glucose ($R_{a\ meal}$), endogenous glucose production (EGP) and glucose disposal (R_d). Dual-tracer methods have been largely used to assess these fluxes by employing two tracers, one mixed with ingested glucose and a second infused intravenously, and calculating the systemic appearance rate of both ingested

tracer and total (i.e., ingested and endogenously produced) glucose. $R_{a\ meal}$ is then calculated by multiplying the rate of appearance of ingested tracer by specific activity (or tracer-to-tracee ratio if a stable tracer is used) of glucose or carbohydrate contained in the meal. EGP is subsequently calculated by subtracting $R_{a\ meal}$ from total glucose rate of appearance (R_a). Finally glucose R_d is calculated by subtracting rate of change of plasma glucose mass from R_a. However, as extensively discussed [1, 4, 78, 84, 116], the marked tracer nonsteady state that occurs with the dual-tracer method introduces errors and renders the calculation of $R_{a\ meal}$, EGP and R_d dependent on both the model used in the calculation (e.g., one or two compartments) and its parameters (e.g., the volume of distribution).

The triple-tracer technique [4] circumvents these problems, aiming to estimate in a "model-independent" manner $R_{a\ meal}$ and EGP fluxes by minimizing changes in both meal and endogenous plasma TTR (Figure 4.1) thanks to appropriate infusion of three tracers. Changes in the plasma ratios of the intravenous and ingested tracers were minimized by intravenously infusing [6 $-^3$ H]glucose to mimic the systemic $R_{a\ meal}$ of the [1 $-^{13}$ C]glucose contained in a mixed meal. At the same time, changes in the ratio between [6,6 $-^2$ H_2]glucose tracer and endogenous glucose were minimized by infusing [6,6 $-^2$ H_2]glucose mimicking the anticipated pattern of change of EGP. However, this is a circular logic, i.e. tracers infusion is appropriately modified in order to reproduce the unknown pattern. Thus, one can at least to minimize the change in TTR, by adjusting tracers infusion rate based on pilot studies.

Let now define some variable useful for the following calculations:

- *Tracee*: glucose at natural composition, coming from ingested glucose and EGP.
- $Tracer^I$: [1 $-^{13}$ C]glucose tracer above natural ingested during the meal.
- $Tracer^{II}$: [6,6 $-^2$ H_2]glucose tracer infused intravenously, consisting primarly of [6,6 $-^2$ H_2]glucose (tracer purity is 94%), a minor amount of [6,6 $-^2$$H_1$ $-^1$$H_1$]glucose and a negligible amount of [6,6 $-^1$$H_2$]glucose.
- $Tracer^{III}$: [6 $-^3$ H]glucose tracer infused intravenously.

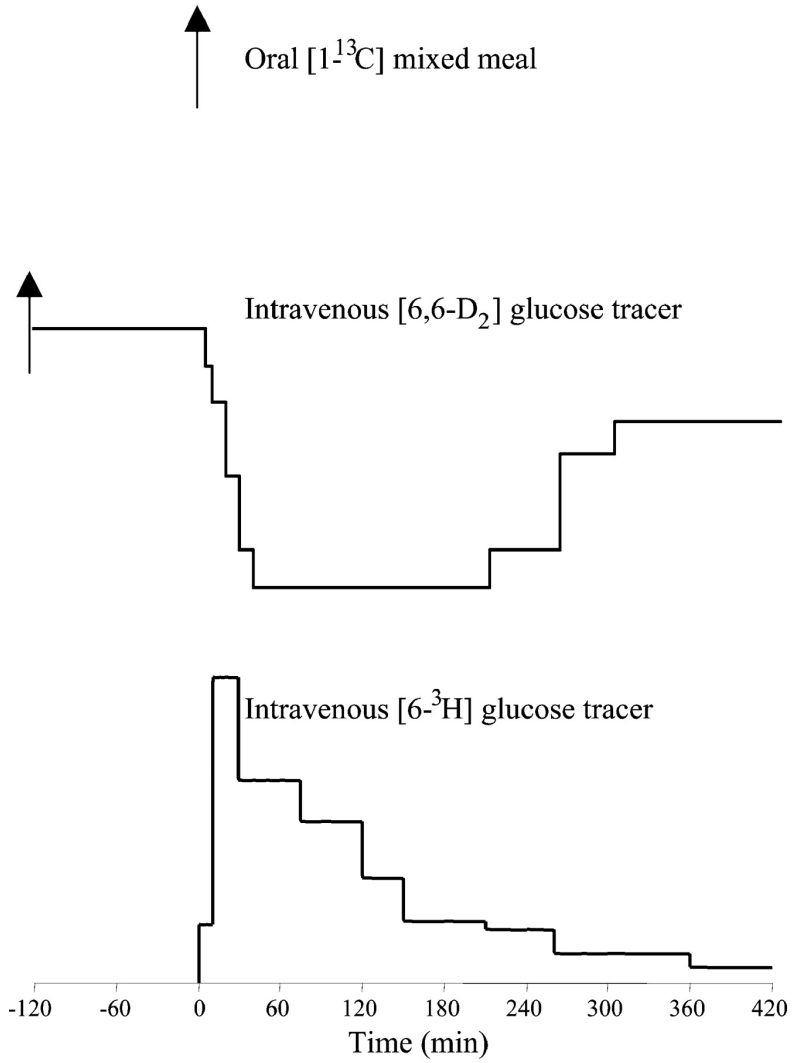

Figure 4.1: Study design of tracers infusion. Adapted from [4].

- G_{nat}: concentration of tracee in plasma [mg/dL].
- G_{13_C}: concentration of tracer$^{\text{I}}$ in plasma [mg/dL].
- G_{2_H}: concentration of tracer$^{\text{II}}$ in plasma [mg/dL].
- G_{3_H}: concentration of tracer$^{\text{III}}$ in plasma [dpm/mL].
- F_{2_H}: rate of intravenous infusion of tracer$^{\text{II}}$ [mg/min].
- F_{3_H}: rate of intravenous infusion of tracer$^{\text{III}}$ [dpm/min].

- G: plasma glucose concentration measured in the arterialized hand vein samples [mg/dL].

First of all, in order to derive the formulas for calculating glucose fluxes, tracer and tracee glucose concentrations in plasma are calculated:

- MR_{13_C} is the ratio of [1 $-^{13}$ C]glucose to [1 $-^{12}$ C]glucose in plasma. MR_{13_C} above natural, i.e. corrected for natural abundance of all atoms, is related to tracer$^{\mathrm{I}}$, tracer$^{\mathrm{II}}$ and tracee by the following formula

$$\begin{aligned} MR_{13_C} - MR_{13_{C,nat}} &= \frac{tracer^I}{tracee + tracer^{II}} \cdot (1 + MR_{13_{C,nat}}) \\ &= \frac{G_{13_C}}{G_{nat} + G_{2_H}} \cdot (1 + MR_{13_{C,nat}}) \end{aligned} \tag{4.1}$$

  where $\mathrm{MR}_{13_{C,nat}}$ represents the ratio between ^{13}C and ^{12}C in natural glucose, equal to 0.011.

- MR_{2_H} is the ratio of $[6,6-^2\mathrm{H}_2]$glucose to $[6,6-^1\mathrm{H}_2]$glucose in plasma corrected for natural abundance. It quantifies 94% of tracer$^{\mathrm{II}}$ divided by tracee plus tracer$^{\mathrm{I}}$

$$MR_{2_H} = \frac{tracer^{II}}{tracee + tracer^I} = \frac{G_{2_H} \cdot 0.94}{G_{nat} + G_{13_C}} \tag{4.2}$$

Total plasma glucose concentration (G) measures the sum of the concentration of tracee, tracer$^{\mathrm{I}}$ and tracer$^{\mathrm{II}}$ in plasma

$$G = G_{nat} + G_{13_C} + G_{2_H} \tag{4.3}$$

From Eqs. 4.1, 4.2 and 4.3, G_{13_C}, G_{2_H} and G_{nat} can be obtained as

$$G_{13_C} = \frac{MR_{13_C} - MR_{13_{C,nat}}}{1 + MR_{13_C}} \cdot G \tag{4.4}$$

$$G_{2_H} = \frac{0.94}{MR_{2_H} - MR_{2_H}} \cdot G \tag{4.5}$$

$$G_{nat} = G - G_{13_C} - G_{2_H} \tag{4.6}$$

The concentration of plasma glucose derived from EGP (G_{end}) can be calculated by subtracting from the total plasma glucose concentration (G_{nat}) the ingested natural glucose, which is related to G_{13_C} through the ratio between $tracer^I$ and natural glucose in the meal (ttr_{meal}) obtained as

$$G_{end} = G_{nat} - G_{13_C}/ttr_{meal} \tag{4.7}$$

Assuming a "perfect" clamp of the plasma TTR of G_{3_H}-to-G_{13_C} (i.e. variations are negligible), $R_{a\ 13_C}$ equals the infusion rate of the tracer (i.e. [6 $-^3$ H]glucose) divided by the plasma TTR (G_{3_H}-to-G_{13_C} ratio)

$$R_{a\ 13_C} = \frac{F_{3_H}}{G_{3_H}/G_{13_C}} \tag{4.8}$$

Then $R_{a\ meal}$ is calculated as

$$R_{a\ meal} = R_{a\ 13_C} \cdot \left(\frac{tracee + tracer^I}{tracer^I}\right)_{meal} = R_{a\ 13_C} \cdot \left(\frac{1}{ttr_{meal}} + 1\right) \tag{4.9}$$

Similarly, assuming a "perfect" clamp of the plasma TTR of G_{2_H}-to-G_{end}, EGP is calculated as

$$EGP = \frac{F_{2_H}}{G_{2_H}/G_{end}} \tag{4.10}$$

Although the estimation of $R_{a\ meal}$ and EGP is virtually model independent, the calculation of R_d requires to use a model.

4.3 Models for fluxes estimation

Since it is almost impossible to realize a "perfect" clamp of the plasma TTR, the use of models is necessary to compensate the non-steady-state errors and, as stated in the previous Section, they are fundamental for the estimation of R_d. In this Section, two compartmental models (i.e., single-compartment and two-compartment) for the calculation of unknown glucose fluxes are presented.

4.3.1 Single-compartment model

This model is based on a single-compartment description of the system and was introduced in [108, 109]. The model assumes that R_a and R_d of glucose and glucose tracers take place in the accessible compartment, which has a volume equal to a fraction p (pool fraction) of the total glucose distribution volume V fixed to population values. Mass balance equation of [6 $-^3$ H]glucose is then

$$pV \cdot \frac{dG_{3_H}}{dt} = F_{3_H} - R_{d\ 3_H} \tag{4.11}$$

where G_{3_H} is the concentration of [6 $-^3$ H]glucose tracer in plasma, F_{3_H} is the rate of [6 $-^3$ H]glucose infusion and R_{d3_H} is the rate of [6 $-^3$ H]glucose tracer disappearance in plasma. Similarly, for the [1 $-^{13}$ C]glucose tracer

$$pV \cdot \frac{dG_{13_C}}{dt} = R_{a\ 13_C} - R_{d\ 13_C} \tag{4.12}$$

where G_{13_C} is the concentration of [1 $-^{13}$ C]glucose tracer in plasma, R_{a3_H} and R_{d13_C} are, respectively, the rate of [1 $-^{13}$ C]glucose tracer apperance and disappearance in plasma.
Isotopic indistinguishability allows one to link the disappearance rate of the two tracers to their amount in the accessible compartment

$$\frac{R_{d\ 3_H}}{pVG_{3_H}} = \frac{R_{d\ 13_C}}{pVG_{13_C}} = k_{01} \tag{4.13}$$

where k_{01} is the disappearance rate parameter, which is assumed to vary during the experiment.
By using Eq. 4.13, Eqs. 4.11 and 4.12 can be rewritten as

$$pV \cdot \frac{dG_{3_H}}{dt} = F_{3_H} - k_{01}pVG_{3_H} \tag{4.14}$$

$$pV \cdot \frac{dG_{13_C}}{dt} = R_{a\ 13_C} - k_{01}pVG_{13_C} \tag{4.15}$$

From the [6 $-^3$ H]glucose mass balance equation (Eq. 4.14), an expression for the disappearance rate parameter k_{01} of [6 $-^3$ H]glucose tracer ($k_{01,3_H}$) is derived

$$k_{01,3_H} = -\frac{dG_{3_H}/dt}{G_{3_H}} + \frac{F_{3_H}}{pVG_{3_H}} \tag{4.16}$$

By using equation Eq. 4.16 into Eq. 4.15, one obtains

$$R_{a\ 13_C} = \frac{F_{3_H}}{G_{3_H}/G_{13_C}} - \frac{pVG_{13_C}}{G_{3_H}/G_{13_C}} \cdot \frac{d(G_{3_H}/G_{13_C})}{dt} \tag{4.17}$$

By applying the same rationale to [6, 6 $-^2$ H_2]glucose and endogenous glucose, an expression for the disappearance rate parameter k_{01} of [6, 6 $-^2$ H_2]glucose tracer ($k_{01,2_H}$) is derived

$$k_{01,2_H} = -\frac{dG_{2_H}/dt}{G_{2_H}} + \frac{F_{2_H}}{pVG_{2_H}} \tag{4.18}$$

By using Eq. 4.18 into endogenous glucose (G_{end}) mass balance equation, one obtains

$$EGP = \frac{F_{2_H}}{G_{2_H}/G_{end}} - \frac{pVG_{end}}{G_{2_H}/G_{end}} \cdot \frac{d(G_{2_H}/G_{end})}{dt} \tag{4.19}$$

Finally, since $R_{a\ meal}$ is calculated by using Eq. 4.9, R_d results

$$R_d = \left(R_{a\ meal} + EGP + F_{2_H}\right) - pV\frac{dG}{dt} \tag{4.20}$$

4.3.2 Two-compartment model

This model is based on a two-compartment description of the system and was introduced in [93]. The model assumes exchange between the accessible and remote compartments and irreversible loss from the accessible compartment only, which has a volume equal to V_1 fixed to population value. Mass balance equation of [6 $-^3$ H]- and [1 $-^{13}$ C]glucose tracers in the accessible

compartment are

$$V_1 \cdot \frac{dG_{3_H}}{dt} = F_{3_H} - \left(R_{01,3_H} + R_{21,3_H}\right) + R_{12,3_H} \tag{4.21}$$

$$V_1 \cdot \frac{dG_{13_C}}{dt} = F_{13_C} - \left(R_{01,13_C} + R_{21,13_C}\right) + R_{12,13_C} \tag{4.22}$$

where $R_{01,3_H}$ and $R_{01,13_C}$ denote the irreversible flux of the two tracers from the accessible compartment and $R_{12,3_H}$, $R_{21,3_H}$, $R_{21,13_C}$ and $R_{21,13_C}$ are exchange fluxes.
Isotopic indistinguishability provides

$$\begin{aligned} \frac{R_{01,3_H}}{V_1 G_{3_H}} &= \frac{R_{01,13_C}}{V_1 G_{13_C}} = k_{01} \\ \frac{R_{21,3_H}}{V_1 G_{3_H}} &= \frac{R_{21,13_C}}{V_1 G_{13_C}} = k_{21} \\ \frac{R_{12,3_H}}{V_2 G_{3_H}} &= \frac{R_{12,13_C}}{V_2 G_{13_C}} = k_{12} \end{aligned} \tag{4.23}$$

The model assumes that parameters k_{12} and k_{21} remain constant and are fixed to population values while k_{01} varies during the experiment. By using Eq. 4.23, Eqs. 4.21 and 4.22 can be rewritten as

$$V_1 \cdot \frac{dG_{3_H}}{dt} = F_{3_H} - (k_{01} + k_{21}) V_1 G_{3_H} + k_{12} Q_{2,3_H} \tag{4.24}$$

$$V_1 \cdot \frac{dG_{13_C}}{dt} = F_{13_C} - (k_{01} + k_{21}) V_1 G_{13_C} + k_{12} Q_{2,13_C} \tag{4.25}$$

where $Q_{2,13_C}$ and $Q_{2,3_H}$ are the amounts of [1$-^{13}$C]glucose and [6$-^{3}$H]glucose tracer in the peripheral compartment. From the [6$-^{3}$H]glucose mass balance equation (Eq. 4.24), an expression for the disappearance rate parameter k_{01} of [6 $-^{3}$ H]glucose tracer ($k_{01,3_H}$) is derived

$$k_{01,3_H} = -\frac{dG_{3_H}/dt}{G_{3_H}} + \frac{F_{3_H}}{V_1 G_{3_H}} - k_{21} + \frac{k_{12} Q_{2,3_H}}{V_1 G_{3_H}} \tag{4.26}$$

By using Eq. 4.26 into Eq. 4.25, one obtains

$$R_{a\ ^{13}C} = \frac{F_{^3H}}{G_{^3H}/G_{^{13}C}} - \frac{V_1 G_{^{13}C}}{G_{^3H}/G_{^{13}C}} \cdot \frac{d(G_{^3H}/G_{^{13}C})}{dt} + k_{12}\Big(\frac{Q_{2,^3H}}{G_{^3H}/G_{^{13}C}} - Q_{2,^{13}C}\Big) \quad (4.27)$$

As result, $R_{a\ ^{13}C}$ is expressed as a function of known ($F_{^3H}$, V_1, k_{12}) or measured ($G_{^3H}$, $G_{^{13}C}$) variables but also of $Q_{2,^{13}C}$ and $Q_{2,^3H}$, which are not measured. These last variables were evaluated by solving the mass balance equations of the [6 $-^3$ H]- and [1 $-^{13}$ C]glucose tracers in the peripheral compartment

$$\frac{dQ_{2,^3H}}{dt} = -k_{12}Q_{2,^3H} + k_{21}V_1 G_{^3H} \quad (4.28)$$

$$\frac{dQ_{2,^{13}C}}{dt} = -k_{12}Q_{2,^{13}C} + k_{21}V_1 G_{^{13}C} \quad (4.29)$$

By applying the same rationale to [6, 6$-^2$H$_2$]glucose and endogenous glucose, an expression for the disappearance rate parameter k_{01} of [6, 6 $-^2$ H$_2$]glucose tracer ($k_{01,^2H}$) is derived

$$k_{01,^2H} = -\frac{dG_{^2H}/dt}{G_{^2H}} + \frac{F_{^2H}}{V_1 G_{^2H}} - k_{21} + \frac{k_{12}Q_{2,^2H}}{V_1 G_{^2H}} \quad (4.30)$$

By using Eq. 4.30 into endogenous glucose (G_{end}) mass balance equation, one obtains

$$EGP = \frac{F_{^2H}}{G_{^2H}/G_{end}} - \frac{V_1 G_{end}}{G_{^2H}/G_{end}} \cdot \frac{d(G_{^2H}/G_{end})}{dt} + k_{12}\Big(\frac{Q_{2,^2H}}{G_{^2H}/G_{end}} - Q_{2,end}\Big) \quad (4.31)$$

where $Q_{2,^2H}$ and $Q_{2,end}$ are the amounts of [6, 6 $-^2$ H$_2$]glucose tracer and endogenous glucose in the peripheral compartment, evaluated by solving the

mass balance equations

$$\frac{dQ_{2,2_H}}{dt} = -k_{12}Q_{2,2_H} + k_{21}V_1G_{2_H} \tag{4.32}$$

$$\frac{dQ_{2,end}}{dt} = -k_{12}Q_{2,end} + k_{21}V_1G_{end} \tag{4.33}$$

Finally, since $R_{a\ meal}$ is calculated by using Eq. 4.9, R_d results

$$R_d = \left(R_{a\ meal} + EGP + F_{2_H}\right) - V_1\frac{dG}{dt} - k_{21}V_1G + k_{12}Q_2 \tag{4.34}$$

where Q_2 is the amount of glucose in the peripheral compartment to be evaluated by integrating model equations.

4.4 Data smoothing and derivative calculation

As reported in the previous Section, the use of models for calculating $R_{a\ meal}$ and EGP, accounting for non-steady-state errors in TTR (Eqs. 4.17, 4.19 and Eqs. 4.27, 4.31), and R_d, accounting for changing in glucose concentration (Eq. 4.20 and Eq. 4.34), needs derivatives calculation. However, since TTR and glucose signals are affected by noise, derivatives calculation cannot be straightforwardly solved due to amplification of the measurement errors.

Traditional methods evaluate time derivatives using a two-step process, i.e. data are first smoothed, then a numerical estimation of the time derivatives is performed. In fact, TTR and glucose signals $y(t)$ can be modeled as

$$y(t) = z(t) + v(t) \tag{4.35}$$

where $z(t)$ is the real unknown input signal and $v(t)$ the measurement error, that can be assumed to be a random white noise process with zero mean and unknown variance, possibly varying with time. Direct estimation of the first derivative of a signal via finite differences is often not satisfactory and the resulting signal is noisy, since differentiation acts as a high-pass

filter amplifying high frequency measurement noise. Thus, several literature approaches can be used to obtain a smoothed version of the of the signal $z(t)$, e.g. Moving Average filters [54]. Such filters are not adaptive, i.e. their parameters remain the same throughout the monitoring and do not efficiently exploit available a priori statistical information in both the regularity of the signal and measurement error. This is why, in this thesis, a Bayesian approach [56] to simultaneously perform both data smoothing and derivative calculations is used.

The problem of estimating the time-derivative $u(t)$ can be considered as a deconvolution problem [36], i.e. defining $u(t)$ such that $u(t) = \dot{z}(t)$ where, for a generic time instant t_0, it holds

$$z(t) = z(t_0) + \int_{t0}^{t} u(\tau)d\tau \tag{4.36}$$

Assuming for simplicity $t_0 = 0$ and $z_0 = 0$, one obtains

$$z(t) = \int_{0}^{t} g(t-\tau)u(\tau)d\tau = g(t) \otimes u(t) \tag{4.37}$$

where

$$g(t) = 1(t) = \begin{cases} 0 & \text{if} \quad t < 0 \\ 1 & \text{if} \quad t > 0 \end{cases} \tag{4.38}$$

The problem can be discretized by integrating $g(t)$ over the time intervals where $u(t)$ is assumed to be constant. The model of data is defined as

$$y = Gu + v \tag{4.39}$$

where G is the integrator in the matrix-vector representation

$$G = \begin{bmatrix} 1 & 0 & \dots & \dots & 0 \\ 1 & 1 & 0 & \dots & 0 \\ 1 & 1 & 1 & \dots & 0 \\ \vdots & \vdots & \vdots & \ddots & \vdots \\ 1 & \dots & \dots & \dots & 1 \end{bmatrix} \tag{4.40}$$

In a Bayesian framework, i.e. u, v and y are considered as stochastic variables, the estimate of u given by y and the model 4.39 can be tackled as a minimum error variance estimate. The solution of this problem coincides with that of determining the vector $\hat{u}$ which minimizes the expected value of the quadratic norm of the estimate error

$$E\Big[||u - \hat{u}||^2\Big] \tag{4.41}$$

Restricting the search into the class of linear estimators, it can be demonstrated that, if u and v are uncorrelated, have zero mean and known covariance matrices Σ_u and Σ_v respectively, the best linear estimate of u given y is the solution of the following optimization problem

$$\min_{\hat{u}}(y - G\hat{u})^T\Sigma_v^{-1}(y - G\hat{u}) + \hat{u}^T\Sigma_u^{-1}\hat{u} \tag{4.42}$$

Notably, the argument of the minimization problem is made of two terms:

- $(y - G\hat{u})^T\Sigma_v^{-1}(y - G\hat{u})$ represents the adherence of the model to the data, i.e. it accounts for the posterior information yielded by the data.
- $\hat{u}^T\Sigma_u^{-1}\hat{u}$ represents the adherence of the unknown vector u to the prior information available on u itself.

Eq. 4.42 has a closed form solution given by

$$\hat{u} = (G^T\Sigma_v^{-1}G + \Sigma_u^{-1})^{-1}G^T\Sigma_v^{-1}y \tag{4.43}$$

In order to solve the minimization problem, it is necessary to have a second-order a priori statistical description of vectors u and v.
For TTR and glucose signals, we can assume the following models for the statistical a priori knowledge:

- *Second order statistical description of vector v*: covariance matrix of vector v described as

  $$\Sigma_v = \sigma^2 B \tag{4.44}$$

  with B known matrix and σ^2 scaling factor, possibly unknown.

- *Second order statistical description of vector u*: for biological signals, the a priori information on the signal to be estimated are qualitative, i.e. the signal is assumed to be smooth and regular. Formally, this can be described considering the components of the vector $u(t)$ to be the realization of a stochastic process that is modeled by a cascade of m integrators driven by a white noise process with zero mean and, possibly, time-varying statistics. Prior covariance matrix is described as

$$\Sigma_u = F^{-1}\Lambda F^{-T} \quad \text{with} \quad F = \Delta^m \tag{4.45}$$

where m represents the penalty index of the m-th order derivatives of $u(t)$, Δ is the lower-triangular Toeplitz matrix

$$\Delta = \begin{bmatrix} 1 & 0 & 0 & \dots & 0 & 0 \\ -1 & 1 & 0 & \dots & 0 & 0 \\ 0 & -1 & 1 & \dots & 0 & 0 \\ \vdots & \vdots & \ddots & \ddots & \vdots & \vdots \\ \vdots & \vdots & \vdots & -1 & 1 & 0 \\ 0 & \dots & \dots & 0 & -1 & 1 \end{bmatrix} \tag{4.46}$$

and Λ is a diagonal matrix representing statistics properties of the white noise process (described below). Eq. 4.45 can be represented as

$$\Sigma_u = \lambda^2 (Q^T Q)^{-1} \quad \text{with} \quad Q = \Omega^{-1} F \tag{4.47}$$

where Ω is given by $\Lambda = \lambda^2(\Omega\Omega^T)$ and λ^2 is a scale factor.

Assuming to have a statistical description of the covariance matrices as defined in Eqs. 4.44 and 4.47, Eq. 4.42 can be rewritten as

$$\hat{u} = (G^T B^{-1} G + \gamma^0 Q^T Q)^{-1} G^T B^{-1} y \tag{4.48}$$

The ratio $\gamma^0 = \sigma^2/\lambda^2$ determines the best trade-off between the adherence to the prior and the data. The Bayesian framework allows to optimally weight the relative importance of the prior and of the data, since the statistical

knowledge on their variance is explicitly considered in the computation of the estimate. Considering the problem defined in Eq. 4.41 and its closed form solution in Eq. 4.48, two quantities can be defined

- *WRSS*: Weighted Residuals Sum of Squares

$$WRSS = (y - G\hat{u})^T B^{-1}(y - G\hat{u}) \tag{4.49}$$

- *WESS*: Weighted Estimates Sum of Squares

$$WESS = \hat{u}^T Q^T Q\hat{u} \tag{4.50}$$

In a stochastic framework, $WRSS$ and $WESS$ are random variables, whose realizations depend on the value of γ. It can be shown [36] that for the optimal value of γ^0, the following properties hold

$$E\Big[WESS(\gamma^0)\Big] = \lambda^2 \cdot q(\gamma^0) \tag{4.51}$$

$$E\Big[WRSS(\gamma^0)\Big] = \sigma^2\{n - q(\gamma^0)\} \tag{4.52}$$

where

$$q(\gamma^0) = trace[B^{-1/2}G(G^T B^{-1}G + \gamma^0 Q^T Q)^{-1}G^T B^{-1/2}] \tag{4.53}$$

with $B^{-1/2}$ is a square matrix such that $B^{-1} = B^{-1/2}B^{-1/2}$. Some consistency criteria can be defined from the properties expressed in Eqs. 4.51 and 4.52 for the choice of the best γ in conditions where σ^2, λ^2 or both are unknown. In particular

Consistency Criterion 1 : if λ^2 is unknown but σ^2 is known, choose γ such that the following condition is matched

$$WESS(\gamma) = \lambda^2 \cdot q(\gamma^0) \quad \text{with} \quad \lambda^2 = \sigma^2/\gamma \tag{4.54}$$

Consistency Criterion 2 : if σ^2 is unknown but λ^2 is known, choose γ

such that the following condition is matched

$$WRSS(\gamma) = \sigma^2\{n - q(\gamma^0)\} \quad \text{with} \quad \sigma^2 = \lambda^2 \cdot \gamma \tag{4.55}$$

Consistency Criterion 3 : when both σ^2 and λ^2 are unknown, choose γ such that the following condition is matched

$$\frac{WRSS(\gamma)}{n - q(\gamma)} = \gamma \cdot \frac{WESS(\gamma)}{q(\gamma)} \tag{4.56}$$

then, when γ is determined from Eq. 4.56, compute the posterior estimate of σ^2 from 4.49 as

$$\hat{\sigma}^2 = \frac{WRSS}{n - q(\gamma)} \tag{4.57}$$

Depending upon the statistical properties of the unknown input signal u, the unknown input signal can be described a priori as multiple integrations of a stationary or time-varying white noise process. Two descriptions of the prior covariance matrix 4.47 are reported.

4.4.1 Standard stochastic deconvolution method

The standard approach is based on the hypothesis that the expectations on the smoothness of the unknown input signal u can be formalized by describing it a priori as multiple integrations of a stationary white noise process. This allow us to define Λ such that

$$\Lambda = \begin{bmatrix} \lambda^2 & 0 & \dots & \dots & 0 \\ 0 & \lambda^2 & 0 & \dots & 0 \\ 0 & 0 & \ddots & \ddots & \vdots \\ \vdots & \vdots & \vdots & \ddots & \vdots \\ 0 & \dots & \dots & \dots & \lambda^2 \end{bmatrix} = \lambda^2 \cdot I \tag{4.58}$$

where I is the identity matrix and λ^2 represents the constant variance of the stationary white noise process.

4.4.2 Improved stochastic deconvolution method

If the unknown input signal shows marked nonstationarity, the standard formulation of the regularization approach in Section 4.4.1 cannot be applied. In [90], an improved stochastic deconvolution method, accounting for nonstationarity in the unknown input signal, is showed. In this work, the biphasic pattern of insulin secretion rate, after a glucose stimulus, consisting of a spike followed by a more regular release, was modeled as a multiple integration of a white noise process with time-varying statistics. More specifically, the white noise process is composed of two different variances: λ_1^2 for $t \leq \tau$ for the first phase secretion, and λ_2^2 for $t > \tau$ for the second phase secretion. Thus matrix Σ_u is the same of Eq. 4.45 but, in this case, Λ is defined as

$$\Lambda = \begin{bmatrix} \lambda_1^2 & 0 & \dots & \dots & 0 \\ 0 & \lambda_1^2 & 0 & \dots & 0 \\ 0 & 0 & \dots & \ddots & \vdots \\ \vdots & \vdots & \vdots & \lambda_2^2 & \vdots \\ 0 & \dots & \dots & \dots & \lambda_2^2 \end{bmatrix} \tag{4.59}$$

The three parameters λ_1^2, λ_2^2 and τ have to be estimated from the data, y, together with the input profile and with the parameter σ^2 which represents the variance of the measurement error. To solve the problem of finding these unknown parameters, in [90] a set of possible values of τ and of the ratio λ_1^2/λ_2^2 is defined and the best combination of λ_1^2, λ_2^2, σ^2 and τ is selected, which maximizes the likelihood function L of y. The choice λ_1^2/λ_2^2 and τ fixed permits to employ the same fast algorithm proposed in [36] where only one regularization parameter was considered in the problem.

General problem

In general, if a priori information on the time-varying statistics of the input signal are unknown, one can build the matrix in Eq. 4.59 by assuming k different variances of the white noise process, thus obtaining

$$\Lambda = \begin{bmatrix} \lambda_1^2 & 0 & \dots & \dots & \dots & \dots & 0 \\ 0 & \lambda_1^2 & \dots & \dots & \dots & \dots & \vdots \\ \vdots & \vdots & \dots & \ddots & \vdots & \vdots & \vdots \\ \vdots & \vdots & \vdots & \lambda_2^2 & \vdots & \vdots & \vdots \\ \vdots & \vdots & \vdots & \vdots & \dots & \vdots & \vdots \\ \vdots & \vdots & \vdots & \vdots & \vdots & \lambda_k^2 & 0 \\ 0 & \dots & \dots & \dots & \dots & 0 & \lambda_k^2 \end{bmatrix} \tag{4.60}$$

The definition of k different variances of the white noise process implies the definition of $k-1$ values for τ, representing the times of variation of the white noise process statistics, and reformatting Eq. 4.60 dividing by λ_1^2 one obtains

$$\Lambda = \lambda_1^2 \begin{bmatrix} 1 & 0 & \dots & \dots & \dots & \dots & 0 \\ 0 & 1 & \dots & \dots & \dots & \dots & \vdots \\ \vdots & \vdots & \dots & \ddots & \vdots & \vdots & \vdots \\ \vdots & \vdots & \vdots & \frac{\lambda_2^2}{\lambda_1^2} & \vdots & \vdots & \vdots \\ \vdots & \vdots & \vdots & \vdots & \dots & \vdots & \vdots \\ \vdots & \vdots & \vdots & \vdots & \vdots & \frac{\lambda_k^2}{\lambda_1^2} & 0 \\ 0 & \dots & \dots & \dots & \dots & 0 & \frac{\lambda_k^2}{\lambda_1^2} \end{bmatrix} \tag{4.61}$$

Then, defining $\alpha_j^2 = \lambda_{j+1}^2/\lambda_1^2$ with $j = 1, \dots, k-1$ as the ratio between the variances of the white noise and λ_1^2, one has

$$\Lambda = \lambda_1^2 \begin{bmatrix} 1 & 0 & \dots & \dots & \dots & \dots & 0 \\ 0 & 1 & \dots & \dots & \dots & \dots & \vdots \\ \vdots & \vdots & \dots & \ddots & \vdots & \vdots & \vdots \\ \vdots & \vdots & \vdots & \alpha_1^2 & \vdots & \vdots & \vdots \\ \vdots & \vdots & \vdots & \vdots & \dots & \vdots & \vdots \\ \vdots & \vdots & \vdots & \vdots & \vdots & \alpha_{k-1}^2 & 0 \\ 0 & \dots & \dots & \dots & \dots & 0 & \alpha_{k-1}^2 \end{bmatrix} = \lambda_1^2(\Omega\Omega^T) \tag{4.62}$$

where Ω was previously defined in Eq. 4.47. Eq. 4.62 allows us to resort to the same algorithm proposed in [90] by fixing a set of possible values for τ and α^2.

Specific problem

Focusing on the present specific problem, since the priori information on time-varying statistics of the input signal due to physical activity is unknown, we hypothesized such a matrix Λ as

$$\Lambda = \begin{bmatrix} \lambda_1^2 & 0 & \dots & \dots & \dots & \dots & \dots & \dots & 0 \\ 0 & \ddots & \dots & \dots & \dots & \dots & \dots & \dots & \vdots \\ \vdots & \vdots & \lambda_1^2 & \ddots & \vdots & \vdots & \dots & \dots & \vdots \\ \vdots & \vdots & \vdots & \lambda_2^2 & \vdots & \vdots & \dots & \dots & \vdots \\ \vdots & \vdots & \vdots & \vdots & \ddots & \vdots & \dots & \dots & \vdots \\ \vdots & \vdots & \vdots & \vdots & \vdots & \lambda_2^2 & \dots & \dots & \vdots \\ \vdots & \dots & \dots & \dots & \dots & \dots & \lambda_3^2 & \dots & \vdots \\ \vdots & \dots & \dots & \dots & \dots & \dots & \dots & \ddots & 0 \\ 0 & \dots & \dots & \dots & \dots & \dots & \dots & 0 & \lambda_3^2 \end{bmatrix} \tag{4.63}$$

where, in Eq. 4.63, three different variances of the white noise process are assumed:

- λ_1^2, i.e. meal phase, starting at $t = 0$ min and lasting till the start of the physical activity session at $t = 120$ min.

- λ_2^2, i.e. exercise phase, starting at $t = 120$ min and lasting till $t = \tau$ min with τ to be estimated, where physical activity effect is assumed to begin sufficiently soon, as can be observed by the rapid falling, on average, of plasma glucose signal (Figure 3.1, top-left).

- λ_3^2, i.e. recovery phase, starting at $t = \tau$ min and lasting till the end of the experiment at $t = 360$ min.

Thus, four parameters $\lambda_1^2, \lambda_2^2, \lambda_3^2$ and τ have to be estimated from the data. Applying the same rationale used in [90], we can reformulate the problem defining $\alpha_1^2 = {}^{\lambda_2^2}/_{\lambda_1^2}$ and $\alpha_2^2 = {}^{\lambda_3^2}/_{\lambda_1^2}$ in order to rewrite Eq. 4.63 as

$$\Lambda = \lambda_1^2 \begin{bmatrix} 1 & 0 & \dots & \dots & \dots & \dots & \dots & \dots & 0 \\ 0 & \ddots & \dots & \dots & \dots & \dots & \dots & \dots & \vdots \\ \vdots & \vdots & 1 & \ddots & \vdots & \vdots & \dots & \dots & \vdots \\ \vdots & \vdots & \vdots & \alpha_1^2 & \vdots & \vdots & \dots & \dots & \vdots \\ \vdots & \vdots & \vdots & \vdots & \ddots & \vdots & \dots & \dots & \vdots \\ \vdots & \vdots & \vdots & \vdots & \vdots & \alpha_1^2 & \dots & \dots & \vdots \\ \vdots & \dots & \dots & \dots & \dots & \dots & \alpha_2^2 & \dots & \vdots \\ \vdots & \dots & \dots & \dots & \dots & \dots & \dots & \ddots & 0 \\ 0 & \dots & \dots & \dots & \dots & \dots & \dots & 0 & \alpha_2^2 \end{bmatrix} \tag{4.64}$$

To solve the problem of finding these unknown parameters a set of possible values for the following parameters was assumed:

- α_1^2 and α_2^2 were assumed to vary, on average, between 10^{-2} to 10^2, where lower values represent less variability while higher values represent high variability of the white noise process.

- τ was assumed to vary from the start of physical activity ($t = 120$), i.e. no effect of physical activity, to the end of physical activity ($t = 195$),

i.e. for the entire duration of physical activity session, with the same time step of the sampling grid.

The choice of fixing parameters to a limited, but sufficiently large, set of possible values allows us to resort the same fast algorithm proposed in [36], where only one regularization parameter was considered in the problem at each step and to repeat the search to all possible values. Finally, the method proposed in [90] suggests to select the best combination of parameters (α_1^2, α_2^2 and τ) which maximizes the likelihood function L of the data.

Moreover, in addition to the method proposed in [90] for the choice of optimal combination of parameters, in this study, a new criterion is proposed. This new method is based on the statistical properties of weighted residuals of the deconvolution technique. As a matter of fact, assuming measurement error to be a white gaussian noise with zero-mean and possibly unknown variance, weighted residuals should be an approximation of measurement errors normalized to their standard deviation (possibly unknown), i.e. a realization of a random process having unit variance. The aim is to satisfy all these hypothesis and minimize the objective function $WRSS + \gamma \cdot WESS$, where the regularization parameter γ is estimated from the data and represents the best trade-off between the adherence to the data and the a priori information. The use of the objective function above may help in choosing the optimal combination of parameters in the case of similar statistical characteristics of weighted residuals. Then two indices to be maximized, one for TTR and one for glucose signals, are obtained:

- TTR: the optimal combination of parameters for TTR signal is obtained by maximizing

$$\frac{p_{(\text{t-test})} \cdot p_{(\text{runs-test})} \cdot p_{(\text{KS-test})}}{WRSS + \gamma \cdot WESS} \tag{4.65}$$

  where in the numerator one can find the p-value of 3 statistical tests, i.e. Student's t-test ($p_{(\text{t-test})}$), Wald-Wolfowitz runs test ($p_{(\text{runs-test})}$) and

Kolmogorov-Smirnov test ($p_{(\text{KS-test})}$) in order to respectively quantify the zero-mean, randomness and normality of the distribution of weighted residuals, and in the denominator the objective function $WRSS + \gamma \cdot WESS$.

- *Glucose*: the optimal combination of parameters for glucose signal is obtained by maximizing

$$\frac{p_{(\text{t-test})} \cdot p_{(\text{runs-test})} \cdot p_{(\text{KS-test})} \cdot p_{(\chi^2\text{-test})}}{WRSS + \gamma \cdot WESS} \tag{4.66}$$

in this case in the numerator, at variance with the index obtained for the TTR signal, also the Chi-square test for the variance ($p_{(\chi^2\text{-test})}$) is used since, for glucose signal, the variance is a priori known. This test is not used for TTR signal in order not to overestimate the effect of the variance on the smoothing procedure of TTR data since it is already estimated from the data.

4.5 Results

Data are presented as mean ± SE, if not differently indicated. Rates of glucose turnover are expressed as milligrams per kilogram of body weight per minute. Postprandial glucose fluxes were averaged on a total of 11 subjects, since an error on the measurement of meal enrichment was reported in one subject. Values obtained at $t = 0$ min were considered as basal. In the following Figures, shaded box between $t = 120$ and $t = 195$ min represents the exercise period at 50% $\dot{\text{V}}\text{O}_{2\text{max}}$.

4.5.1 Plasma glucose, hormones and tracers data

In Figure 3.1 plasma glucose, insulin, C-peptide and glucagon concentration data are reported. Plasma glucose concentration rose from baseline of 89.6 ± 3.24 mg/dL to a peak of 164.6 ± 10.45 mg/dL at $t = 60$ min, then

dropped to 112.7 ± 10.64 mg/dL at $t = 120$ min (start of exercise), and reached a nadir of 71.6 ± 5.03 mg/dL at $t = 140$ min. Thereafter, plasma glucose concentration gradually rose to 78.0 ± 2.70 mg/dL at $t = 195$ min (end of exercise) before returning to baseline 89.7 ± 2.81 mg/dL at $t = 250$ min, remaining constant thereafter until $t = 360$ min. Plasma insulin concentration rose from baseline of 3.7 ± 0.61 μU/mL to a peak of 54.1 ± 6.81 μU/mL at $t = 60$ min, then dropped to 32.8 ± 6.78 μU/mL at $t = 120$ min (start of exercise), and reached a nadir of 4.9 ± 1.14 μU/mL at $t = 195$ min (end of exercise) before gradually drifting to 4.5 ± 1.41 μU/mL at $t = 360$ min. Plasma C-peptide concentration rose from a baseline of 0.55 ± 0.05 nmol/L to a peak of 3.46 ± 0.32 nmol/L at $t = 90$ min, then dropped to 2.88 ± 0.36 nmol/L at $t = 120$ min (start of exercise), and reached 0.88 ± 0.11 nmol/L at $t = 195$ min (end of exercise) before gradually drifting down to 0.58 ± 0.08 nmol/L at $t = 360$ min. In contrast, plasma glucagon concentration at baseline were 59.3 ± 4.49 pg/mL, then briefly rose on meal ingestion before falling to a nadir of 54.3 ± 4.19 pg/mL at $t = 60$ min, then slowly rose to 64.0 ± 7.41 pg/mL at $t = 120$ min (start of exercise) before rapidly rising more than two-fold to a peak of 135 ± 18.85 pg/mL at $t = 180$ min. Subsequently, glucagon concentration rapidly fell to 70.9 ± 6.89 pg/mL at $t = 360$ min.
In Figure 3.2 $[1-^{13}\mathrm{C}]$ MR above natural, $[6,6-^{2}\mathrm{H}_2]$ MR and $[6-^{3}\mathrm{H}]$ glucose counts data are reported. $[1-^{13}\mathrm{C}]$ MR above natural rose to a peak of $3.34 \pm 0.09\%$ at $t = 120$ min after meal ingestion and then declined to $0.89 \pm 0.13\%$ at the end of the experiment. $[6,6-^{2}\mathrm{H}_2]$ MR declined from baseline of $4.47 \pm 0.23\%$ to a plateau of approximately $0.82 \pm 0.06\%$ between $t = 120$ and $t = 150$ min, then increased to $3.00 \pm 0.15\%$ at the end of the experiment. $[6-^{3}\mathrm{H}]$ glucose counts rose to a peak of 1728.7 ± 181.09 dpm/mL at $t = 60$ min and then decreased to 425.0 ± 27.33 dpm/mL at the end of the experiment.

Then, starting from plasma glucose (Figure 3.1, top-left), molar ratios and counts data (Figure 3.2), glucose tracers concentration $G_{13_{\mathrm{C}}}$, $G_{3_{\mathrm{H}}}$, $G_{2_{\mathrm{H}}}$ and endogenous glucose G_{end} are calculated (Figure 4.2) by using Eqs. 4.4, 4.5 and 4.7. As can be observed in Figure 4.2, on average, profiles of $G_{13_{\mathrm{C}}}$

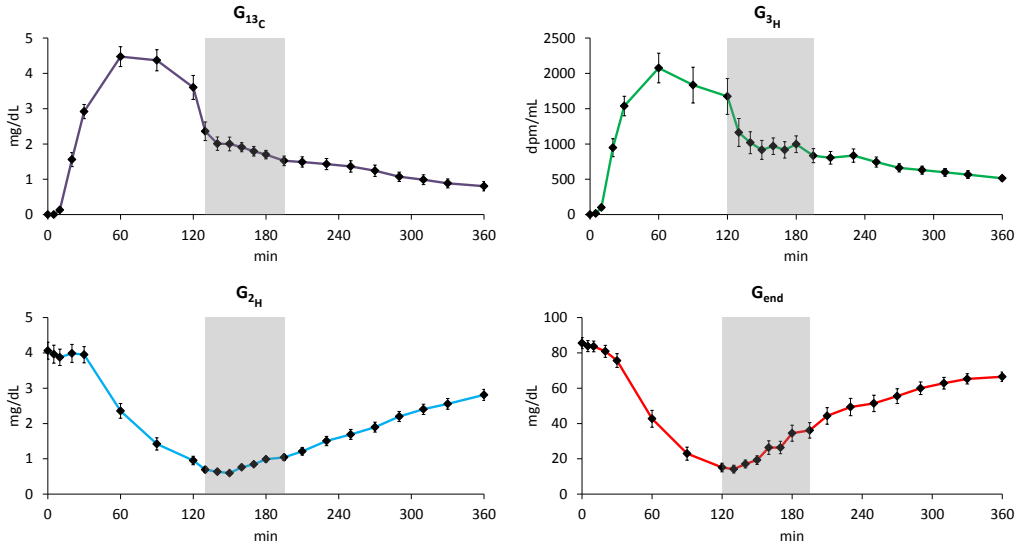

Figure 4.2: [1 $-^{13}$ C]glucose (top-left), [6 $-^{3}$ H]glucose (top-right), [6,6 $-^{2}$ H_2]glucose (bottom-left) and endogenous glucose (bottom-right) concentrations calculated from $t = 0$ and $t = 360$ min.

to G_{3_H} and G_{2_H} to G_{end} are very similar, respectively, thus indicating a good clamp of the respective tracer-to-tracee ratios. However, this may not always be the case for individual signals, since, as previously remarked, it is almost impossible to realize a "perfect" clamp of the plasma TTR. In fact, usually it may happen that:

- [6 $-^{3}$ H]glucose-to-[1 $-^{13}$ C]glucose ratio shows, especially in the initial few minutes after meal ingestion, unavailable measurements (either G_{13_C} or G_{3_H} below the limit of detection) or very high values and of uncertain reliability, as indicated by an error propagation analysis.

- [6,6 $-^{2}$ H_2]glucose-to-endogenous glucose ratio shows, especially in the endogenous glucose suppression phase, very high or even negative values due to very low or negative values, respectively, of endogenous glucose concentration. This can be due to measurement error on both tracer and tracee data from which G_{end} is derived (Eq. 4.7).

Thus, when the above described events occur, we are required to exclude these measurements, in one hand, to eliminate unacceptable values of TTR

and, on the other hand, to avoid errors on derivative calculation.

Then, starting from glucose tracers concentration G_{13_C}, G_{3_H}, G_{2_H} and endogenous glucose G_{end} we can calculate tracer-to-tracee ratios (Figure 4.3) as

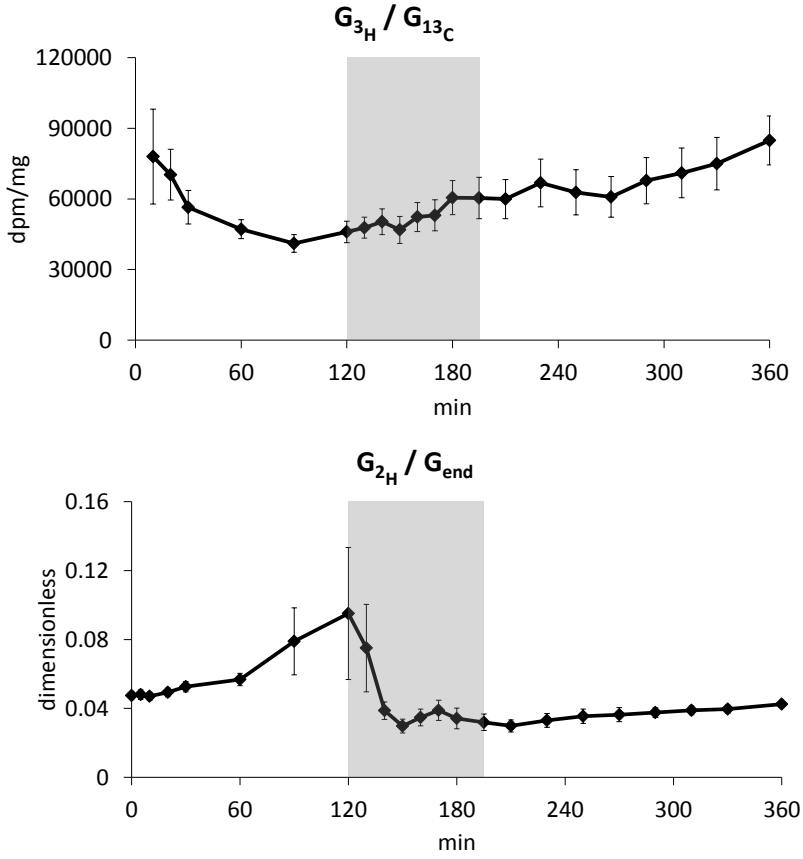

Figure 4.3: [6 $-^3$ H]glucose-to-[1 $-^{13}$ C]glucose ratio (top) and [6,6 $-^2$ H_2]glucose-to-endogenous glucose ratio (bottom).

- G_{3_H}/G_{13_C}, called also "specific activity" (SA), where [6 $-^3$ H]glucose is considered as tracer while [1 $-^{13}$ C]glucose is considered as tracee (Figure 4.3, top). As can be observed, the ratio G_{3_H}/G_{13_C} is fairly constant for almost the entire duration ($t = 10 - 360$ min) of the study apart form the initial perturbation ($t = 0 - 10$ min) that is

unavoidable, as previously explained, when the intravenously infused and orally ingested tracee are entering the systemic circulation. In contrast, physical activity starting at $t = 120$ min does not alter SA, since the plasma concentrations of tracer and tracee changed in parallel throughout the study.

- G_{2_H}/G_{end} where $[6,6\,{}^{-2}\,H_2]$glucose is considered as tracer while endogenous glucose is considered as tracee (Figure 4.3, bottom). As can be observed, the ratio G_{2_H}/G_{end} is also fairly constant apart from a slight fall at $t = 120$ min at the start of exercise. This nonstationary has to be carefully taken into account when TTR derivative is calculated.

4.5.2 Methods for glucose fluxes estimation

As shown in Figure 4.3, it is almost impossible to realize a "perfect" clamp of the plasma TTR. Thus postprandial glucose fluxes can be calculated using either a single-compartment or a two-compartment model (1CM and 2CM, respectively) to compensate the non-steady-state errors and to estimate R_d. Model parameters are fixed to population values: $V = 200$ mL/kg and $p = 0.65$ for the one-compartment [109], while $V_1 = 130$ mL/kg, $k_{12} = 0.07$ min^{-1} and $k_{21} = 0.05$ min^{-1} for the two-compartment [4, 93]. However the use of models requires derivatives calculation for G_{3_H}/G_{13_C}, G_{2_H}/G_{end} and glucose signals, here approached adopting a deconvolution technique. Two possible implementations of the deconvolution technique have been considered, both working in a Bayesian framework, but each assuming a particular statistical property of the unknown input signal.

Standard stochastic deconvolution method

The standard stochastic deconvolution approach hypothesizes that the expectations on the smoothness of the unknown input signal u can be formalized by describing it, a priori, as multiple integrations of a stationary white noise process. For each signal, the same assumptions used in [4] have been considered:

- G_{3_H}/G_{13_C}: since the clamp of the SA is often a smooth signal, thanks to pilot studies information and given the subjects' normal gastric emptying, its derivative can be assumed as a realization of a stochastic process modeled by a cascade of two integrators ($m = 2$) driven by a white noise process with unknown constant variance (λ^2), while measurement error is assumed to be constant with unknown coefficient of variation ($\sigma^2 = (CV \cdot y)^2$).

- G_{2_H}/G_{end}: since the clamp of TTR is often more difficult to realize due to the high variability of G_{end}, its derivative can be assumed as a realization of a stochastic process modeled by an integrator ($m = 1$) driven by a white noise process with unknown constant variance (λ^2), while measurement error is assumed to be constant with unknown coefficient of variation ($\sigma^2 = (CV \cdot y)^2$).

- *Glucose*: glucose signal is known to be smooth and generally it is described by an integrated random-walk model, thus its derivative can be described as a realization of a stochastic process modeled by an integrator ($m = 1$) driven by a white noise process with unknown constant variance (λ^2), while measurement error on glucose signal is generally assumed to be constant with a known coefficient of variation equal to 2% ($\sigma^2 = (0.02 \cdot y)^2$).

In Figure 4.4 average data vs. reconvolution (left) and weighted residuals (right) of G_{3_H}/G_{13_C}, G_{2_H}/G_{end} and glucose signals obtained with the standard stochastic deconvolution method are showed. On top panels of Figure 4.4 and one can observe that the method provides an accurate regularized version of SA since, as previously reported, physical activity does not alter SA. In contrast, the method is not able to follow the rapid changes on TTR signal (Figure 4.4, middle panels) and data overfitting can be observed on glucose signal (Figure 4.4, bottom panels). The inability of the method to provide an accurate regularization of TTR and glucose signals, and thus their derivatives, is due to the effect of physical activity that, in this case, has not been taken into account.

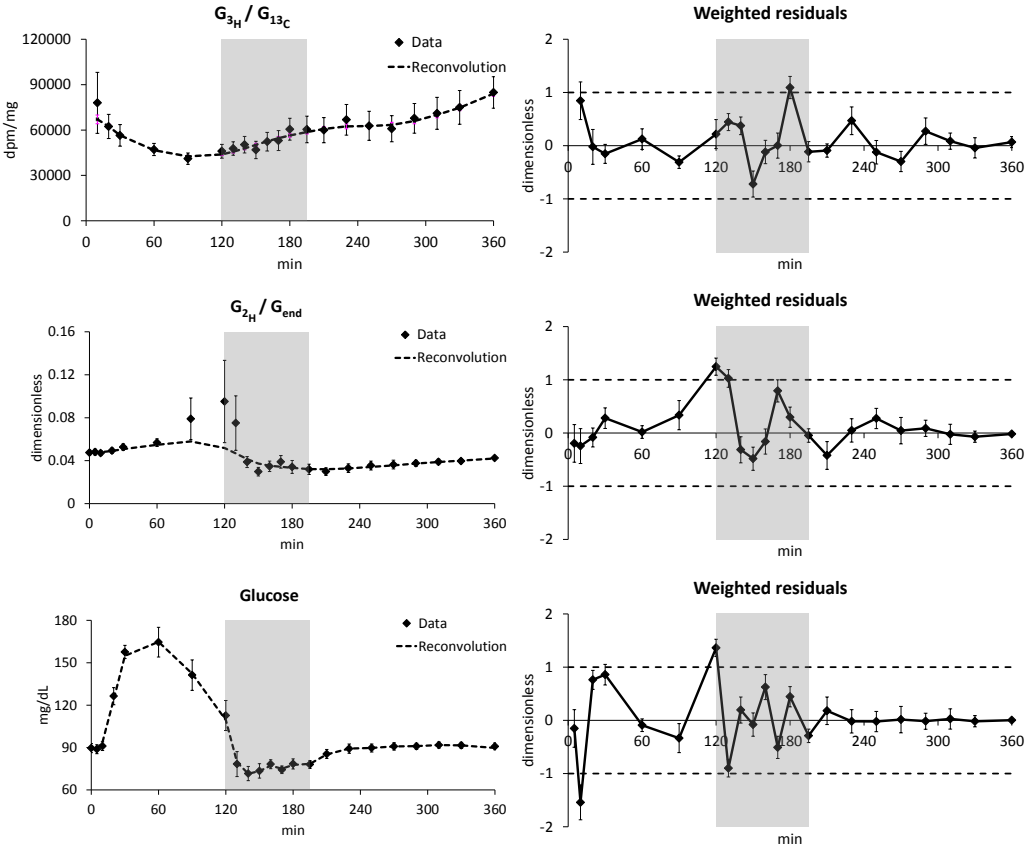

Figure 4.4: Average data vs. reconvolution (left) and weighted residuals (right) obtained with the standard stochastic deconvolution method. [6 $-^3$ H]glucose-to-[1 $-^{13}$ C]glucose ratio (top), [6,6 $-^2$ H_2]glucose-to-endogenous glucose ratio (center-right) and glucose signal (bottom).

Finally, in Figure 4.5, average postprandial glucose fluxes obtained with the one- and two-compartment model using derivatives of SA, TTR and glucose signals calculated with the standard stochastic deconvolution method are showed. As can be observed, $R_{a\ meal}$ obtained with the one- and two-compartment model are very similar one to each other thanks to the well clamped SA. In contrast, EGP and R_d are not perfectly superimposable, possibly due to the rapid changes in both G_{2_H}/G_{end} and glucose signals which amplify models errors. However, even if the slight superiority of the two- vs. one-compartment model in the postprandial setting [4], in this experimental conditions, EGP and R_d calculated with the two-compartment model

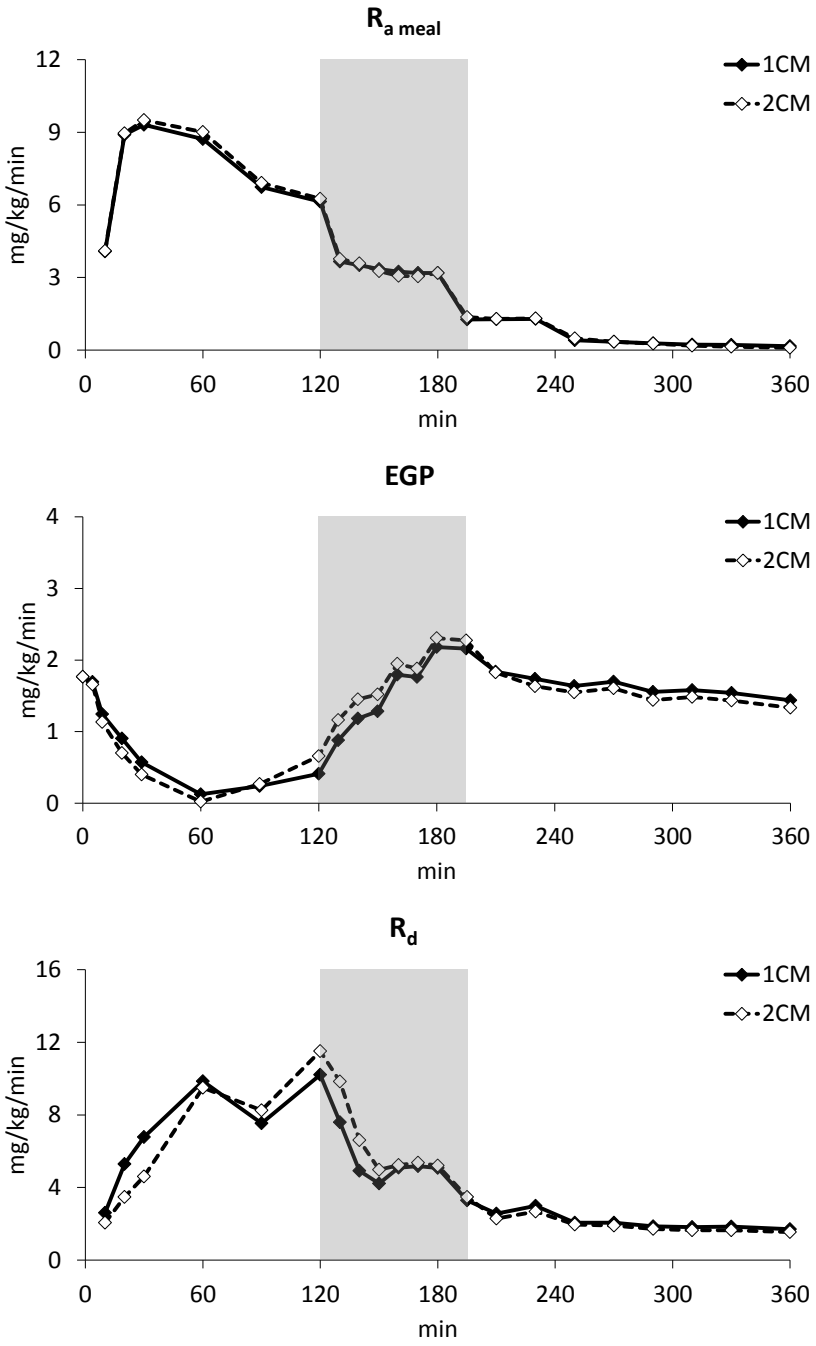

Figure 4.5: Average $R_{a\ meal}$ (top), EGP (middle) and R_d (bottom) fluxes obtained with the one- (1CM) and two-compartment (2CM) model with derivatives of SA, TTR and glucose signals obtained with the standard stochastic deconvolution method.

exhibit, in some cases, unphysiological behaviours, e.g negative values and less smoother signals, respect to the one-compartment model. Likely, these are due to unknown effects of physical activity on the exchange parameters between the two glucose compartments, fixed to population values, and this error may be amplified due to TTR and glucose rapid variations.

Improved stochastic deconvolution method

Assuming that a nonstationarity is introduced due to physical activity, an improved stochastic deconvolution method is adopted. It assumes that the expectations on the smoothness of the unknown input signal can be modeled as a multiple integration of a white noise process but, in this case, with time-varying statistics. This effect is particularly remarkable on both TTR and glucose signals (Figure 4.4), but not on SA. For this reason, this method is not applied to SA, but only to TTR and glucose signals.

In Figures 4.6 average data vs. reconvolution (left) and weighted resid-

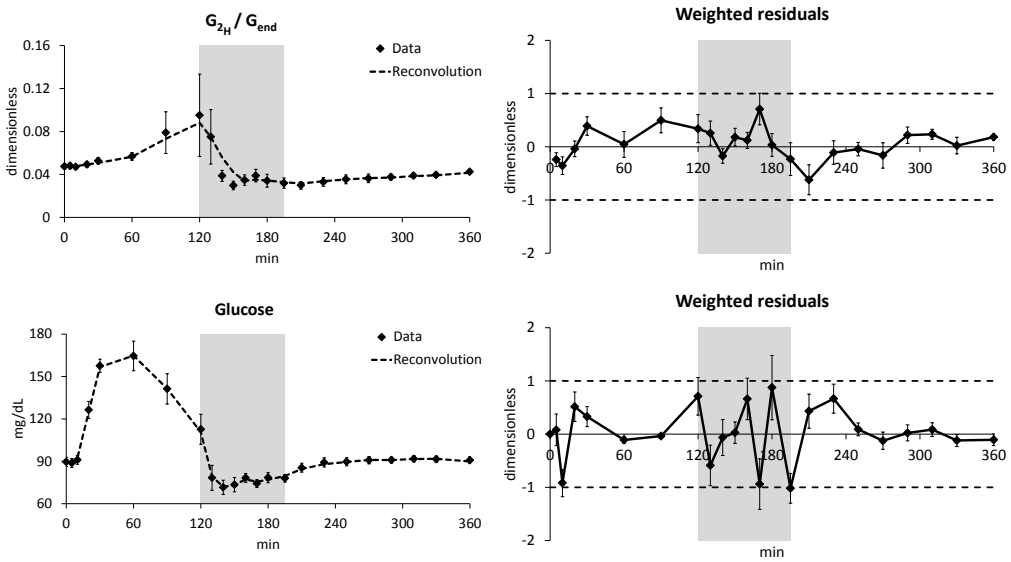

Figure 4.6: Average data vs. reconvolution (left) and weighted residuals (right) obtained with the improved stochastic deconvolution method maximizing the likelihood function L of the data for the estimation of the optimal combination of parameters (α_1^2, α_2^2 and τ). $[6,6\,-^2\,H_2]$glucose-to-endogenous glucose ratio (top) and glucose signal (bottom).

uals (right) of G_{2_H}/G_{end} and glucose signals obtained with the improved stochastic deconvolution method are showed. One can observe that this method provides an accurate regularized version of both TTR and glucose signal. In fact, the reconvoluted TTR (Figure 4.6, top panel) well follows the rapid changes of TTR signal, while weighted residuals of glucose signal (Figure 4.6, lower panel) are well distributed. Median and interquartile range of parameters α_1^2, α_2^2 and τ, estimated maximizing the likelihood function L of the data, are reported in Table 4.1.

For TTR and glucose signals, on average, α_1^2 and α_2^2 are greater and lower,

	α_1^2	α_2^2	τ
TTR	9.5	0.117	160
	$(1.55 - 15)$	$(0.05 - 2.5)$	$(147.5 - 165)$
Glucose	6	0.053	160
	$(0.28 - 8.5)$	$(0.027 - 1)$	$(150 - 170)$

Table 4.1: Median and interquartile range of parameters α_1^2, α_2^2 and τ estimated applying the improved stochastic deconvolution method on TTR (top) and glucose (bottom) signals maximizing the likelihood function L of the data for the estimation of the optimal combination of parameters (α_1^2, α_2^2 and τ).

respectively, than 1 (which would have meant same statistical properties during meal and exercise phase). This can be due to physical activity which introduces a nonstationarity from the start of the exercise phase (α_1^2) to approximately $\tau = 160$ min, while a more stationary phase, the recovery phase (α_2^2), lasts till the end of the experiment for both signals.

In Figure 4.7, average EGP and R_d fluxes obtained with the one- and two-compartment model using derivatives calculated with the improved stochastic deconvolution method are showed. As can be observed, EGP and R_d are slightly different from those obtained with the standard stochastic deconvolution method (Figure 4.5), especially during exercise. In fact, EGP rises faster, thanks to a more accurate estimation of TTR derivatives which better follows the rapid changes in TTR signal, while R_d is more smoothed, thanks to a smoother glucose derivatives in this phase.

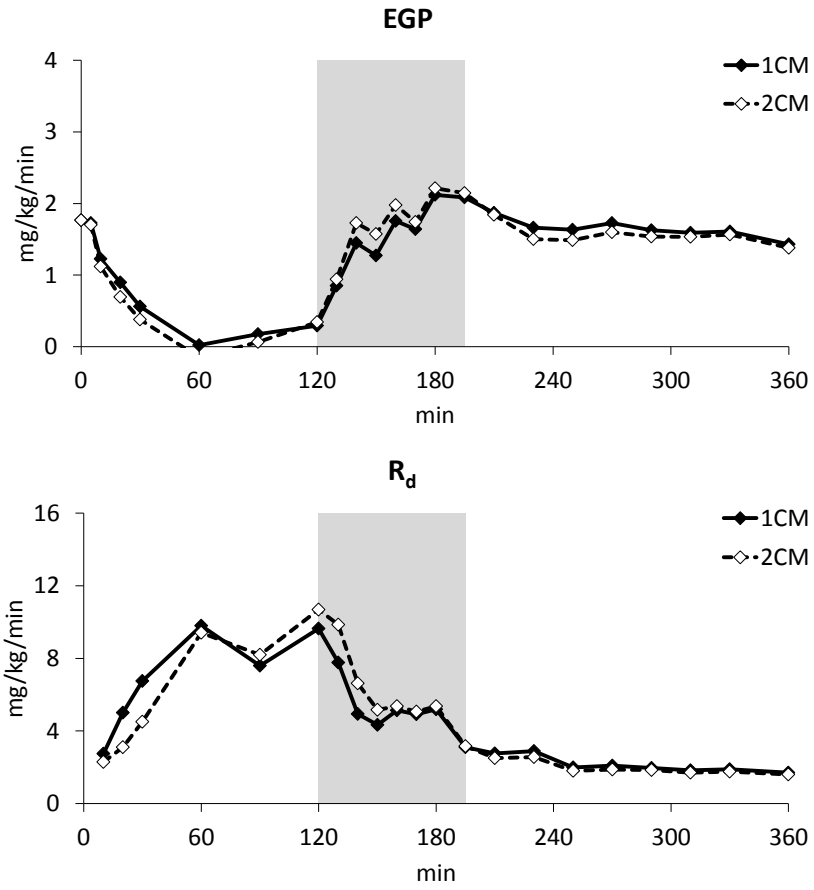

Figure 4.7: Average EGP (top) and R_d (bottom) fluxes obtained with the one- (1CM) and two-compartment (2CM) model with derivatives of TTR and glucose signals obtained with the improved stochastic deconvolution method maximizing the likelihood function L of the data for the estimation of the optimal combination of parameters (α_1^2, α_2^2 and τ).

However, the use of the block matrix Λ (Eq. 4.64) and a criterion for the choice of the optimal combination of parameters (α_1^2, α_2^2 and τ) which consider signals as made up of discontinuous components due to sudden variations of statistics properties of the a priori model, can lead sometimes to undersmoothing, probably caused by compensation effects between the estimated parameters.

For example, in Figure 4.8, the criterion proposed in [90], i.e. maximization of the likelihood function L of the data for the estimation of the optimal

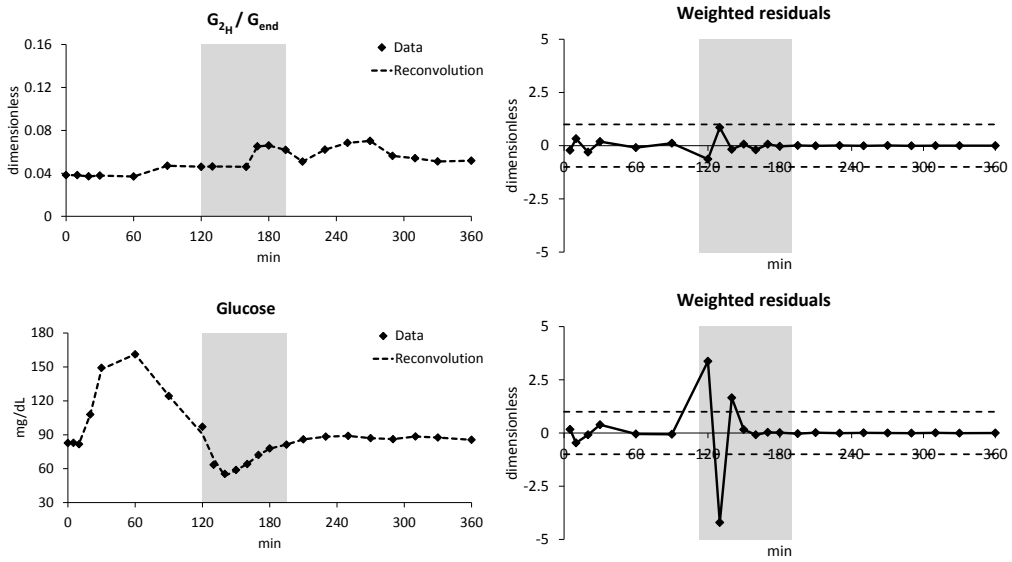

Figure 4.8: Data vs. reconvolution (left) and weighted residuals (right) obtained with the improved stochastic deconvolution method maximizing the likelihood function L of the data for the estimation of the optimal combination of parameters (α_1^2, α_2^2 and τ). $[6,6-^2\mathrm{H}_2]$glucose-to-endogenous glucose ratio of subject 04 (top) and glucose signal of subject 01 (bottom).

combination of parameters (α_1^2, α_2^2 and τ), leads both TTR and glucose signals to be undersmoothed. This issue can be related to the fact that the variations on the regularity of the a priori model of TTR and glucose signals may not always be modeled as a sudden variation, i.e. in some cases this variation may change more smoothly.

For this reason here the new criterion, based on the statistical properties of weighted residuals, for the estimation of the optimal combination of parameters is used (Eqs. 4.65 and 4.66), in order to maintain the structure of Eq. 4.64 but avoiding oversmoothing.

By comparing reconvoluted TTR and glucose signals obtained with the two criteria in Figures 4.8 and 4.9, one can observe the improvements introduced by the new criterion (Eqs. 4.65 and 4.66) which allows a better fit of the data, reducing the undersmoothing phenomena. However, as can be observed by comparing Figures 4.6 and 4.10, this may always be the case. In fact, on average, results obtained with the two criteria are very similar, meaning that

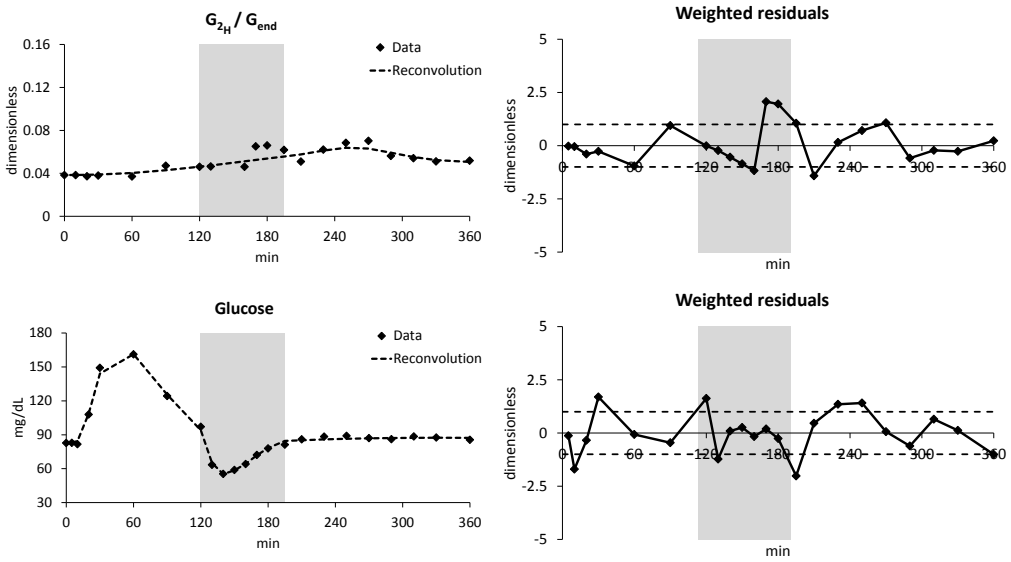

Figure 4.9: Data vs. reconvolution (left) and weighted residuals (right) obtained with the improved stochastic deconvolution method using the new criterion proposed for the estimation of the optimal combination of parameters (α_1^2, α_2^2 and τ). $[6,6-^2\mathrm{H}_2]$glucose-to-endogenous glucose ratio of subject 04 (top) and glucose signal of subject 01 (bottom).

the assumption of a rapid variation of stationarity introduced by physical activity is valid in most cases. However, the use of the new criterion worsens weighted residuals, but this was an expected consequence since the new criterion allows a more smoothed reconstruction of TTR and glucose signals, leading to a lower adherence to noisy experimental data. Median and interquartile range of parameters α_1^2, α_2^2 and τ, estimated with the new criterion proposed are reported in Table 4.2.

As reported in Table 4.2, on average, α_1^2 of TTR signal is greater than 1 while α_1^2 of glucose signal is approximately equal to 1. This means that the nonstationarity introduced by physical activity is more pronounced in the TTR signal between the exercise and meal phase. In contrast, both α_2^2 of TTR and glucose signals are lower than 1 leading to a more regular recovery phase, as expected. As a remark, looking at the average value of τ reported in Table 4.1, here the effect of exercise seems to last a bit longer.

In Figure 4.11, average EGP and $\mathrm{R_d}$ fluxes obtained with the one- and two-

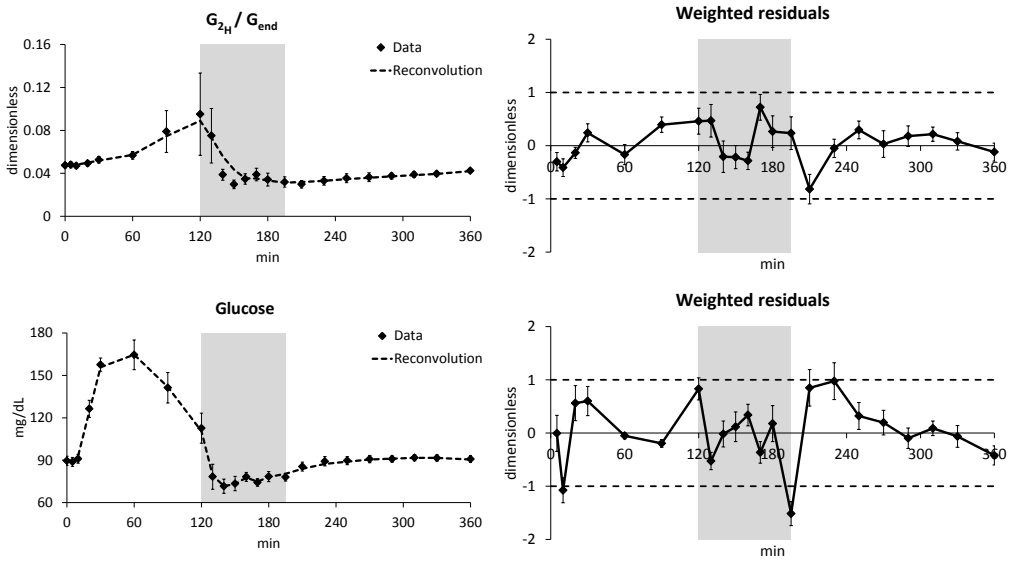

Figure 4.10: Average data vs. reconvolution (left) and weighted residuals (right) obtained with the improved stochastic deconvolution method using the new criterion proposed for the estimation of the optimal combination of parameters (α_1^2, α_2^2 and τ). [6,6 −^{2} H_2]glucose-to-endogenous glucose ratio (top) and glucose signal (bottom).

	α_1^2	α_2^2	τ
TTR	4	0.167	170
	(1.625 − 11.75)	(0.032 − 0.625)	(150 − 195)
Glucose	1	0.031	187.5
	(1 − 2)	(0.014 − 0.087)	(180 − 195)

Table 4.2: Median and interquartile range of parameters α_1^2, α_2^2 and τ estimated applying the improved stochastic deconvolution method on TTR (top) and glucose (bottom) signals using the new criterion proposed for the estimation of the combination of parameters (α_1^2, α_2^2 and τ).

compartment model using derivatives calculated with the improved stochastic deconvolution method and the new criterion are showed. As TTR and glucose reconvoluted signals (Figure 4.7), EGP and R_d are very similar to the ones obtained with the other improved deconvolution method.

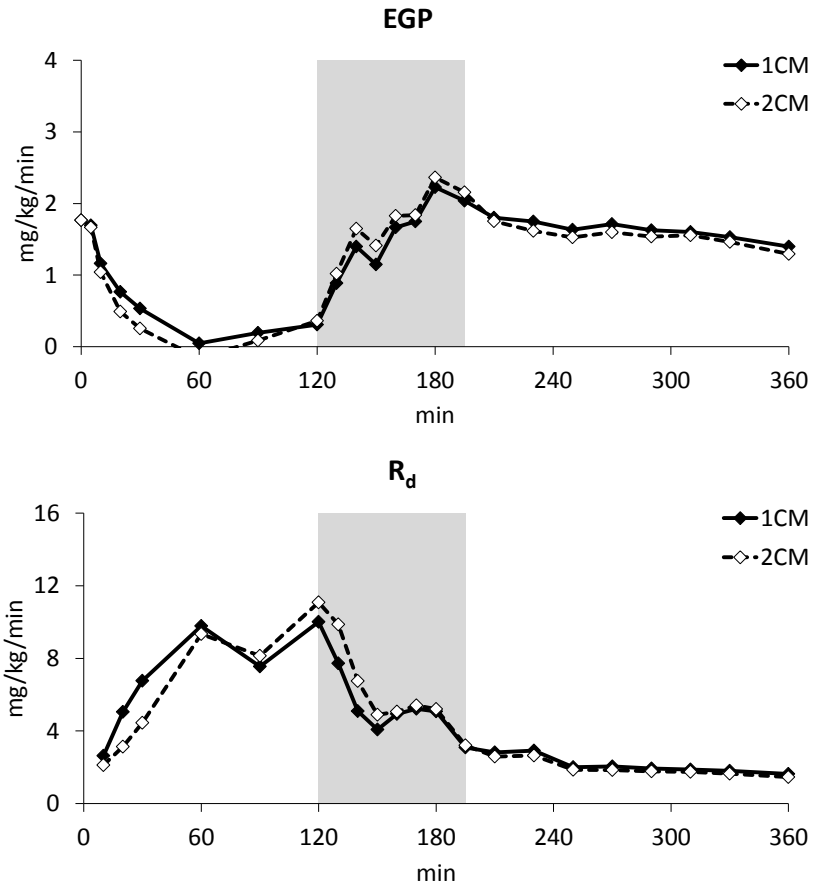

Figure 4.11: Average EGP (top) and R_d (bottom) fluxes obtained with the one- (1CM) and two-compartment (2CM) model with derivatives of TTR and glucose signals obtained with the improved stochastic deconvolution method using the new criterion proposed for the estimation of the optimal combination of parameters (α_1^2, α_2^2 and τ).

4.5.3 Postprandial glucose fluxes

Here a brief discussion about postprandial glucose fluxes estimated with the triple-tracer approach is reported. $R_{a\ meal}$ obtained with the one- and two-compartment were very similar one to each other because plasma concentrations of tracer and tracee changed in parallel throughout the study and, for this reason, the standard deconvolution technique was adequate to allow an accurate reconstruction of SA and its derivative. In contrast, the reconstruction of EGP and R_d fluxes has been more complicated since the rapid changes

in both G_{2_H}/G_{end} and glucose signals probably due to nonstationarity introduced by physical activity. For these two signals, the one-compartment model and the improved stochastic deconvolution method for derivatives calculation were chosen. The one-compartment model was selected since, in this particular conditions (moderate-intensity physical activity), estimated glucose fluxes showed a more physiological behaviour, i.e. smoother signals and avoiding negative values, with respect to the two-compartment. In addition, a part from the clear advantages of the improved stochastic deconvolution method in reconstructing TTR and glucose signals, the adoption of the new criterion proposed allows a more regular reconstruction of both TTR and glucose profiles.

As reported in the upper panel of Figure 4.5, $R_{a\ meal}$ fell rapidly during the first 10 min of exercise ($t = 120 - 130$ min) but thereafter reached a plateau at rates similar to that observed at $t = 10$ min for the remaining duration of the exercise period. Subsequently, $R_{a\ meal}$ rapidly declined to near zero by $t = 240$ min (i.e., within 35 min) after completion of exercise. The transient plateau in $R_{a\ meal}$ during exercise could be because of an exercise-induced increase in visceral sympathetic nerve activity delaying gastric emptying rates. Prior reports on the direct effects of exercise on rates of gastric emptying have been conflicting, with reports demonstrating either delayed [77, 94] or no effects [15, 42] on gastric emptying rates in healthy adults. It is possible that the timing of exercise in relation to the meal is an important determinant of $R_{a\ meal}$. Therefore, an earlier start to the exercise after the meal could have had a greater effect on $R_{a\ meal}$. Furthermore, a humoral factor that could have contributed to the plateau in $R_{a\ meal}$ includes the rise in glucagon concentrations during exercise (Figure 3.1, left-lower panel), since glucagon is known to possess decelerating effects on gastric motility [129].
Glucose concentration at any given time point is a function of the rate of glucose entering and leaving the circulation. This concept is true in both the postabsorptive and postprandial situations. Because exercise is known to increase the rate of glucose leaving the circulation (i.e., R_d), rates of glucose entering the circulation in the postprandial state (i.e., EGP and/or

$R_{a\ meal}$) must also increase to compensate for the physiological increase in R_d to prevent hypoglycemia. Because glucose concentrations fell below baseline fasting levels during exercise in all subjects, the rate of glucose leaving the circulation (i.e., R_d) must have exceeded the rate of glucose entering the circulation (i.e., combined rates of EGP and $R_{a\ meal}$). It is noteworthy, however, that these dynamic changes were occurring in the presence of rapidly falling insulin concentrations during exercise. Although the almost eightfold rise in rates of EGP from the start to the end of exercise (Figure 4.11, top panel) could be explained by both falling insulin and rising glucagon concentrations, the plateau in R_d (Figure 4.11, bottom panel) during exercise ($t = 140 - 180$ min) can be explained by increasing muscle glucose uptake by both insulin-independent and -dependent mechanisms. The sustained rate of R_d during exercise, however, was only in part compensated by the eightfold increase in EGP and a transient plateau in the rate of $R_{a\ meal}$ from the gastrointestinal tract. Furthermore, exercise is also known to increase rates of blood flow to exercising muscles [2, 92], thereby contributing, at least in part, to enhanced muscle glucose uptake [53].
In conclusion, in this section, a description of postprandial glucose turnover, during moderate-intensity physical activity, has been presented. A rapid eightfold increase in rates of EGP with a plateau in the rates of both $R_{a\ meal}$ and R_d were showed, while glucose concentrations rapidly fell below baseline fasting levels in all subjects accompanied by a rapid fall in insulin concentrations together with greater than twofold rise in glucagon concentrations.

The implemented methods for the estimation of glucose fluxes and their results have been published in [104].

5 Estimation of Insulin Sensitivity during Exercise

5.1 Introduction

Excellent, but complex, methods are available for the quantitative assessment of insulin sensitivity (S_I), i.e. the ability of insulin to stimulate glucose disposal (R_d) and inhibit endogenous production (EGP), employing intravenous administration of insulin and/or glucose, e.g. hyperinsulinemic euglycemic clamp [37] and intravenous glucose tolerance test (IVGTT) [6]. However, given the difficulty of venous administration and the nonphysiological experimental conditions, it would have been highly desirable to obtain an accurate measure of S_I from oral administration. More recently, methods based on meal and oral glucose tolerance test (MTT and OGTT, respectively), e.g. the oral glucose minimal model [30, 32] and surrogate measures [55, 85, 112], have been developed. However, none of these methods have been tested and validated when these perturbations are further challenged by exercise.

In this Chapter a method is presented to assess the effect and effect size of physical activity on insulin sensitivity, which employs the glucose fluxes estimated in Chpater 4. To do that, insulin sensitivity is estimated in absence and in presence of physical activity. Thanks to glucose fluxes availability, it

was possible also to tease out the contribution of liver and disposal insulin sensitivity. Then, a well-established integral formula [21], for the estimation of net insulin sensitivity, based on plasma glucose and insulin concentration data, was used to compare and validate the obtained results.

5.2 Insulin sensitivity estimation

In this Section two integral formulas for the estimation of insulin sensitivity during a meal are presented. Both methods rely on the minimal model of glucose regulation [6], but with some fundamental differences.
The first one is based on reconstructed postprandial glucose fluxes and the model is coupled with a simple mathematical description of the effect of glucose and insulin on EGP and R_d, while the other one is based on glucose and insulin data and the model is coupled with a simple mathematical description of glucose absorption from the gastrointestinal tract.

5.2.1 Insulin sensitivity from postprandial glucose fluxes

In this Section a method for the estimation of net (S_I^{TOT}), liver (S_I^L) and disposal (S_I^D) insulin sensitivity, based on reconstructed postprandial glucose fluxes is proposed. The method is based on the minimal model of glucose regulation [6] by adopting a simple mathematical description of the effect of glucose and insulin on EGP and R_d (Fig. 5.1). The model describing EGP is given by

$$EGP(t) = EGP_b - GE^L \cdot (G(t) - G_b) - S_I^L \cdot X'(t)G(t)$$
$$EGP(0) = EGP_b \quad (5.1)$$

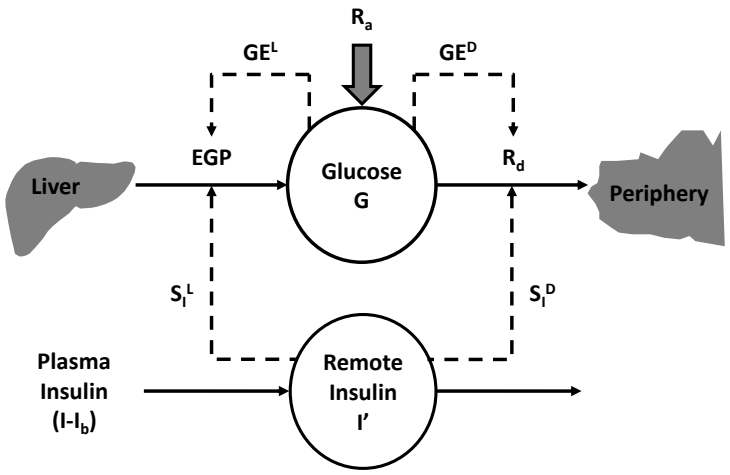

Figure 5.1: Minimal model of glucose regulation [6] adopting a simple description of the effect of glucose and insulin on EGP and R_d.

while the model describing R_d is given by

$$R_d(t) = R_{db} + GE^D \cdot (G(t) - G_b) + S_I^D \cdot X'(t)G(t)$$
$$R_d(0) = R_{db} \quad (5.2)$$

where EGP_b and R_{db} are basal EGP and R_d, GE^L and GE^D are the liver and disposal glucose effectiveness, S_I^L and S_I^D are liver and disposal insulin sensitivity, respectively. X' is the delayed insulin action (deviation from basal) defined as

$$\dot{X}'(t) = -p_2 \cdot X'(t) + p_2 \cdot [I(t) - I_b] \qquad X(0) = 0 \qquad (5.3)$$

where p_2 is the speed of rise and decay of insulin action.
Moreover, combining Eqs. 5.1 and 5.2, a model describing the net effect of insulin and glucose on both disposal and production is obtained

$$R_d(t) = EGP(t) + GE^{TOT} \cdot [G(t) - G_b] + S_I^{TOT} \cdot X'(t)G(t)$$
$$R_d(0) = EGP_b \quad (5.4)$$

where $GE^{TOT} = GE^{L} + GE^{D}$ and $S_I^{TOT} = S_I^{L} + S_I^{D}$. By integrating Eq. 5.3 describing insulin action and assuming that at the end of the perturbation the insulin system returns at the pretest steady state, the following expression is obtained

$$\int_0^\infty X(t)dt = \int_0^\infty [I(t) - I_b]dt \tag{5.5}$$

whereas integrating Eqs. 5.1, 5.2 and 5.4 we obtain, rescpectively

$$S_I^L \cdot \int_0^\infty X(t)dt = \int_0^\infty \frac{-\Delta EGP(t) - GE^L \cdot \Delta G(t)}{G(t)}dt \tag{5.6a}$$

$$S_I^D \cdot \int_0^\infty X(t)dt = \int_0^\infty \frac{\Delta R_d(t) - GE^D \cdot \Delta G(t)}{G(t)}dt \tag{5.6b}$$

$$S_I^{TOT} \cdot \int_0^\infty X(t)dt = \int_0^\infty \frac{R_d(t) - EGP(t) - GE^{TOT} \cdot \Delta G(t)}{G(t)}dt \tag{5.6c}$$

Thus, substituting Eq. 5.5 into Eqs. 5.6, the following expression for liver, disposal and total insulin sensitivity are obtained

$$S_{I,TT}^L = \frac{\int_0^\infty \frac{-\Delta EGP(t) - GE^L \cdot \Delta G(t)}{G(t)}dt}{\int_0^\infty [I(t) - I_b]dt} \tag{5.7a}$$

$$S_{I,TT}^D = \frac{\int_0^\infty \frac{\Delta R_d(t) - GE^D \cdot \Delta G(t)}{G(t)}dt}{\int_0^\infty [I(t) - I_b]dt} \tag{5.7b}$$

$$S_{I,TT}^{TOT} = S_{I,TT}^L + S_{I,TT}^D = \frac{\int_0^\infty \frac{R_d(t) - EGP(t) - GE^{TOT} \cdot \Delta G(t)}{G(t)}dt}{\int_0^\infty [I(t) - I_b]dt} \tag{5.7c}$$

where the subscript "TT" indicates that these indices are derived from the fluxes measured with the triple tracer approach.

As can be observed in Eqs. 5.7, calculation of liver, disposal and net insulin sensitivity from postprandial glucose fluxes, requires values for GE^{L}, GE^{D} and GE^{TOT} which are generally fixed to population values [21, 33] since individual estimates are not available.

5.2.2 Insulin sensitivity from plasma glucose and insulin data

In this Section a method for the estimation of S_I, in healthy subjects, based on plasma glucose and insulin data [21] is presented. The method is based on an integral formula obtained coupling the classical minimal model of glucose kinetics [6] with a simple mathematical description of glucose absorption from the gastrointestinal tract.
During an oral test (e.g. a meal) the food is ingested and nutrients, including glucose, encounter the systemic circulation only after absorption from the gastrointestinal tract and passage through the liver. The general formu-

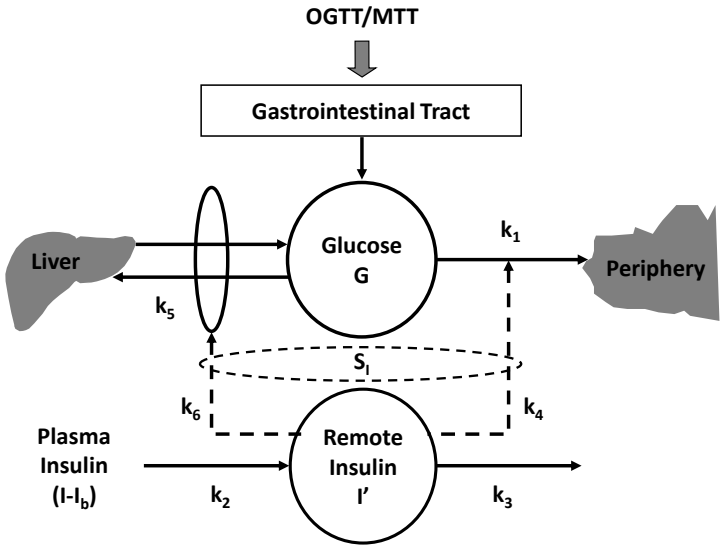

Figure 5.2: Classic representation of the minimal model [6] where the k_i are linked to p_i of Eq. 5.8 as follows: $p_1 = k_1 + k_5$, $p_2 = k_3$ and $p_3 = k_2 \cdot (k_4 + k_6)$. I' is remote insulin related to X as $X = (k_4 + k_6) \cdot I'(t)$. R_a is the rate of appearance of glucose in plasma after oral ingestion.

lation of the oral minimal model [30], making explicit the rate of appearance of exogenous glucose (Fig. 5.2), yields

$$\begin{cases} \dot{G}(t) = -[p_1 + X(t)] \cdot G(t) + p_1 \cdot G_b + \frac{R_a(t)}{V} & G(0) = G_b \\ \dot{X}(t) = -p_2 \cdot X(t) + p_3 \cdot [I(t) - I_b] & X(0) = 0 \end{cases} \tag{5.8}$$

where G is glucose concentration, X is insulin action, I is insulin plasma concentration, R_{a} is the generic expression for the rate of appearance of glucose in plasma, V is the volume distribution, suffix "b" denotes basal (pretest) values, p_1 is the fractional (i.e. per unit distribution volume) glucose effectiveness (GE) measuring glucose ability per se to promote glucose disposal and inhibit glucose production, p_2 is the speed of rise and decay of insulin action and p_3 is a scale factor governing the size of insulin action.
In [21], R_{a} is represented as an anticipated version of glucose excursion above basal

$$\Delta\dot{G}(t) = -a \cdot \Delta G(t) + b \cdot R_a(t) \tag{5.9}$$

where a is a parameter governing the delay and smoothness of ΔG (glucose excursion above basal) with respect to R_{a}, and b is s scale factor. Substituting the expression of Eq. 5.9 into Eq. 5.8 one obtains

$$\begin{cases} \dot{G}(t) = -[p_1 + X(t)] \cdot G(t) + p_1 \cdot G_b + \frac{a \cdot \Delta G(t) + \cdot \Delta\dot{G}(t)}{bV} & G(0) = G_b \\ \dot{X}(t) = -p_2 \cdot X(t) + p_3 \cdot [I(t) - I_b] & X(0) = 0 \end{cases} \tag{5.10}$$

By integrating the the second differential equation of Eq. 5.10 and assuming that at the end of the perturbation the insulin system returns at the pretest steady state, the following expression for $\mathrm{S_I}$ is obtained

$$S_I = \frac{p_3}{p_2} \cdot V = \frac{\int_0^\infty X(t)dt}{\int_0^\infty [I(t) - I_b]dt} V \tag{5.11}$$

By integrating the first differential equation of Eq. 5.10 we obtain

$$\int_0^\infty X(t)dt = \left(\frac{a}{b \cdot V} - p_1\right) \int_0^\infty \frac{\Delta G(t)}{G(t)} dt + \left(\frac{1}{b \cdot V} - 1\right) \int_0^\infty \frac{\Delta\dot{G}(t)}{G(t)} dt \tag{5.12}$$

Assuming that at the end of the perturbation the glucose system returns at the pretest steady state, which is a valid assumption especially in healthy subjects, we obtain that the second integral in the right member is zero. Moreover, assuming that the ratio a/b is proportional to the amount of gluc-

ose absorbed during the test one obtains

$$\frac{a}{b} = \frac{\int_0^\infty R_a(t)dt}{\int_0^\infty \Delta G(t)dt} = \frac{{}^{(f\cdot D)}/_{BW}}{\int_0^\infty \Delta G(t)dt} \tag{5.13}$$

where the integral of R_a is expressed as a fraction f of the amount of glucose D per body weight (BW) that has reached the systemic circulation and $p_1 \cdot V$ is the glucose effectiveness (GE).
Thus, substituting Eqs. 5.12 and 5.13 into Eq. 5.11, the following expression for insulin sensitivity is obtained

$$S_I = \frac{{}^{(f\cdot D)}/_{BW} \cdot \frac{\int_0^\infty {}^{\Delta G(t)}/_{G(t)}dt}{\int_0^\infty \Delta G(t)dt} - GE \cdot \int_0^\infty \frac{\Delta G(t)}{G(t)}dt}{\int_0^\infty [I(t) - I_b]dt} \tag{5.14}$$

However, particularly when a session physical activity is performed, the case in which glucose exhibits excursions below the pretest basal level has to be considered. Denoting τ_k with $k = 1, \ldots, n$ as the time instants when glucose concentration crosses the baseline level G_b, evaluated by linearly interpolating the glucose samples immediately precede and follow the subject-specific threshold, the description of R_a throughout the experiment has to be accordingly modifying in order to cope with its nonphysiological negative values. Thus R_a, for each $\tau_{k-1} < t < \tau_k$, can be defined as

$$R_a(t) = \begin{cases} \frac{[a\cdot G(t) + \Delta\dot{G}(t)]}{b} & \text{if } G(t) \geq G_b \\ -\frac{[a\cdot G(t) + \Delta\dot{G}(t)]}{b} & \text{if } G(t) < G_b \end{cases} \tag{5.15}$$

Thus, using the same rationale outlined above with R_a described as Eq. 5.15, one has the following expression for $\mathrm{S_I}$

$$S_I = \frac{{}^{(f\cdot D)}/_{BW} \cdot \frac{\int_0^\infty |{}^{\Delta G(t)}/_{G(t)}|dt}{\int_0^\infty |\Delta G(t)|dt} - GE \cdot \int_0^\infty \frac{\Delta G(t)}{G(t)}dt}{\int_0^\infty [I(t) - I_b]dt} \tag{5.16}$$

As can be observed in Eq. 5.16, calculation of S_I requires values both for GE and f which generally are fixed to population values [21, 30] since individual estimates are not available.

5.3 Quantification of exercise effect on insulin sensitivity

Exercise is known to improve insulin action in the postexercise period [51, 52], but quantification of this effect, especially in the postprandial state has been difficult to estimate.
The approach proposed here for the quantification of the effect size of physical activity on postprandial insulin sensitivity relies on calculating S_{I} both in absence and in presence of physical activity. Since at $t = 0$ min the meal was ingested, between $t = 120$ min and $t = 195$ min the exercise session was performed and at $t = 360$ min the experiment ended, two indices of insulin sensitivity can be calculated: one in absence of physical activity (rest), i.e. between $t = 0 - 120$ min, and one in presence of physical activity (overall), i.e. between $t = 0 - 360$ min.
The same rationale is thus extended to insulin sensitivity indices calculated from postprandial glucose fluxes as well as from glucose and insulin data as outlined below.

Insulin sensitivity from postprandial glucose fluxes

Starting from Eqs. 5.7 one can calculate liver, disposal and net insulin sensitivity both in absence and in presence of physical activity:

- $S_{\mathrm{I,TT}}^{\mathrm{rest}}$: calculated for $t = 0 - 120$ min, i.e. integrating Eqs. 5.7 from the beginning of the meal to the beginning of the exercise session, thus

calculating $S_{\mathrm{I,TT}}$ in absence of physical activity:

$$S_{I,TT}^{rest,L} = \frac{\int_0^{120} \frac{-\Delta EGP(t) - GE^L \cdot \Delta G(t)}{G(t)} dt}{\int_0^{120} [I(t) - I_b] dt} \tag{5.17a}$$

$$S_{I,TT}^{rest,D} = \frac{\int_0^{120} \frac{\Delta R_d(t) - GE^D \cdot \Delta G(t)}{G(t)} dt}{\int_0^{120} [I(t) - I_b] dt} \tag{5.17b}$$

$$S_{I,TT}^{rest,TOT} = \frac{\int_0^{120} \frac{R_d(t) - EGP(t) - GE^{TOT} \cdot \Delta G(t)}{G(t)} dt}{\int_0^{120} [I(t) - I_b] dt} \tag{5.17c}$$

- $S_{\mathrm{I,TT}}^{\mathrm{overall}}$: calculated for $t = 0 - 360$ min, i.e. integrating Eqs. 5.7 from the beginning of the meal to the end of experiment, thus calculating $S_{\mathrm{I,TT}}$ in presence of physical activity:

$$S_{I,TT}^{overall,L} = \frac{\int_0^{360} \frac{-\Delta EGP(t) - GE^L \cdot \Delta G(t)}{G(t)} dt}{\int_0^{360} [I(t) - I_b] dt} \tag{5.18a}$$

$$S_{I,TT}^{overall,D} = \frac{\int_0^{360} \frac{\Delta R_d(t) - GE^D \cdot \Delta G(t)}{G(t)} dt}{\int_0^{360} [I(t) - I_b] dt} \tag{5.18b}$$

$$S_{I,TT}^{overall,TOT} = \frac{\int_0^{360} \frac{R_d(t) - EGP(t) - GE^{TOT} \cdot \Delta G(t)}{G(t)} dt}{\int_0^{360} [I(t) - I_b] dt} \tag{5.18c}$$

Insulin sensitivity from plasma glucose and insulin data

Starting from Eq. 5.16 one can calculate net insulin sensitivity both in absence and in presence of physical activity:

- $S_{\mathrm{I}}^{\mathrm{rest}}$: calculated for $t = 0 - 120$ min, i.e. from the beginning of the meal to the beginning of the exercise session, i.e. in absence of physical activity:

$$S_I^{rest} = \frac{{}^{(f^{rest} \cdot D)}/_{BW} \cdot \frac{\int_0^{120} |{}^{\Delta G(t)}/_{G(t)}| dt}{\int_0^{120} |\Delta G(t)| dt} - GE \cdot \int_0^{120} \frac{\Delta G(t)}{G(t)} dt}{\int_0^{120} [I(t) - I_b] dt} \tag{5.19}$$

where f^{rest} represents the fraction of the meal absorbed during the interval $t = 0 - 120$ min (its calculation is described below).

- $S_{\text{I}}^{\text{overall}}$: calculated for $t = 0 - 360$ min, i.e. from the beginning of the meal to the end of experiment, i.e. in presence of physical activity:

$$S_I^{overall} = \frac{{}^{(f^{overall}.D)}/_{BW} \cdot \frac{\int_0^{360} |{}^{\Delta G(t)}/_{G(t)}| dt}{\int_0^{360} |\Delta G(t)| dt} - GE \cdot \int_0^{360} \frac{\Delta G(t)}{G(t)} dt}{\int_0^{360} [I(t) - I_b] dt} \tag{5.20}$$

where f^{overall} represents the fraction of the meal absorbed during the interval $t = 0 - 360$ min (its calculation is described below). However, it is important to remark that this value includes either the rest and the physical activity effect on S_I.

It is worth noting that at $t = 120$ min the meal has not been fully absorbed and this has to be taken into account when calculating the amount of $R_{\text{a meal}}$ which appears in the circulation. In this study, thanks to the triple-tracer technique, we actually estimated the $\text{R}_{\text{a meal}}$ profile. This allowed the calculation of the time-varying fraction of the ingested dose f as the ratio between the area under the $\text{R}_{\text{a meal}}$ curve and the amount of ingested glucose D. For our purpose, we calculated two values for f

$$f^{rest} = \frac{\int_0^{120} R_{a\ meal}}{{}^{D}/_{BW}} \qquad f^{overall} = \frac{\int_0^{360} R_{a\ meal}}{{}^{D}/_{BW}} \tag{5.21}$$

representing the fraction of the glucose dose which appears into systemic circulation from the beginning of the meal to the beginning of exercise (Eq. 5.21, left) and for the whole experiment (Eq. 5.21, right), respectively.

5.4 Results

Data are presented as mean ± SE, if not differently indicated. Student's paired two-sample t-test (significance level set to 5%) was used for comparison. Pearson's correlation was used to evaluate univariate correlation.

Insulin sensitivity indices were averaged on a total of 11 subjects, since an error on the measurement of meal enrichment was reported in one subject. Values obtained at $t = 0$ min were considered as basal.

Insulin sensitivity from postprandial glucose fluxes

In this model, for the calculation of liver, disposal and net insulin sensitivity from postprandial glucose fluxes, one has to fix GE^{L} and GE^{D} to population values. From previous studies [33], we know that the ratio between GE^{L} and GE^{D} to GE^{TOT} can be approximated to $^{1}/_{3}$ and $^{2}/_{3}$, respectively, of total glucose effectiveness (GE^{TOT}), which is generally fixed to population value (0.02 dL/kg/min) according to [21].

In Figure 5.3 average values of rest vs overall liver ($S^{L}_{I,TT}$), disposal ($S^{D}_{I,TT}$) and net ($S^{TOT}_{I,TT}$) insulin sensitivity indices (top) and individual values of rest vs overall net ($S^{rest,TOT}_{I,TT}$ vs $S^{overall,TOT}_{I,TT}$) insulin sensitivity index (bottom) estimated from postprandial glucose fluxes are reported. No significant difference has been found between $S^{rest,L}_{I,TT}$ and $S^{overall,L}_{I,TT}$ (2.56 ± 0.54 vs 3.36 ± 1.26 10^{-4} dL/kg/min per μU/mL, $p>0.05$), while $S^{rest,D}_{I,TT}$ and $S^{rest,TOT}_{I,TT}$ are significantly lower than $S^{overall,D}_{I,TT}$ (13.06 ± 2.79 vs 22.16 ± 4.43 10^{-4} dL/kg/min per μU/mL, $p<0.005$) and $S^{overall,TOT}_{I,TT}$ (15.62 ± 3.27 vs 25.52 ± 5.02 10^{-4} dL/kg/min per μU/mL, $p<0.005$), respectively. Moreover, if one observes the individual estimates of rest vs overall net insulin sensitivity, each $S^{overall,TOT}_{I,TT}$ value is significantly higher than the corresponding $S^{rest,TOT}_{I,TT}$.

These results show that overall insulin sensitivity, i.e. the average of insulin sensitivity during the entire experiment, is $76 \pm 12\%$ higher respect to rest insulin sensitivity and that this effect is due to an enhancement in glucose disposal rather than a further suppression of EGP. In fact, the absence of systematic variation in $S^{L}_{I,TT}$, before and after the exercise session, means that insulin seems do not exert a significant effect on EGP during physical activity. This effect may be due to either, from a modeling point of view, to having fixed to population values the ratio between GE^{L} and GE^{D}, and,

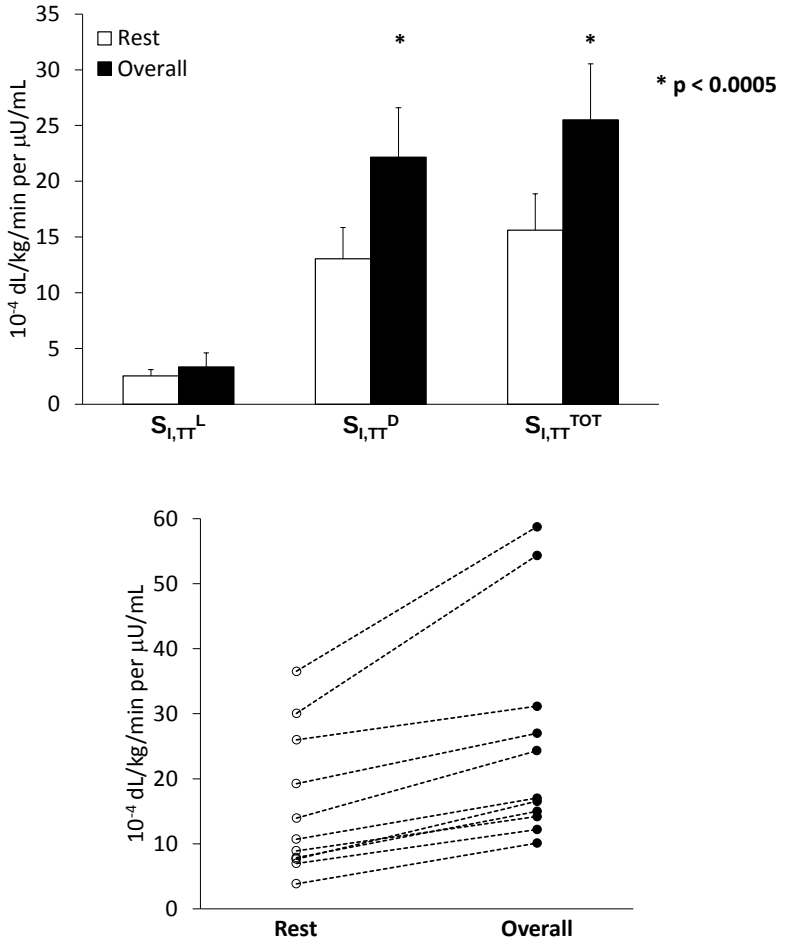

Figure 5.3: Rest vs overall of average values of liver, disposal and net insulin sensitivity indices (top) and of individual values of net insulin sensitivity index (bottom) estimated from postprandial glucose fluxes with the method proposed in Section 5.2.1.

from a physiological point of view, that the inhibitory effect of insulin on EGP is relatively minor compared to the stimulatory effect of glucagon on EGP. On the contrary, a significant effect seems to be exerted by insulin on glucose disposal: even though insulin and glucose rapidly fall, sustained rate of R_d are showed during exercise, possibly due to an increased glucose uptake by insulin-dependent mechanisms. It is known, however, that glucose disposal during and after exercise is also determined by insulin-independent

effects [48, 49, 114, 128], but this method cannot specifically tease out the insulin-independent effects on muscle glucose uptake induced by exercise.

Insulin sensitivity from glucose and insulin data

In this model, for the calculation of net insulin sensitivity from glucose and insulin concentration data, one has to fix GE and f to population values. GE is generally fixed to 0.02 dL/kg/min, according to [21] while f can vary between 0.8 to 0.9, as reported in [21, 29, 30, 32]. In this study, since we actually estimated the $R_{a\ meal}$ profile, we can calculate the value of f. Here high values of $f^{overall}$ have been calculated on average equal to 1.09 ± 0.22. We thus fixed all $f^{overall}$ calculated equal to 1. The same rationale is thus extended also to the calculation of f^{rest}, where each value has been normalized respect to its $f^{overall}$.

In Figure 5.4 average (top) and individual values of rest vs overall net (S_I^{rest} vs $S_I^{overall}$) insulin sensitivity index (bottom) estimated from glucose and insulin concentration data are reported. As can be observed S_I^{rest} is significantly lower than $S_I^{overall}$ (12.83 ± 2.22 vs $21.92 \pm 3.99\ 10^{-4}$ dL/kg/min per μU/mL, $p<0.005$). Moreover, if one observes the individual estimates of rest vs overall net insulin sensitivity, each $S_I^{overall}$ value is higher than the corresponding S_I^{rest}.

These results show that, in agreement with prior results on net insulin sensitivity index calculated from postprandial glucose fluxes ($S_{I,TT}^{TOT}$), $S_I^{overall}$ is $74 \pm 8\%$ higher than S_I^{rest}. At variance with the method proposed above, here the method does not allow to segregate the effect of insulin on glucose production and disposal before, during and after exercise due to the impossibility to tease out the contribution of the two components only using glucose and insulin concentration data. However, it allows to quantify the effects of physical activity on insulin sensitivity just using glucose and insulin concentration data which needed a much simpler protocol respect to the triple-tracer one. As a remark, since GE is fixed to population values, also this method does not allow to tease out the relative contribution of insulin-independent glucose uptake induced by exercise.

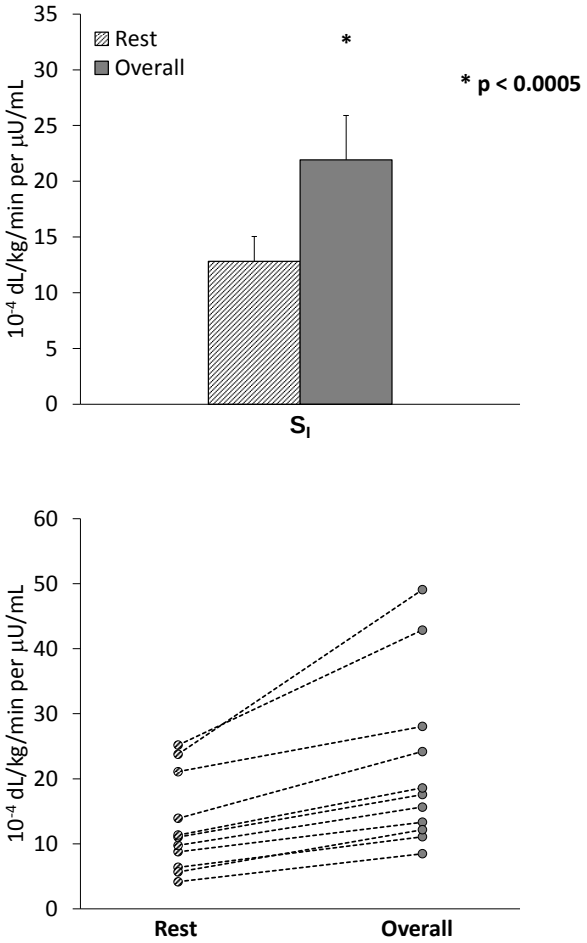

Figure 5.4: Rest vs overall of average (top) and individual (bottom) values of net insulin sensitivity index estimated from glucose and insulin concentration data with the method proposed in Section 5.2.2.

The implemented methods for the quantification of the effect size of exercise on insulin sensitivity calculated from glucose and insulin data and their results have been published in [104].

Comparison

Here the aim is to compare and validate the values of net insulin sensitivity calculated with the formula proposed in Section 5.2.1 with the well-established integral formula proposed in [21]. As a remark, for the calculation of S_I with the method proposed in Section 5.2.2, we have normalized the values of f^{overall} to 1. Thus, in order to do a fair comparison, for the calculation of $S_{I,TT}$ with the method proposed in Section 5.2.1, it is necessary to rescale the $R_{a\ meal}$ profile of each subject in relation to its f^{overall}. For what concerns GE, in both model, it is fixed to population value (0.02 dL/kg/min) according to [21].

In Figure 5.5 comparison between average values (top) of rest vs overall (S_I^{rest} vs $S_{I,TT}^{\text{rest}}$ and S_I^{overall} vs $S_{I,TT}^{\text{overall}}$, respectively) and correlation between rest and overall (bottom) of the two indices calculated (S_I vs $S_{I,TT}$) are reported. Average values of net insulin sensitivity at rest (12.83 ± 2.22 vs 13.97 ± 2.54 10^{-4} dL/kg/min per μU/mL, p=0.06) and overall (21.92 ± 3.99 vs 23.12 ± 3.93 10^{-4} dL/kg/min per μU/mL, p=0.05) net insulin sensitivity indices estimated with the two methods are very similar, even if $S_{I,TT}$ is significant higher than S_I (p=0.0044). However, on average, both rest $S_{I,TT}$ and S_I values are significantly lower respect to their corresponding overall estimates ($p<0.005$). Moreover, we found a very strong correlation (r=0.989, $p \ll 0.005$) between the two indices which allows us to validate the results obtained with the proposed formula.

These results confirmed that for both $S_{I,TT}$ and S_I indices, during a session of moderate-intensity exercise, insulin sensitivity is $77 \pm 12\%$ and $74 \pm 8\%$ higher, respectively. However, it is important to remark that, the overall insulin sensitivity represents the average insulin sensitivity during the entire duration of the experiment, i.e. it accounts for insulin sensitivity before, during and after the session of physical activity. Moreover, with the proposed method, we are able only to quantify an insulin-dependent effects of exercise on glucose uptake while, unfortunately, it is not possible to tease out the relative contribution of the well-established insulin-independent mech-

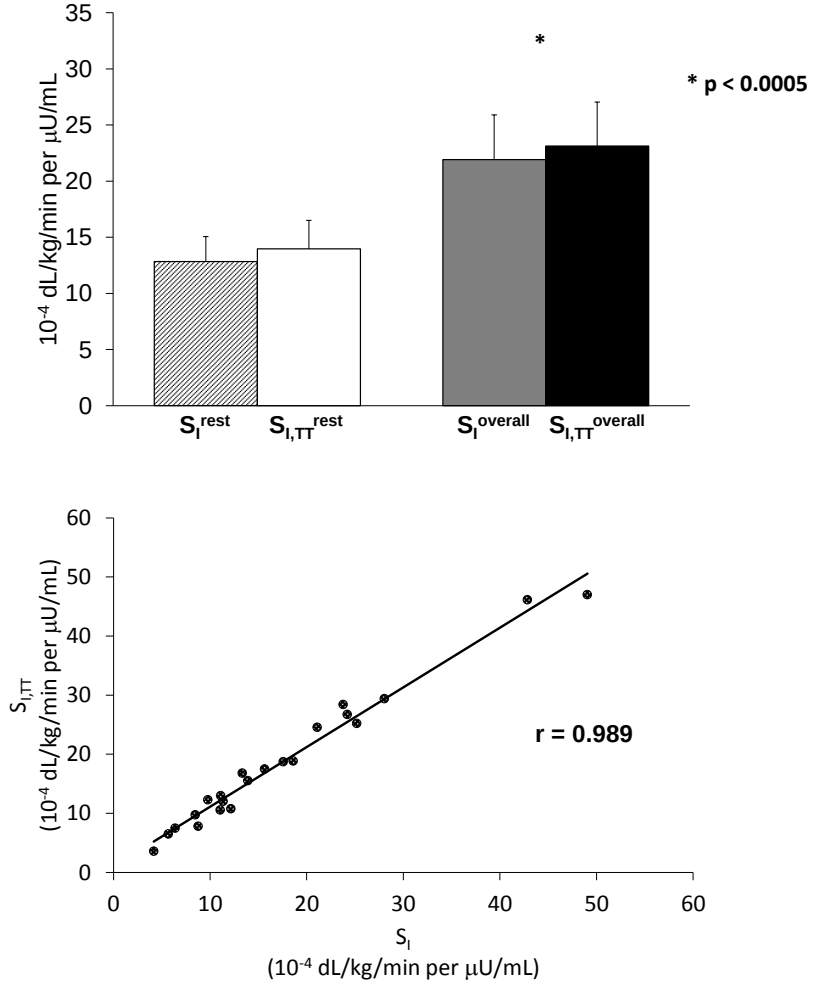

Figure 5.5: Comparison between average rest vs overall (top) of S_I and $S_{I,TT}$ and correlation (bottom) between all S_I and $S_{I,TT}$ values (rest and overall) estimated with the methods proposed in 5.2.1 and 5.2.2, respectively.

anisms induced by exercise, e.g. increase in muscle blood flow [2, 92], capillary recruitment and exercise-induced translocation of GLUT-4 protein [48, 49, 114, 128].

5.5 Use of results

This Section has been realized in collaboration with our clinical partners, exploiting information on the effect of moderate-exercise physical activity in healthy subjects, to suggest an optimization strategy of insulin therapy in T1DM patients during exercise.
Here, an in silico study aimed to assess the effect of moderate-intensity physical activity in T1DM subjects under continuous subcutaneous insulin infusion (CSII) therapy regimen and to propose a strategy for the optimization of subcutaneous insulin infusion rate during exercise. The results presented in Section 5.4, i.e. the almost doubled increase in insulin sensitivity after a session of moderate-intensity physical activity in healthy subjects, have been incorporated in the UVA/Padova T1DM simulator [35, 70] to simulate a session of moderate-intensity physical activity. In order to evaluate the effect of physical activity with different insulin therapy regimens, two in silico experiments, including a session of physical activity, have been performed: one maintaining the insulin infusion rate at the same level used at rest and one with different degrees of reductions and durations of basal insulin infusion rates. Results showed that physical activity markedly affects glucose control and an insulin therapy optimization strategy would be useful to improve diabetes management during exercise.

If the reader is not interested in this particular application, he can skip this paragraph without compromising the understanding of the following chapters.

5.5.1 Introduction

Due to the inability of the pancreas to produce insulin, patients with T1DM use exogenously administered insulin to maintain blood glucose (BG) concentration in the near-normal range (70-180 mg/dL). Severe hypoglycemia can be very dangerous, possibly leading to coma and ultimately to death, while sustained hyperglycemia may cause long-term microvascular and

macrovascular complications. However, BG control is extremely challenging due to the delay between insulin administration and action, physiological perturbations (i.e. meals and physical activity) and intrasubject variability. Thanks to the availability of continuous glucose monitoring (CGM) systems and continuous subcutaneous insulin infusion (CSII) pumps, researchers have focused on the development of a wearable artificial pancreas (AP), a system able to modulate subcutaneous insulin infusion rates automatically based on CGM readings, thus helping in optimally controlling BG [26]. Artificial pancreas prototypes have been tested successfully in inpatient trials, demonstrating reduced occurrence of hypoglycemia with respect to standard therapy, increased time spent in the target range, and reduction of mean glucose [11, 62, 66, 79, 110, 130]. Some of these trials [11, 79] included a session of physical activity in order to test the ability of the control algorithm to deal with the rapid changes in insulin sensitivity due to exercise and prevent the risk of immediate and delayed hypoglycemia associated with daily activity. In standard therapy, subjects usually, but not always, reduce their basal insulin infusion by a given percentage, starting up to 2 h before exercise session, but each patient follows his/her own routine and physician suggestions.
It remains a question if one needs to inform the control algorithm regarding impending physical activity and, if this is the case, the degree and duration of changes to insulin infusion rates in relation to physical activity. In particular, model predictive control algorithms (e.g., [89, 107]) may benefit greatly from the availability of this information because they can use it to predict future glucose level and adjust insulin infusion rates accordingly. The issue is particularly important because maintaining unchanged basal infusion rates in the presence of physical activity often leads to hypoglycemia.

5.5.2 Incorporating the effect of physical activity into the UVA/Padova T1DM simulator

In this Section the inclusion of the effect of physical activity in the UVA/Padova T1DM simulator, by using the results shown in Section 5.4,

is presented.

The UVA/Padova T1DM simulator

The UVA/Padova T1DM simulator [35, 70] is a tool accepted by the Food and Drug Administration as a substitute for preclinical trials of certain insulin treatments, including closed-loop control algorithms (Figure 5.6). It describes the glucose dynamics during a meal by putting in relation plasma glucose, insulin, and glucagon concentrations with glucose fluxes (endogenous glucose production, glucose rate of appearance, glucose utilization, renal excretion), insulin fluxes (rate of insulin appearance from subcutaneous tissue, insulin degradation), and glucagon fluxes (glucagon secretion, glucagon degradation). However, the effect of physical activity was not yet been included in the simulator.

The primary effect of physical activity is to enhance glucose utilization by the tissues [17] (Figure 5.6, red arrow). The model of glucose utilization currently implemented in the simulator assumes that glucose kinetics are described by two compartments, that insulin-independent glucose utilization by the brain and the erythrocytes takes place in the first compartment (plasma and rapidly equilibrating tissues) and is constant, while insulin-dependent glucose utilization (U_{id}) takes place in the remote compartment (slowly equilibrating tissues) and depends nonlinearly from glucose in the tissues: insulin system returns at the pretest steady state, the following expression is obtained

$$U_{id}(t) = \frac{[V_{m0} + V_{mX} \cdot X(t) \cdot (1 + r_1 \cdot risk)] \cdot G_t(t)}{K_{m0} + G_t(t)} \tag{5.22}$$

where $G_t(t)$ is glucose mass in the peripheral compartment; V_{m0}, V_{mX}, K_{m0}, and p_{2U} are model parameters; and, in particular, V_{mX} represents insulin sensitivity, i.e., the ability of insulin to stimulate glucose utilization. Insulin action $X(t)$ on glucose utilization is described by

$$\dot{X}(t) = -p_{2U} \cdot X(t) + p_{2U} \cdot [I(t) - I_b] \tag{5.23}$$

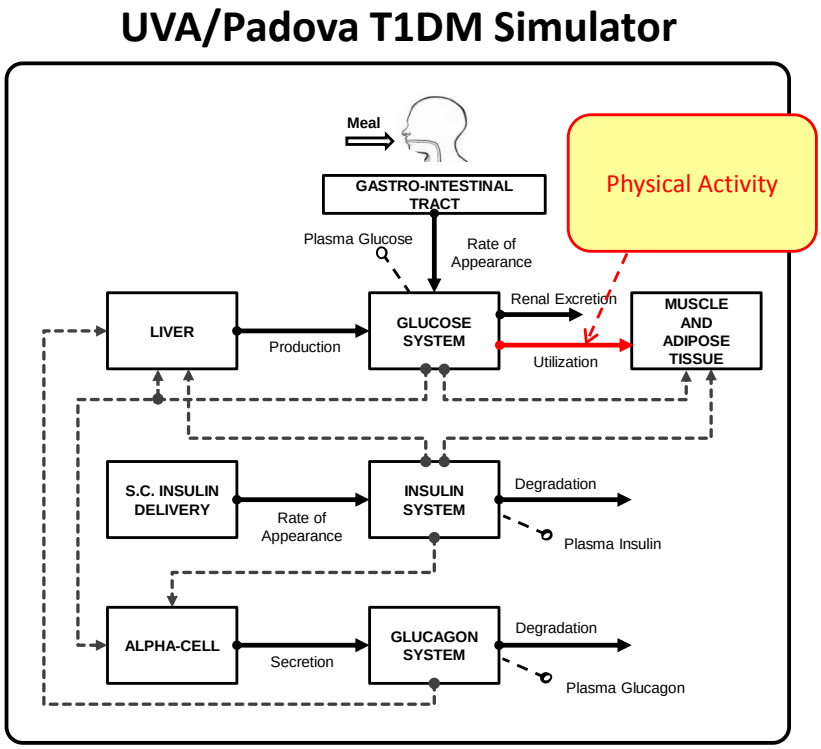

Figure 5.6: The new version of T1DM simulator [35] with the effect of physical activity evidenced. S.C. stays for subcutaneous.

where p_{2U} is the rate constant of insulin action on the peripheral glucose utilization and $I(t)$ is plasma insulin concentration (suffix b denotes basal state). Moreover, to describe insulin action in the hypoglycemic range, $X(t)$ is modulated by the glucose risk function [69]:

$$risk = \begin{cases} 0 & \text{if } G \geq G_b \\ 10 \cdot [f(G)]^2 & \text{if } G_{th} \leq G < G_b \\ 10 \cdot [f(G_{th})]^2 & \text{if } G < G_{th} \end{cases} \tag{5.24}$$

with G_b the basal glucose, G_{th} the hypoglycemic threshold (set at 60 mg/dL), and

$$f(G) = log\left(\frac{G}{G_b}\right)^{r_2} \tag{5.25}$$

with r_1 and r_2 model parameters.
Please refer to [35] for more details on the complete set of model equations.

Modeling the effect of physical activity

Results presented in Section 5.4 showed that insulin sensitivity in healthy subjects, after a moderate-intensity session of physical activity ($S_I^{overall}$), almost doubled respect to the rest value (S_I^{rest}). However, $S_I^{overall}$ is basically the average of S_I in the entire duration of the experiment. To single out the actual value of S_I during exercise (S_I^{ex}), one can assume that S_I is equal to S_I^{rest} for $t \leq 120$, equal to S_I^{ex} for $120 < t \leq 195$ and decreases linearly from S_I^{ex} to S_I^{rest} in $195 < t \leq 360$ (Figure 5.7, top panel, pink line). With this assumption, the average S_I during the whole experiment ($S_I^{overall}$) can be calculated by integrating the S_I profile of Figure 5.7 from t_{meal} and t_{end} and dividing it by the length of the integration interval ($t_{end} - t_{meal}$):

$$S_I^{overall} = \frac{S_I^{rest} \cdot (t_{ex,start} - t_{meal}) + S_I^{ex} \cdot (t_{ex,end} - t_{ex,start}) + \frac{(S_I^{ex} + S_I^{rest}) \cdot (t_{end} - t_{ex,end})}{2}}{(t_{end} - t_{meal})} \tag{5.26}$$

thus

$$S_I^{rest} \cdot (t_{ex,start} - t_{meal}) + S_I^{ex} \cdot (t_{ex,end} - t_{ex,start}) + \frac{(S_I^{ex} + S_I^{rest}) \cdot (t_{end} - t_{ex,end})}{2} = S_I^{overall} \cdot (t_{end} - t_{meal}) \tag{5.27}$$

Moreover, assuming that S_I^{ex} is $\alpha \cdot S_I^{rest}$ and, as reported in Chapter 5, approximating $S_I^{overall}$ as twice S_I^{rest}, we can explicitly calculate α from

$$S_I^{rest} \cdot (t_{ex,start} - t_{meal}) + \alpha \cdot S_I^{rest} \cdot (t_{ex,end} - t_{ex,start}) + \frac{(1 + \alpha) \cdot S_I^{rest}) \cdot (t_{end} - t_{ex,end})}{2} = 2 \cdot S_I^{rest} \cdot (t_{end} - t_{meal}) \tag{5.28}$$

where t_{meal} and t_{end} are time of the meal and time of the end of experiment, while $t_{ex,start}$ and $t_{ex,end}$ are time of the start and end of the exercise session, respectively, obtaining $\alpha = 3.29$. This approximation, i.e. the nonphysiological step increase in insulin sensitivity, is acceptable as far as the duration of the experiment is much longer than the time constant of exercise action on glucose utilization. However, simulations can be redefined if a reliable physiological model is formulated.

Finally, this effect of exercise on glucose dynamics was incorporated into the

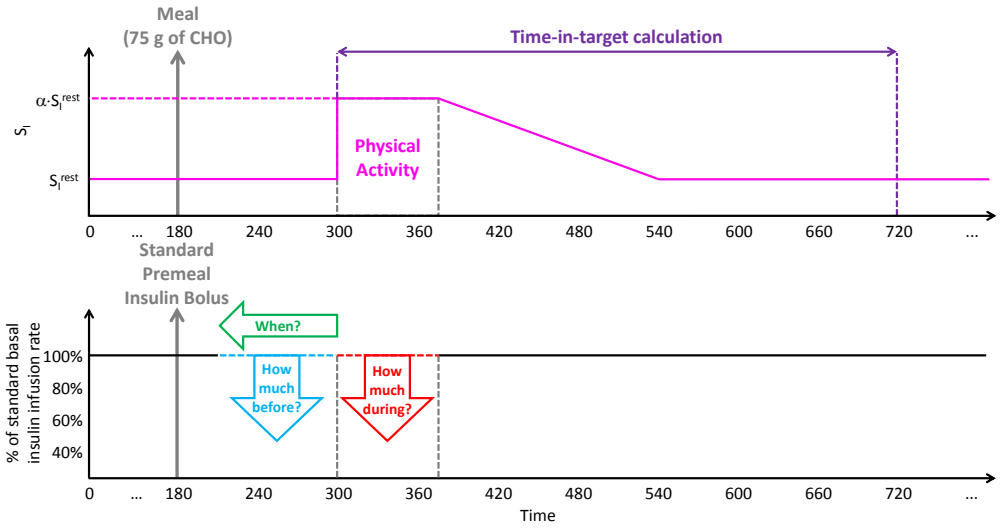

Figure 5.7: Simulation scenario mimicking the experimental protocol reported in Chapter 3 (top) with the exercise session (pink line). Standard premeal insulin bolus given at mealtime and basal insulin infusion rate adjustments, with respect to the patient's profile, during (red arrow) and/or before (blue and green arrows) the exercise session (bottom). CHO stays for carbohydrate.

UVA/Padova T1DM simulator by modifying accordingly the parameter V_{mX}, while all other parameters are maintained fixed to standard UVA/Padova T1DM population parameters. However, as previously discussed, it is well-known that physical activity also stimulates non-insulin mediated glucose transport, but with the method proposed in Chapter 5 the contribution of this insulin-independent effect of physical activity has not yet been quantitatively assessed, and thus it is not possible at this time to simulate the relative contributions of insulin-dependent and insulin-independent effects on glucose

utilization.

5.5.3 In silico experiments

The simulation scenario, mimicking the experimental protocol described in Chapter 3, consists of a meal (containing 75g of carbohydrates) administered 3 h after the start of the experiment to 100 in silico adults with T1DM. The exercise session was simulated to start 2 h after the meal and to last 75 min (Figure 5.7, top panel). The simulation of the exercise session was obtained by modifying parameter V_{mX} as shown in Figure 5.7 (top panel, pink line). The virtual subjects received a standard premeal insulin bolus based on each individual's insulin-to-carbohydrate ratio, while basal insulin infusion rate was first maintained fixed to patient basal profile (Experiment 1) and then decreased in various degrees and durations in relation to usual basal insulin infusion rates (Experiment 2).
The optimization strategy aims to explore, in a simulation context, the best combination of basal insulin infusion rate before and during physical activity that would prevent hypoglycemia during and after exercise.

Experiment 1

The virtual subjects received their own basal insulin profile, a subject-specific constant insulin infusion rate able to maintain glucose at steady state in the absence of external disturbances such as meals and physical activity. This provided the worst-case scenario to which to compare the simulation results of Experiment 2.

Experiment 2

The virtual subjects received their own basal insulin profile lowered by step reductions of 10% during and/or before the exercise session to prevent hypoglycemia (Figure 5.7, bottom panel), while outside these ranges, they

received constant rates of basal insulin infusion. In particular, before the exercise session, step reductions of basal insulin rates ranging from 10% to 60%, with a 10% step, starting 90, 60, and 30 min before the beginning of the exercise (Figure 5.7, bottom panel, blue and green arrows)were simulated. During the exercise, reductions ranging from 10% to 60% with a 10% step have been tested, lasting for the entire exercise duration (Figure 5.7, bottom panel, red arrow). Outside these time intervals, basal insulin infusion rate was maintained constant and equal to the patient's basal insulin profile (Figure 5.7, bottom panel, black line).

5.5.4 Results

Results are presented as mean ± SD. Safety (reduction of hypoglycemia) and efficacy (attenuation of hyperglycemia) of different simulated adjustments to basal insulin infusion rates have been assessed by using the control-variability grid analysis (CVGA) [81] and by computing the time spent in the target range of 90-140 mg/dL. For this calculation, simulated glucose profiles from the start of exercise session to 7 h later, i.e., 3 h after that V_{mX} has returned to its rest value (Figure 5.7, top panel) were used.

Experiment 1

Simulated plasma glucose concentrations in the 100 T1DM virtual subjects are shown in Figure 5.8 (top-left panel). As expected, most of the subjects experienced hypoglycemia (defined as glucose concentration below 70 mg/dL), with several of them having severe hypoglycemic episodes (defined as glucose concentration below 50 mg/dL). This is confirmed by the CVGA (Figure 5.8, bottom-left panel), which shows 15% of the subjects in the lower C zone, 73% in the lower D zone, no subject in the A zone, and only 12% of the subjects in the B zone. The average time in target was $28.8 \pm 16.1\%$.

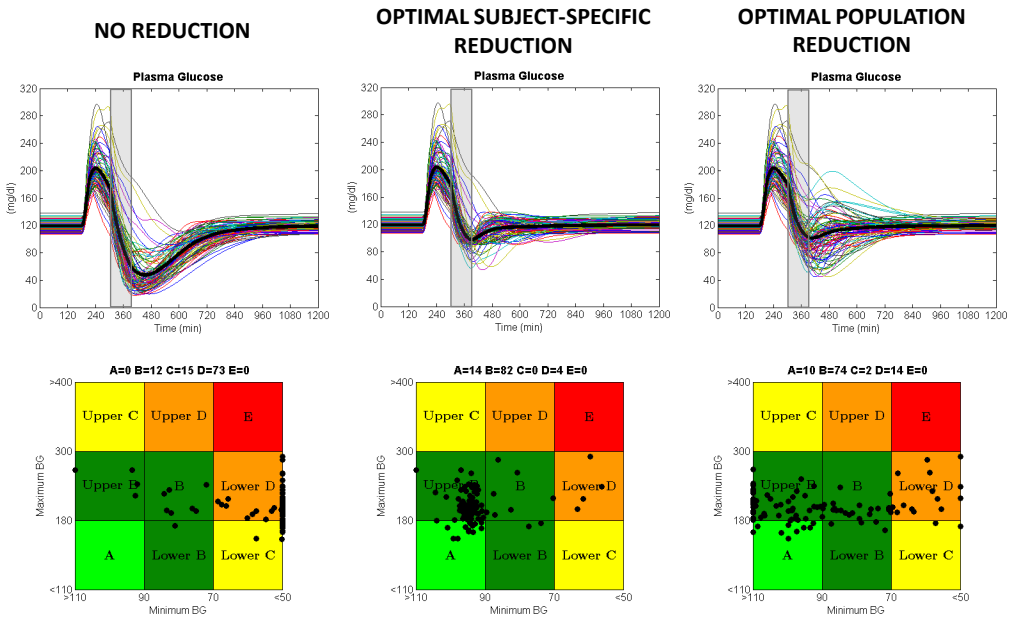

Figure 5.8: Simulated plasma glucose concentrations (top panel) and CVGA (bottom panel) in the 100 T1DM virtual subjects: no basal insulin infusion rate adjustment (left panel), optimal mobination of subject-specific adjustments (middle panel) and optimal combination of population (on average) adjustments (right panel). Shaded box represents the exercise period.

Experiment 2

The distribution of the optimal combination of basal reductions in the 100 in silico subjects are shown in Figure 5.9. Most of the subjects needed to reduce their basal insulin of 60% (middle panel) from 90 min before the start of exercise (Figure 5.9, left panel) and maintain this reduction until the end of the physical activity (Figure 5.9, right panel). However, there is large intersubject variability, and the optimal reduction strategy is different from the one described earlier in a significant proportion of subjects. Therefore, ideally, one should apply a personalized strategy to each subject. In this case, in fact, simulations show that the average time in target increases to $90.2 \pm 11.4\%$ and that 96% of the subjects does not experience hypoglycemia (Figure 5.8, top-middle panel) while the remaining 4% only shows mild hypoglycemia episodes (plasma glucose between 50 and 70 mg/dL). This is also confirmed

by the CVGA (Figure 5.8, bottom-middle panel), which shows 14% of the subjects in zone A, 82% in zone B, and only 4% in lower zone D.

Unfortunately, a patient-specific optimal basal reduction strategy is not

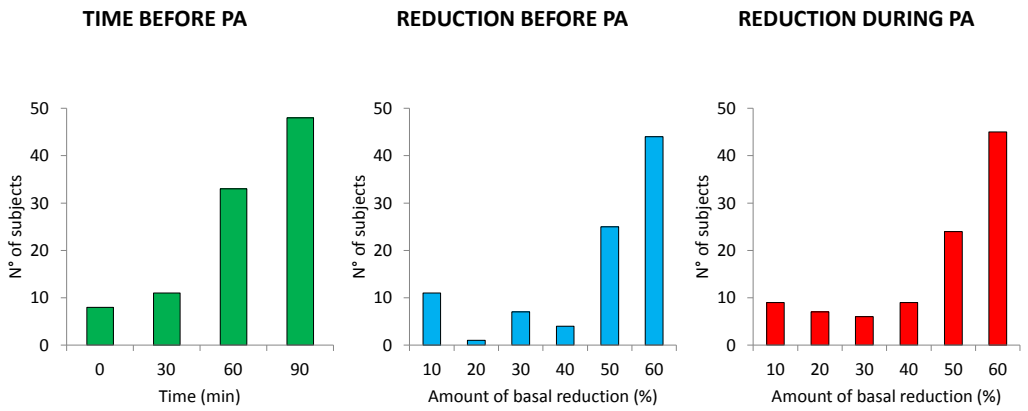

Figure 5.9: Distribution of the optimal subject-specific combination of basal reductions in the 100 T1DM virtual subjects: time before the start of physical activity (left), reduction before physical activity (middle) and reduction during physical activity (right). PA stays for physical activity.

always available. The simulation results can provide some guidelines in case this patient-specific information is missing. The basal reduction pattern that maximizes efficacy and safety in all the 100 in silico subjects, using as a metric the time spent in the target range of 90-140 mg/dL, was selected. In this case, a 30% reduction of basal insulin rates during physical activity, preceded by 50% reduction starting 90 min before the start of physical activity, is the combination that most effectively guarantees safety and efficacy in most of the 100 in silico population. As a matter of fact, if this adjustment is applied to all virtual subjects, average time in target is $72.7 \pm 23.5\%$. The glucose-simulated profiles are shown in Figure 5.8 (top-right panel), with 84% of the subjects avoiding hypoglycemia. This was confirmed by the CVGA (Figure 5.8, bottom-right panel): 10% of the subjects lie in the A zone, 74% in the B zone, 14% in the lower D zone, and 2% in the lower C zone.

5.5.5 Conclusions

In standard open-loop therapy, subjects usually, but not always, reduce their basal insulin infusion rates in order to prevent the risk of hypoglycemia due to the rapid change in insulin sensitivity caused by exercise. In closed-loop therapy, the need to inform control algorithms regarding impending physical activity, in order to appropriately reduce insulin infusion rates and prevent hypoglycemia both during and after exercise, remains debatable.
Here, the results obtained in Section 5.4 on the quantification of the effect size of physical activity on insulin sensitivity have been incorporated into the UVA/Padova T1DM simulator. In order to evaluate the effect exercise on insulin therapy, two in silico experiments, including an exercise session, have been simulated: one maintaining subject-specific basal insulin infusion profile and another with varying degrees of reductions and durations of basal insulin infusion rates. As expected, physical activity markedly affects glucose control and most of the virtual subjects (88%) experienced hypoglycemia when no announcement of upcoming physical activity was provided. On the other hand, if the information on modifications to basal insulin infusion rates during physical activity is provided to the algorithm, then the safest and most effective "generic" reduction of basal insulin rates (16% of hypoglycemic events) is a 30% reduction during physical activity, preceded by 50% reduction starting 90 min before the start of physical activity.
These results suggests that any control algorithm would benefit by knowing in advance that physical activity is impending to reduce the risk of hypoglycemia, because the large delay between subcutaneous insulin infusion and its effect on plasma glucose concentration preclude the possibility of simply stopping subcutaneous basal insulin infusion when physical activity is detected. Moreover, here, if patient-specific basal insulin reduction pattern is not available, a "generic" basal reduction strategy is proposed that has been proved to be rather safe and effective.

The simulation study and its results have been published in [105].

6 Models to Assess the Effect of Exercise on Glucose Kinetics

6.1 Introduction

It is well established that physical activity increases rates of glucose uptake (R_d) and numerous factors determine this effect during and after exercise. One of the most important regulatory responses is an increase in blood flow [2, 92] to the contracting skeletal muscles. Moreover, it was found that exercise increases glucose uptake in skeletal muscle through the translocation of GLUT-4 isoform from an intracellular compartment to the surface of the cell [48, 49, 114, 128] and increasing its transcription [39, 95], and this effect has been demonstrated to be independent of insulin [88, 91, 97, 123]. Then, in addition to the acute effects of exercise to increase muscle glucose uptake, the postexercise period has been characterized by muscle being more sensitive to the action of insulin [51, 52], even if the mechanisms are still under investigation.

Thus, the effect of physical activity on glucose kinetics, although qualitatively well established from a physiological point of view, has been difficult to quantify. As shown in the literature, the parameters of the minimal model of glucose kinetics can change significantly during and after physical activity [10, 13, 38]. For instance, in [38] a simple mathematical approach is presented, roughly illustrating the effect of physical activity in increasing glucose

uptake and improving insulin sensitivity. In [10] this model was used in T1DM subjects during an euglyemic-hyperinsulinemic clamp and expanded in order to link these effects to heart rate signal. This model was further extended in [34] to take into account for physical activity duration and intensity. However, as reported in [10], some important observed dynamics have not been addressed due to the lack of experimental data. Thus, to the best of our knowledge, a model quantitatively describing the effect of physical activity on postprandial glucose kinetics has never been developed and this is an important practical issue since many people, with and without diabetes, exercise a few hours after a meal.

In this Chapter the development of a model to assess the effect of physical activity on glucose kinetics is presented. To do that, a good model of glucose kinetics in the specific experimental conditions described in Chapter 3 is presented. Then, using the knowledge on exercise physiology presented in Chapter 2, a battery of models of system, incorporating the effect of physical activity, will be tested against data. Finally, the selection of the best models on the basis of standard criteria [24] will be discussed.

6.2 Models of glucose kinetics

In order to develop a model of the effect of physical activity on glucose kinetics, first a model describing the glucose-insulin system at rest is required. As a remark, thanks to the availability of virtually model-independent estimates of $R_{a\ meal}$ and EGP, we can focus specifically on modeling the effect of physical activity on glucose utilization without describing its action, if any, on $R_{a\ meal}$ and EGP.

The first model considered was a single-compartment labeled glucose minimal model presented in [31]. This model exploits $R_{a\ meal}$ as known input and it is identified from G_{meal}, i.e. the exogenous glucose deriving from the

meal, and insulin data. For our purpose, the same model can be identified on total glucose data by using $R_{a\ meal}$ and EGP as known inputs, i.e. the total rate of glucose appearance.

However, as previously discussed in Chapter 4, the rapid variations on glucose kinetics introduced by physical activity make this model inadequate to describe glucose kinetics also during MTT/OGTT. As already reported for the more rapid IVGTT perturbation, in this particular experimental conditions, a two-compartment model better describes glucose kinetics [19, 20]. This last model has been used to accurately assess glucose metabolism in a single individual during labeled-IVGTT [120].

The model (Figure 6.1) is reported below in its uniquely identifiable para-

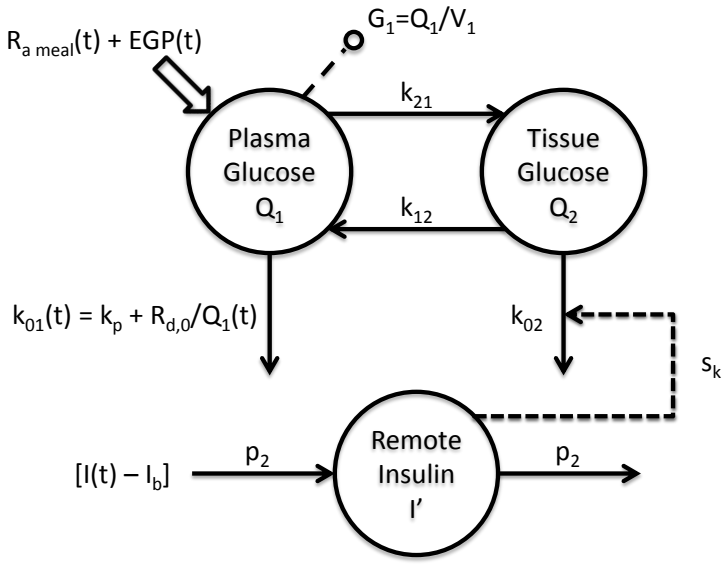

Figure 6.1: The two-compartment minimal model in its uniquely identifiable parameterization. Q_1 and Q_2, glucose masses in the first (accessible pool) and second (slowly equilibrating) compartments, respectively; I', concentration of insulin remote from plasma; G, plasma glucose concentration; $R_{a\ meal}$ and EGP rate of meal glucose appearance and endogenous glucose production, respectively; V_1, volume of the accessible pool; $R_{d,0}$, constant component of glucose disposal that accounts for inhibition of glucose clearance by glucose itself; k_p, proportionality constant; k_{21}, k_{12} and k_{02}, glucose kinetic parameters; p_2 and s_k, insulin action parameters. Adapted from [120].

meterization

$$\begin{cases} \dot{Q}_1(t) = -\left[k_p + \frac{R_{d,0}}{Q_1(t)} + k_{21}\right] Q_1(t) + k_{12} Q_2(t) + EGP(t) + R_{\text{a meal}}(t) \\ \qquad\qquad\qquad\qquad\qquad\qquad\qquad\qquad Q_1(0) = G_b \cdot V_1 \\ \dot{Q}_2(t) = k_{21} Q_1(t) - \left[k_{02} + X(t) + k_{12}\right] Q_2(t) \\ \qquad\qquad\qquad\qquad\qquad\qquad\qquad\qquad Q_2(0) = \frac{k_{21}}{k_{02}+k_{12}} G_b \cdot V_1 \\ \dot{X}(t) = -p_2\{X(t) + s_k[I(t) - I_b]\} \\ \qquad\qquad\qquad\qquad\qquad\qquad\qquad\qquad X(0) = 0 \\ G(t) = \frac{Q_1(t)}{V_1} \end{cases} \tag{6.1}$$

where $Q_1(t)$ and $Q_2(t)$ denote glucose masses in the first (plasma plus insulin-independent tissues, rapid equilibrating with plasma) and the second compartment (insulin-dependent or slowly equilibrating tissues) compartments, respectively (mg/kg); G_b is the basal glucose concentration (mg/dL); $X(t) = s_k \cdot I'(t)$ is insulin action (min^{-1}), where $I'(t)$ is the concentration of insulin remote from plasma (μU/mL); $I(t)$ and I_b are plasma insulin and basal insulin, respectively (μU/mL); $G(t)$ is plasma glucose concentration (mg/dL); $\text{R}_{\text{a meal}}$ and EGP are the rate of meal glucose appearance and endogenous glucose production, respectively (mg/kg/min); V_1 is the volume of the accessible compartment (dL/kg); $R_{d,0}$ is the constant component of glucose disposal (mg/kg/min) [20, 119] whereas k_p (min^{-1}) is the proportionality constant between glucose disposal from the accessible compartment and glucose mass in the same compartment; k_{21} (min^{-1}), k_{12} (min^{-1}) and k_{02} (min^{-1}) are parameters describing glucose kinetics; and p_2 (min^{-1}) and s_k (mL/μU/min) are parameters describing insulin action.

Glucose disposal from the accessible pool is the sum of two components, one constant ($R_{d,0}$) and the other proportional to glucose mass Q_1 (k_p), thus accounting for inhibition of glucose clearance by glucose itself. Glucose disposal from the slowly equilibrating pool is the sum of two components both proportional to glucose mass in the second compartment, Q_2, one insulin-independent (k_{02}) and one insulin-dependent, this last assumed to be

controlled by insulin in a remote compartment (X). Achieving the a priori unique identifiability of the model requires two assumptions [20]: first, in normal subjects, in the basal stead state, insulin-independent glucose disposal is three times insulin-dependent glucose disposal [23] leading to an additional relation among the model parameters:

$$k_p + \frac{R_{d,0}}{G_b V_1} = 3 \cdot \frac{k_{21} k_{12}}{k_{02} k_{12}} \tag{6.2}$$

The second assumption in [120] is that $R_{d,0}$ is fixed to 1 mg/kg/min [7]. The uniquely identifiable parameterization, as shown in [20], is thus V_1, k_{21}, k_{12}, k_{02}, p_2 and s_k.
However, these model assumptions do not guarantee positive values for parameters k_p in all circumstances, in fact this parameter is positive only if the component $R_{d,0}$, which is fixed equal in all subjects (see above), is lower than the steady-state value of glucose disposal from the accessible compartment. Thus, to ensure positive values of k_p, in [115] a new description of the constraint on $R_{d,0}$ is formulated which puts it in relation with the total glucose disposal in steady state (R_d^{ss}). In particular, it is assumed that $R_{d,0}$ account for a fixed fraction of R_d^{ss}:

$$R_{d,0} = \alpha R_d^{ss} \tag{6.3}$$

where α is constant among individuals. Values of $R_{d,0}$ and R_d^{ss} measured in a group of nondiabetic subjects [3] suggested to fix $\alpha = 0.465$. The new assumption in Eq. 6.3, while still ensuring a priori identifiability of the model structure, is also able to guarantee positive values of k_p obtaining

$$k_p = \frac{k_{21} k_{12}}{k_{02} k_{12}} (3 - 4\alpha) \tag{6.4}$$

Finally, the model allows the estimation of:

- *Glucose effectiveness* (GE^*, dL/kg/min) which quantifies the ability of glucose to promote its own disposal at steady state

$$GE^* = \left. \frac{\partial R_d(t)}{\partial G(t)} \right|_{ss} = \left(k_p + \frac{k_{21} k_{12}}{k_{02} k_{12}} \right) V_1 \tag{6.5}$$

where the symbol "*" indicates that this is glucose effectiveness on glucose disposal only.

- *Plasma clearance rate* (PCR, dL/kg/min) which measures glucose disposal at basal steady state, per unit glucose concentration

$$PCR = \frac{R_d^{ss}}{G_b} = \Big(k_p + \frac{R_{d,0}}{V_1 G_b} + \frac{k_{21}k_{12}}{k_{02}k_{12}}\Big)V_1 \tag{6.6}$$

- *Insulin sensitivity* (S_I^*, dL/kg/min per μU/mL) which quantifies the ability of insulin to enhance disposal glucose effectiveness

$$S_I^* = \frac{\partial^2 R_d(t)}{\partial G(t)\partial I(t)}\bigg|_{ss} = s_k \frac{k_{21}k_{12}}{(k_{02}+k_{12})^2}V_1 \tag{6.7}$$

6.3 Models of exercise effect on glucose kinetics

Here, a set of models incorporating the effect of physical activity into the model of glucose kinetics presented in Section 6.2 are presented. Since the physiological interpretation of the two-compartment minimal model of glucose kinetics is that the first compartment represents the plasma plus rapid equilibrating tissues while the second one represents the slowly equilibrating tissues, such as skeletal muscles, the effect of physical activity has been incorporated in the second compartment. It is an accepted knowledge that physical activity increases rates of glucose uptake by numerous factors during and after exercise, such as increasing in blood flow [2, 92] to the contracting skeletal muscles, insulin-independent [91, 97, 123] translocation of GLUT-4 isoform [48, 49, 114, 128] and its transcription [39, 95], and insulin sensitivity in the postexercise period [51, 52].
Thus, ten models incorporating all or part of these effects have been tested assuming that physical activity could affect:

- k_{21}, representing the rate constant of influx from the first to the second compartment.

- s_k, representing the magnitude of insulin-dependent glucose disposal of the second compartment.
- k_{02}, representing the magnitude of insulin-independent glucose disposal of the second compartment.

Physical activity (PA) has been represented as a square-wave signal of unit amplitude and its effect of glucose kinetics parameters has been assumed to act instantaneously or delayed by a parameter d, which has also been estimated from the data:

Model 1 : it assumes a proportional instantaneous action on k_{21}

$$k_{21}^{PA} = k_{21} \cdot [1 + \alpha \cdot PA(t)] \tag{6.8}$$

where α is a parameter modulating the effect of physical activity (Figure 6.2).

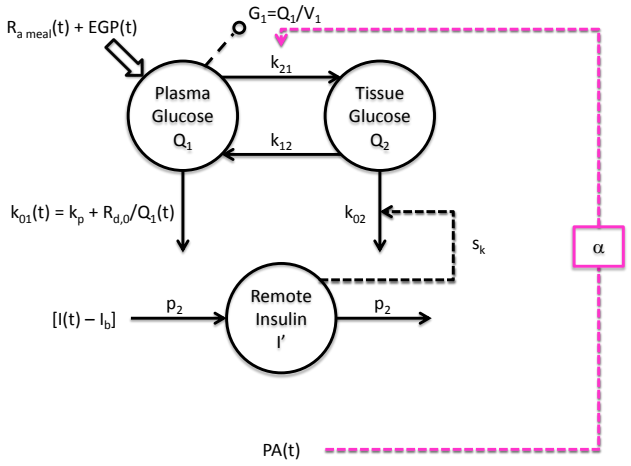

Figure 6.2: Model 1 graphic representation.

Model 2 : it assumes a proportional instantaneous action on s_k

$$s_k^{PA} = s_k \cdot [1 + \beta \cdot PA(t)] \tag{6.9}$$

where β is a parameter modulating the effect of physical activity (Figure 6.3).

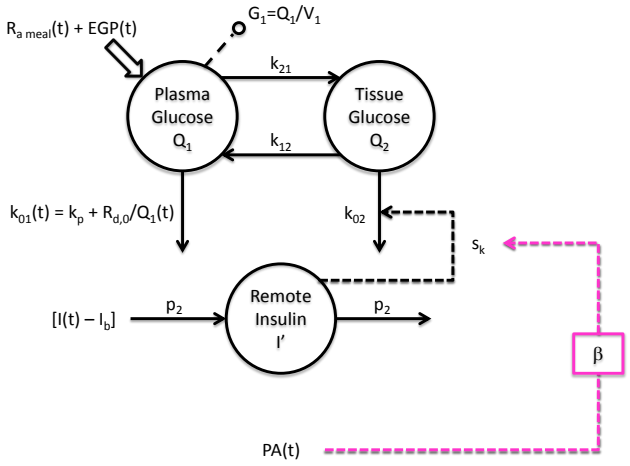

Figure 6.3: Model 2 graphic representation.

Model 3 : it assumes a proportional instantaneous action onk_{02}

$$k_{02}^{PA} = k_{02} \cdot [1 + \gamma \cdot PA(t)] \tag{6.10}$$

where γ is a parameter modulating the effect of physical activity (Figure 6.4).

Model 4 : it is the combination of model 1 and model 2 assuming both a proportional instantaneous action on k_{21} and s_k

$$\begin{aligned} k_{21}^{PA} &= k_{21} \cdot [1 + \alpha \cdot PA(t)] \\ s_k^{PA} &= s_k \cdot [1 + \beta \cdot PA(t)] \end{aligned} \tag{6.11}$$

where α and β are parameters modulating the effect of physical activity (Figure 6.5).

Model 5 : it is the combination of model 1 and model 3 assuming both a

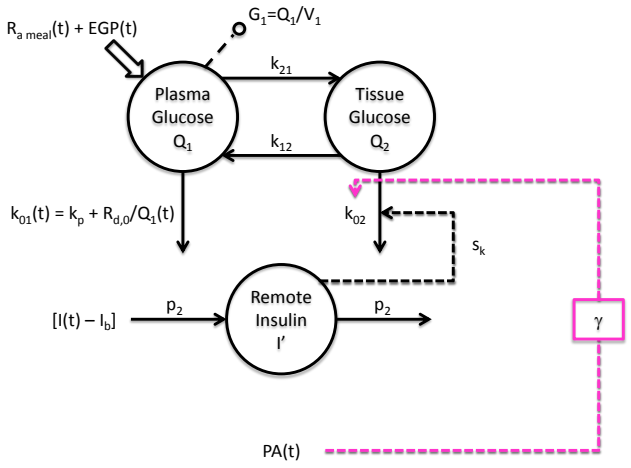

Figure 6.4: Model 3 graphic representation.

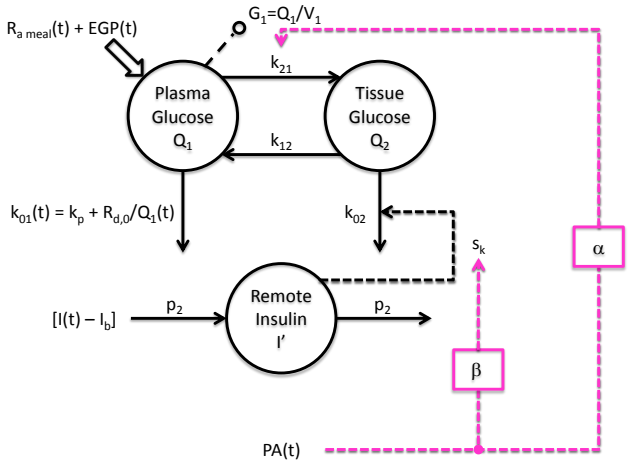

Figure 6.5: Model 4 graphic representation.

proportional instantaneous action on k_{21} and k_{02}

$$\begin{aligned} k_{21}^{PA} &= k_{21} \cdot [1 + \alpha \cdot PA(t)] \\ k_{02}^{PA} &= k_{02} \cdot [1 + \gamma \cdot PA(t)] \end{aligned} \tag{6.12}$$

where α and γ are parameters modulating the effect of physical activity (Figure 6.6).

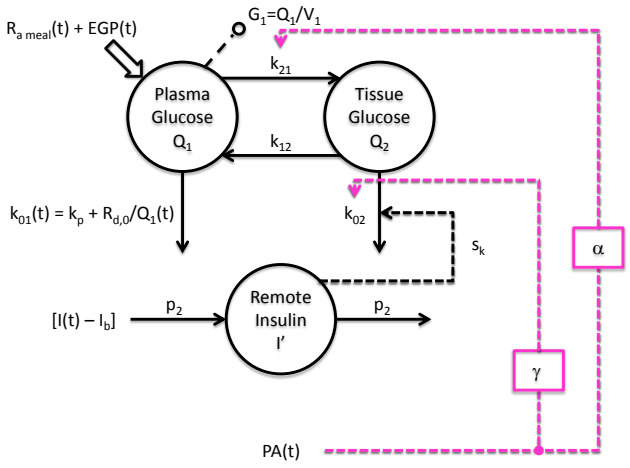

Figure 6.6: Model 5 graphic representation.

In some of the following models a delayed version of physical activity PA'(t)

$$\dot{PA'}(t) = -d \cdot PA'(t) + d \cdot PA(t) \tag{6.13}$$

may be used, instead of PA.

Model 6 : it assumes a proportional delayed action on k_{21}

$$k_{21}^{PA'} = k_{21} \cdot [1 + \alpha \cdot PA'(t)] \tag{6.14}$$

where α is a parameter modulating the effect of physical activity (Figure 6.7).

Model 7 : it assumes a proportional delayed action on s_k

$$s_k^{PA'} = s_k \cdot [1 + \beta \cdot PA'(t)] \tag{6.15}$$

where β is a parameter modulating the effect of physical activity (Figure 6.8).

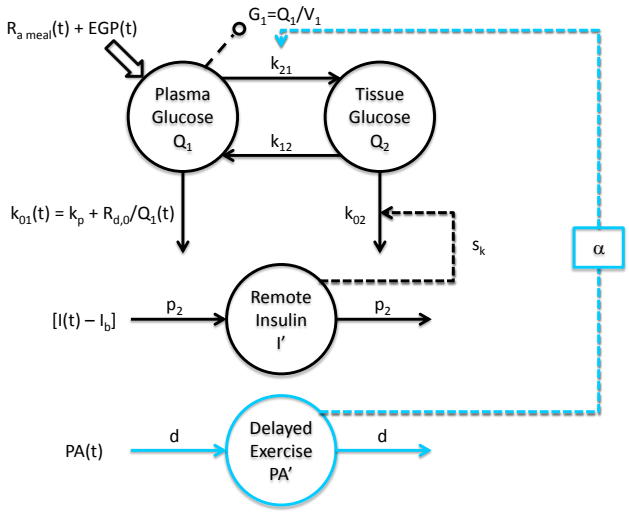

Figure 6.7: Model 6 graphic representation.

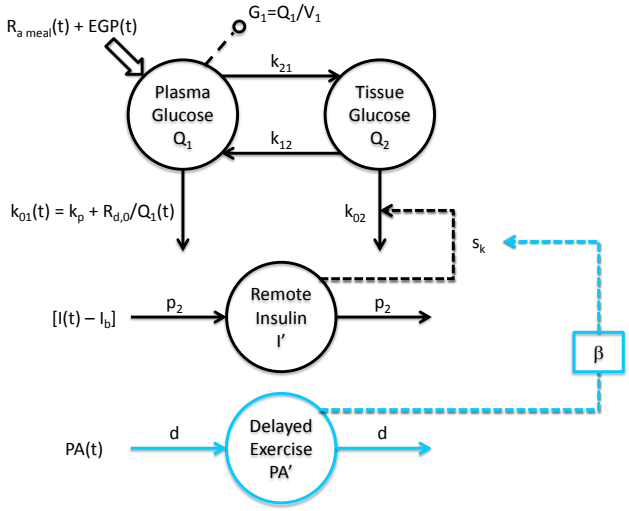

Figure 6.8: Model 7 graphic representation.

Model 8 : it assumes a proportional delayed action on k_{02}

$$k_{02}^{PA'} = k_{02} \cdot [1 + \gamma \cdot PA'(t)] \tag{6.16}$$

where γ is a parameter modulating the effect of physical activity (Figure 6.9).

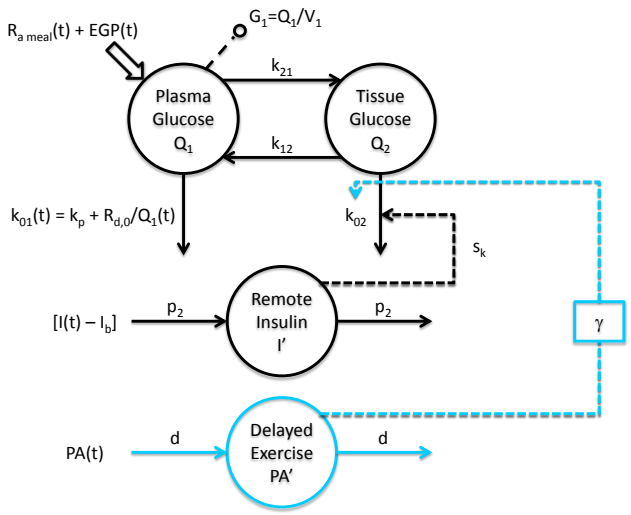

Figure 6.9: Model 8 graphic representation.

Model 9 : it is the combination of model 1 and model 7 assuming a proportional instantaneous action on k_{21} and a proportional delayed action on s_k

$$\begin{aligned} k_{21}^{PA} &= k_{21} \cdot [1 + \alpha \cdot PA(t)] \\ s_k^{PA'} &= s_k \cdot [1 + \beta \cdot PA'(t)] \end{aligned} \tag{6.17}$$

where α and β are parameters modulating the effect of physical activity (Figure 6.10).

Model 10 : it is the combination of model 1 and model 8 assuming a proportional instantaneous action on k_{21} and a proportional delayed action on k_{02}

$$\begin{aligned} k_{21}^{PA} &= k_{21} \cdot [1 + \alpha \cdot PA(t)] \\ k_{02}^{PA'} &= k_{02} \cdot [1 + \gamma \cdot PA'(t)] \end{aligned} \tag{6.18}$$

where α and γ are parameters modulating the effect of physical activity (Figure 6.11).

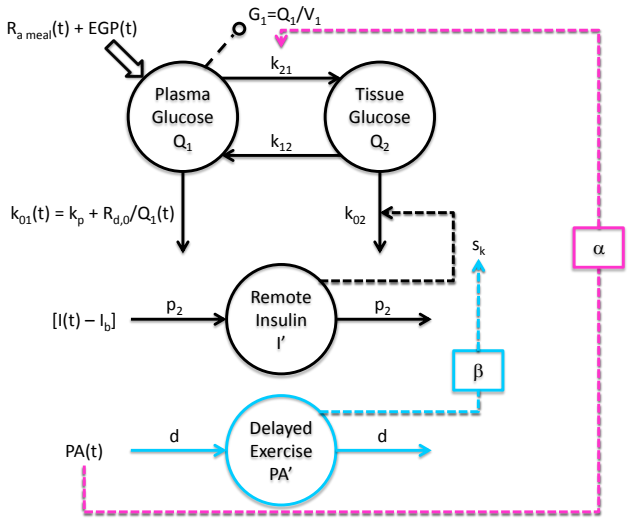

Figure 6.10: Model 9 graphic representation.

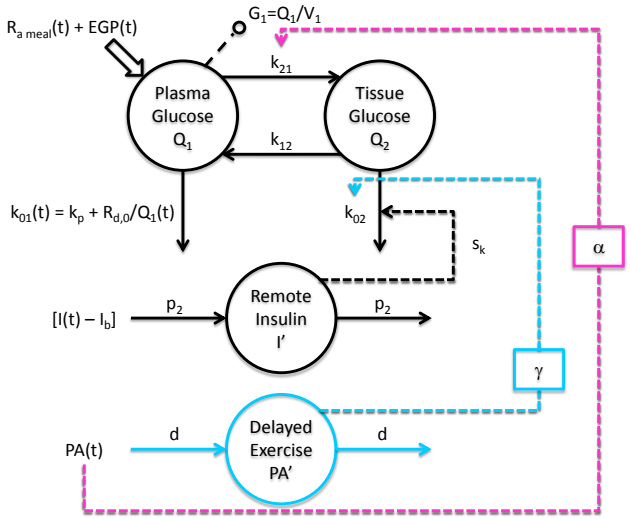

Figure 6.11: Model 10 graphic representation.

6.4 Model identification

As reported in [115, 120] the parameters of glucose kinetics are a priori uniquely identifiable. Moreover, in each presented model, the inclusion of the parameters describing the effect of physical activity did not modify the identifiability properties of the whole model, thus allowing to estimate all parameters at the same time. However, due to the high numbers of paramet-

ers to be estimated in relation to available data, a Maximum A Posteriori (MAP) Bayesian estimator approach was adopted to improve a posteriori identifiability of the model. Data are weighted with the inverse of the variance of glucose measurement errors, which was assumed to be independent, Gaussian with zero mean and known coefficient of variation equal to 2%. Plasma insulin and physical activity signals were the models forcing functions assumed to be known without error. In particular, physical activity was assumed to be a square-wave signal of unit amplitude between $t = 120 - 195$ min and zero elsewhere. The method provided both optimal values for model parameters and a measure of their precision.

6.5 Model selection

Each model described in Section 6.3 has been identified against data. Data are presented as mean ± SE, if not differently indicated. All results were averaged on a total of 11 subjects, since an error on the measurement of meal enrichment was reported in one subject. Values obtained at $t = 0$ min were considered as basal. In the following Figures, shaded box between $t = 120$ and $t = 195$ min represents the exercise period at 50% $\dot{V}O_{2max}$.

Models were compared on the basis of standard criteria [24]:

- Residual independence (Runs Test).
- Ability to describe the data (Weighted Residual Sum of Squares, WRSS).
- Precision of parameter estimates (expressed as CV).
- Model parsimony (Bayesian Information Criterion, BIC).

Table 6.1 shows the quantitative results used for model selection. All the tested models fitted the data sufficiently well, as confirmed by the Runs Test, which supported randomness of residuals in most of individuals for each model. Among models, one can observe that parameter α was always

estimated with a good precision and its identification guarantees full randomness of residuals and provided, on average, lower weighted residuals and parsimony indices (model 1, model 4, model 5, model 6, model 9 and model 10). However, comparing model 1 and model 6, the presence of the delay parameter on the effect of physical activity d in model 6 worsens model prediction against data (higher average WRSS) and reduces the capability of the model to the estimate an exercise-induced effect in 18% of subjects with respect to model 1. For this reason, all the models including an effect on k_{21} assumed an instantaneous effect of physical activity on k_{21} (α).
In contrast, model 2 and model 7 (assuming the effect of physical activity on s_k) provided the worst model predictions against data, with respect to the other candidates, with low precision of parameters estimates. Furthermore, model 3 and model 8 (assuming the effect of physical activity on k_{02}) provided better model predictions if compared to model 2 and model 7, respectively, but worse than model 1 and model 6, respectively. For this reason, these models have been discarded. Finally, the improvement in model prediction introduced by parameter β with respect to simpler or similar models suggested that, in this particular database, this effect is not as relevant as expected. Increasing the complexity of the model, model 4, model 5, model 9 and model 10 allowed to better describe data, i.e. supporting the randomness of the residuals in all subjects, reducing WRSS and the parsimony index, although the number of parameters is greater than their simpler versions. However, the risk of increasing the number of parameters is that sometimes not all the parameters are a posteriori identifiable. In fact, model 4 collapsed in model 1 in 4 subjects, since parameter β was estimated equal to zero, and in model 2 in 1 subject, since parameter α was estimated equal to zero; model 5 collapsed in model 1 in 6 subjects, since parameter γ was estimated equal to zero; model 9 collapsed in model 1 in 3 subjects, since parameter d and/or s_k were estimated equal to zero.

	Residual Independence (Runs Test)	**Data Fit (WRSS)**	**Precision (CV)** α	β	γ	d	**Parsimony Criterion (BIC)**	**No. Parameters**	**Nonzero Parameters (%)**
Model 1	100%	320	13%				323	1	100%
Model 2	64%	436		69%			439	1	82%
Model 3	91%	432			20%		435	1	82%
Model 4	100%	318	12%	36%			325	2	77%
Model 5	100%	311	26%		17%		318	2	73%
Model 6	100%	326	20%			46%	333	2	82%
Model 7	64%	462		100%		23%	468	2	91%
Model 8	73%	457			24%	51%	464	2	91%
Model 9	100%	319	17%	43%		91%	329	3	82%
Model 10	100%	287	12%		42%	39%	296	3	100%

Table 6.1: Models of the effect of exercise on glucose kinetics comparison.

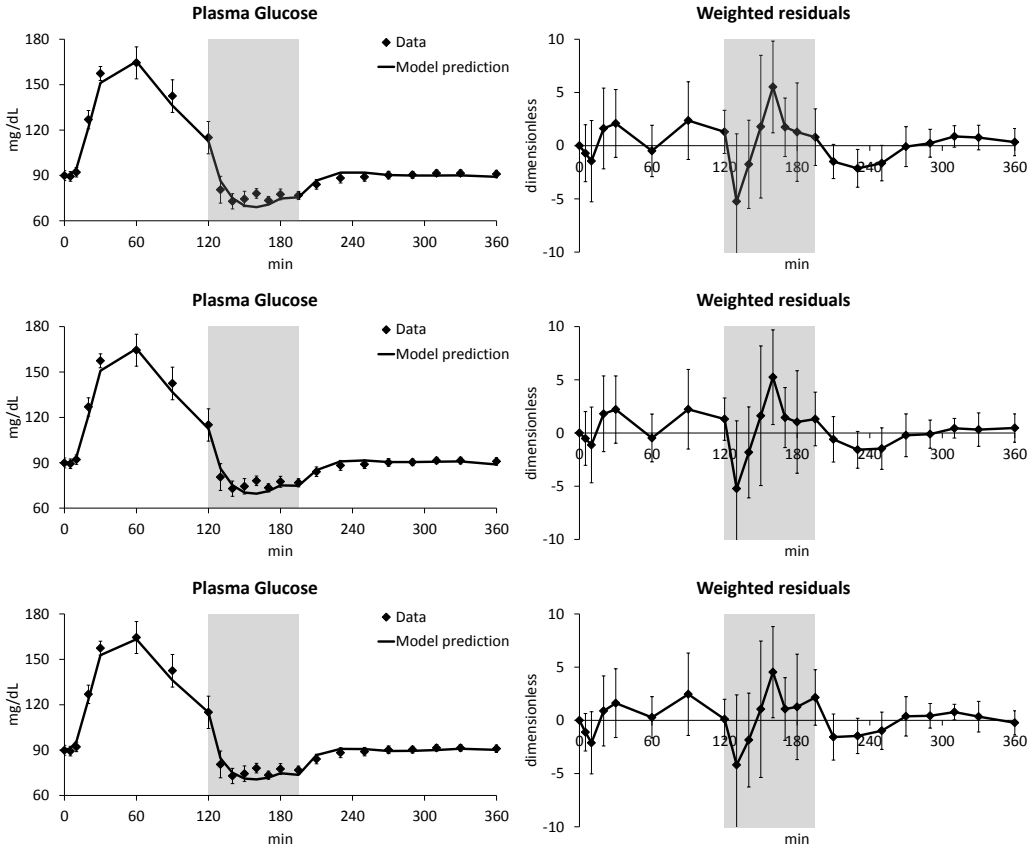

Figure 6.12: Average glucose data vs. models prediction (left) and weighted residuals (right). Model 1 (top), model 5 (middle) and model 10 (bottom). Vertical bars represent SE for glucose data and SD for weighted residuals.

In general, the parsimony criterion indicates model 10 as the most parsimonious (lowest BIC) despite being the most complicated. This is due to the ability of the model to well describe the data (lowest WRSS) still providing a good precision of parameter estimates. However, the main drawback of this model is the large variability of d estimates (range: $1 \div 0.004$ min^{-1}), resulting in an average value of 0.11 ± 0.30 min^{-1}, and in the fact that d in some cases is difficult to estimate. This is likely due to the sampling schedule (every 10 min during exercise session) and the duration of the experiment (360 min). In addition, despite being less accurate than model 10, the two models which satisfy most of the selection criteria are model 1 and model 5. These 3 models share parameter α, which always guaranteed full random-

ness of residuals and was accurately and precisely estimated (0.49 ± 0.32, 0.56 ± 0.22 and 0.56 ± 0.22 for model 1, model 5 and model 10, respectively; with CV equal to $13 \pm 12\%$, $26 \pm 39\%$ and $12 \pm 4\%$ for model 1, model 5 and model 10, respectively); while model 5 and model 10 share parameter γ (12.8 ± 8.0 and 13.2 ± 7.9, respectively).
In Figure 6.12, average glucose data vs. models prediction and weighted residuals for model 1, model 5 and model 10 are reported. As can be observed, all models fitted the data well as confirmed by inspection of visual predictive check (VPC) of model prediction vs. plasma glucose data and the corresponding weighted residuals, which present zero mean and are sufficiently random.

All the models proposed here have been developed based on the available knowledge on exercise physiology, and thus allowing a direct physiological interpretation of the estimated parameters. A set of models, model 1, model 5 and model 10, have been demonstrated to significantly improve prediction of glucose data during physical activity.
The best models proposed share the assumption that exercise affects parameter k_{21} and this is seemed to be fundamental to describe glucose kinetics during physical activity. From a physiological point of view, this effect may be interpreted as the increase in muscle blood flow, in agreement with [2, 92], and, at least in part, glucose uptake by the muscles. In fact, as can be observed in Eqs. 6.5 and 6.7, an increase in k_{21} augments both glucose effectiveness and insulin sensitivity. In addition, model 5 and model 10 also assume that physical activity stimulates the insulin-independent glucose disposal which takes place in the second compartment, k_{02}. From a physiological point of view, this effect may be interpreted as an increase in insulin-independent glucose uptake, e.g. increased translocation and transcription of GLUT-4 isoform and/or glucose oxidation, in agreement with [39, 48, 49, 88, 91, 95, 97, 114, 123, 128]. In contrast, in this particular database, we were not able to specifically modeling the well-known postexercise increase in insulin action [51, 52]. This is likely due to the fact that, in healthy subjects, insulin is markedly suppress during physical activity

(Figure 3.1, top right). It is worth noting that, since insulin is returned to its basal value in this phase, the effect of exercise of insulin-dependent utilization may be included in the estimated increase of k_{02}, thus including both insulin-independent and -dependent effect. Furthermore, as reported in [45, 60], another possible explanation may be due the time-domain of this database in relation to time at which the increase in insulin sensitivity may occur (3-4 hours later).
However, the above reported results are not in contrast with those reported in Chapter 5, i.e. that exercise increase the overall insulin sensitivity by almost 75%. In fact, the overall insulin sensitivity can be calculated from model parameters using Eq. 6.7, thus an increase in k_{21} implies an exercise-induced increase in overall S_I.

In conclusion, the models presented in this Chapter well describe the data and allow the quantification of physiologically interpretable parameters. However, future studies with different protocols, e.g. injecting an insulin bolus after the exercise session or lasting longer, are needed to validate the proposed models and better understand the contribution of insulin-independent and -dependent effect of physical activity on glucose disposal.

7 Conclusions

In healthy subjects, glucose regulation relies on a complex control system that keeps blood glucose level within a narrow range around its basal value. An important component of everyday life challenging this complex mechanism, although offering a net benefit for most individuals with and without diabetes, is regular physical activity.

Regular physical activity is known to have several potential benefits that apply to both diabetic and nondiabetic individuals such as enhancing insulin sensitivity, improving glycemic control and reducing the risk of cardiovascular mortality. Psychological benefits of exercise, such as an increased sense of well-being, improved self-esteem and enhanced quality of life may also be important for those with either type 1 and type 2 diabetes [61]. Although persons with diabetes may derive many benefits from regular physical activity, there are also a number of hazards that make exercise difficult to manage if not properly addressed.

Numerous studies have demonstrated increased rate of glucose disappearance (R_d) and endogenous glucose production (EGP) during physical activity in individuals with and without diabetes [46, 64] in the postabsorptive state, while very few have examined the effects of exercise in the postprandial state in individuals with and without type 2 diabetes [17, 18, 58, 65, 74, 75] and none in individuals with type 1 diabetes, although many people, with and without diabetes, exercise a few hours after a meal. Furthermore, very few

studies [27] have used methods that minimize fluctuations in tracer-to-tracee specific activity to enable accurate continuous (every 10 min) measurement of glucose turnover and during the transition from rest to exercise in nondiabetic subjects.
A method for the quantification of the effect and effect size of exercise on insulin sensitivity and a physiological model quantitatively describing the effect of exercise on glucose turnover in the postprandial state have never been developed so far. This represents a significant knowledge gap, especially in type 1 diabetes, because this information could be incorporated into currently available artificial pancreas control algorithms, thus extending their applicability to treat people with type 1 diabetes. However, such tools will need to be developed and tested in healthy subjects before validating in those with diabetes.

The aim of this contribution is to develop a methodology to accurately quantifying the effect of moderate-intensity physical activity on postprandial glucose turnover in healthy subjects. A novel method for the estimation of postprandial glucose turnover during physical activity with the state-of-the-art techniques has been established. Then, exploiting the obtained results, first a method for the quantification of the effect and effect size of exercise on postprandial insulin sensitivity has been developed, then a whole-body mathematical model describing the effect of physical activity on glucose-insulin system was developed and tested on the available data. To address these tasks, data of 12 healthy individuals who underwent a triple-tracer mixed-meal and a moderate-intensity exercise session 2 hours after meal ingestion for 75 minutes have been used [104].

The tracer-to-tracee clamp technique is a well-established method [4] which allows to accurately estimate postprandial glucose fluxes continuously after a meal in a "model-independent" way by infusing tracers in order to minimize fluctuations in tracer-to-tracee ratio (TTR). However, since it is almost impossible to realize a "perfect" clamp of the plasma tracer-to-tracee ratio,

the use of models, to compensate the non-steady-state errors, is needed. Use of models requires the estimation of derivatives both for tracer-to-tracee ratio and glucose signals. Due to ill-conditioning, this issue was first addressed thanks to a stochastic deconvolution technique [36], where the expectations of the smoothness of the unknown input signal is a priori described as multiple integrations of a stationary white noise process. However, because of physical activity, signals represented marked nonstationarity leading us to resort to an improved stochastic deconvolution method [90]. The proposed method allows to relax the usual stationarity assumption and, since prior information of the input signal was unknown, an hypothesis to account for the different behaviours of the input signal has been assumed. Results show that, at variance with the standard technique, the proposed method provides a good regularization of TTR and glucose signals, and thus their derivatives, able to follow the rapid changes in these signals induced by exercise. Moreover, in addition to the method proposed in [90] for the quantification of the parameters describing the different behaviours of the input signal, a new criterion is proposed that has been proved to allow a more smoothed reconstruction of TTR and glucose signals. The proposed method allows an accurate reconstruction of postprandial glucose fluxes after the meal, during and after the exercise session. Fluxes analysis show a rapid eightfold increase of EGP with a pleateau in the rates of both $R_{a\ meal}$ and R_d during exercise, while glucose concentrations rapidly falls below basal fasting levels in all subjects, accompanied by a rapid fall in insulin concentrations and a greater than twofold rise in glucagon concentrations.

A method for the quantification of the effect and effect size of exercise on net insulin sensitivity (S_I), i.e. the ability of insulin to stimulate glucose disposal (R_d) and suppress endogenous glucose production (EGP), and evaluate the relative contribution of liver and disposal insulin sensitivity is also presented. The method is based on the estimation of S_I using data of first 2 hours after the meal, i.e. in absence of physical activity (rest), and then using the data of the whole experiment, i.e. in presence of physical activity (overall).

S_I is thus derived from reconstructed postprandial glucose fluxes. Results show that net insulin sensitivity increases by almost 76±12% during moderate-intensity exercise and that this increase is due to an enhancement in glucose disposal rather than a further suppression of EGP. This effect, from a physiological point of view, may be due to the relatively minor inhibitory effect of insulin on EGP compared to the stimulatory effect of glucagon, while a significant effect seems to be exerted by insulin on glucose disposal due to sustained rate of R_d during exercise, even though insulin and glucose rapidly fell.
In order to validate the obtained results, the same rationale was applied to the well-established integral formula proposed in [21] to estimate S_I from plasma glucose and insulin concentrations. Results show a similar increase in net insulin sensitivity (74±8%). The comparison between the two methods shows that they provide similar values of net insulin sensitivity and the correlation between the two was very high ($r=0.989$, $p \ll 0.005$).
However it is important to remark that, with the proposed method, it is possible only to measure an insulin-dependent effect of exercise on glucose disposal while, unfortunately, it is not possible to tease out the relative contribution of well-established insulin-independent mechanisms induced by physical activity [48, 49, 114, 128].
Incidentally, these results have been incorporated into the UVA/Padova T1DM simulator in order to suggest the best strategy that could be adopted during artificial pancreas clinical trials that involves a session of moderate physical activity. In this work it is showed that, in order to prevent hypoglycemia during and after exercise, any control algorithm would benefit by knowing in advance of upcoming physical activity, due to the large delay between subcutaneous insulin infusion and its effect on plasma glucose. Moreover, in the case that patient-specific basal insulin reduction pattern is not available, an optimal basal reduction strategy is suggested which has been proved to be rather safe and effective in simulation studies [105].

As previously discussed, the method for the quantification of the effect size of exercise on insulin sensitivity is not able to tease out the insulin-

independent effect of exercise on glucose uptake. Therefore, to discriminate the effect of exercise on insulin-dependent and -independent glucose turnover, the development of a model of system is needed.
Starting from a two-compartment model to describe glucose kinetics, a set of models of increasing complexity, incorporating the modulating effect of physical activity on glucose kinetics parameters were developed. The selection of the best models was tackled using standard criteria (e.g. ability to describe the data, precision of parameter estimates, model parsimony, residual independence). The best selected models share the assumption that exercise increase the model parameter representing the rate constant influx from the first (plasma plus insulin-independent tissues, rapid-equilibrating with plasma) to the second compartment (insulin-dependent or slowly-equilibrating tissues, such as skeletal muscles). This effect may be interpreted as an increase in muscle blood flow, in agreement with [2, 92], and, at least in part, glucose uptake by the muscles. In addition, more complicated models also assume that exercise stimulates the insulin-independent glucose disposal parameter in the second compartment, which may be interpreted as an increase in insulin-independent glucose uptake, in agreement with [39, 48, 49, 88, 91, 95, 97, 114, 123, 128]. In contrast, in this particular database, we were not able to specifically modeling the well-known postexercise increase in insulin action, mainly due to the fact that, in healthy subjects, insulin is markedly suppress during physical activity.
However, it is important to remark that these results are not in contrast with those obtained with the integral method, since the calculation of an index of insulin sensitivity from model parameters, incorporating the above estimated effects of physical activity, implies an exercise-induced increase in the overall insulin sensitivity.

In conclusion, in this study, a methodology to accurately quantifying the effect of moderate-intensity physical activity on postprandial glucose turnover in healthy subjects has been developed. A novel method, using the triple-tracer technique, for the estimation of postprandial glucose turnover which accounts for the nonstationarity introduced by physical activity has

been established. Then, a method for the quantification of the effect of physical activity on whole-body insulin sensitivity has been developed. Finally, a whole-body mathematical model describing the effect of physical activity on glucose-insulin system was developed.

Future studies with different protocols, e.g. injecting an insulin bolus after the exercise session and lasting longer, and/or with different subjects, e.g. T1DM subjects, are needed to validate the proposed techniques and to expand the knowledge on the effect of physical activity on glucose-insulin regulation.

Bibliography

[1] **Allsop J.R., Wolfe R.R., Burke J.F.**, The reliability of rates of glucose appearance in vivo calculated from constant tracer infusions, *Biochem* 172: 407-416, 1978.

[2] **Anderson P., Saltin B.**, Maximal perfusion of skeletal muscle in man *J Physiol* 366: 233-249, 1985.

[3] **Basu A., Caumo A., Bettini F., Gelisio A., Alzaid A., Cobelli C.**, Impaired basal glucose effectiveness in NIDMM: contribution of defects in glucose disappearance and production, measured using an optimized minimal model independent protocol, *Diabetes* 46: 421-432, 1997.

[4] **Basu R., Di Camillo B., Toffolo G.M., Basu A., Shah P., Vella A., Rizza R.A., Cobelli C.**, Use of a novel triple-tracer approach to assess postprandial glucose metabolism, *Am J Physiol Endocrinol Metab* 284: E55-E69, 2003.

[5] **Berger M., Berchtold P., Cüppers H.J., Drost H., Kley H.K., Müller W.A., Wiegelmann W., Zimmerman-Telschow H., Gries F.A., Krüskemper H.L., Zimmermann H.**, Metabolic and hormonal effects of muscular exercise in juvenile type diabetics, *Diabetologia* 13(4): 355-365, 1977.

[6] **Bergman R.N., Ider Y.Z., Bowden C.R., Cobelli C.**, Quantitative estimation of insulin sensitivity, *Am J Physiol* 236: E667-E677, 1979.

[7] **Best J.D., Taborsky J.Jr., Halter J.B., Porte D.Jr.**, Glucose disposal is not proportional to plasma glucose level in man, *Diabetes* 30: 847-850, 1983.

[8] **Birnbaum M.J.**, The insulin-sensitive glucose transporter, *Int Rev Cytology* 137A: 239-297, 1992.

[9] **van Bon A.C., Verbitskiy E., von Basum G., Hoekstra J.B., DeVries J.H.**, Exercise in closed-loop control: a major hurdle, *J Diabetes Sci Technol* 5(6): 1337-1341, 2011.

[10] **Breton M.D.**, Physical activity - the major unaccounted impediment to closed loop control, *J Diabetes Sci Technol* 2: 169-174, 2008.

[11] **Breton M., Farret A., Bruttomesso D., Anderson S., Magni L., Patek S., Dalla Man C., Place J., Demartini S., Del Favero S., Toffanin C., Hughes-Karvetski C., Dassau E., Zisser H., Doyle F.J. 3rd, De Nicola G., Avogaro A., Cobelli C., Renard E., Kovatchev B.P.; International Artificial Pancreas Study Group**, Fully integrated artificial pancreas in type 1 diabetes: modular closed-loop glucose control maintains near normoglycemia, *Diabetes* 61(9): 2230-2237, 2012.

[12] **Brooks G.A., Fahey T.D., White T.P., Baldwin K.M.**, Exercise Physiology: Human Bioenergetics and Its Application 3rd Edition, *Mayfield Publishing Company* Mountain View, 1999.

[13] **Brun J.F., Guintrand-Hurget R., Boegner C., Bouix O., Orsetti A.**, Influence of short-term submaximal exercise on parameters of glucose assimilation analyzed with the minimal model, *Metabolism* 44(7): 833-840, 1995.

[14] **Camacho R.C., Galassetti P., Davis S.N., Wasserman D.H.**, Glucoregulation during and after exercise in health and insulin-dependent diabetes, *Exerc Sport Sci Rev* 33(1): 17-23, 2005.

[15] **Carrio I., Estorch M., Serra-Grima R., Ginjaume M., Notivol R., Calabuig R., Vilardell F.**, Gastric emptying in marathon runners, *Gut* 30: 152-155, 1989.

[16] **Cartee G.D., Holloszy J.O.**, Exercise increases susceptibility of muscle glucose transport to activation by various stimuli, *Am J Physiol Endocrinol Metab* 258(21): E390-E393, 1990.

[17] **Carter S.L., Rennie C., Tarnopolsky M.A.**, Substrate utilization during endurance exercise in men and women after endurance training, *Am J Physiol Endocrinol Metab* 280(6): E898-E907, 2001.

[18] **Carter J.M., Jeukendrup A.E., Mann C.H., Jones D.A.**, The effect of glucose infusion on glucose kinetics during a 1-h time trial, *Med Sci Sports Exerc* 36: 1543-1550, 2004.

[19] **Caumo A., Giacca A., Morgese M., Pozza G., Micossi P., Cobelli C.**, Minimal model of glucose disappearance: lessons from the labelled IVGTT, *Diabet Med* 8: 822-832, 1991.

[20] **Caumo A., Cobelli C.**, Hepatic glucose production during labeled IVGTT: estimation by deconvolution with a new minimal model, *Am J Physiol Endocrinol Metab* 264(37): E829-E841, 1993.

[21] **Caumo A., Bergman R.N., Cobelli C.**, Insulin sensitivity from meal tolerance tests in normal subjects: a minimal model index, *J Clinical Endocr Metab* 85(11): 4396-4402, 2000.

[22] **Chimen M., Kennedy A., Nirantharakumar K., Pang T.T., Andrews R., Narendran P.**, What are the health benefits of physical activity in type 1 diabetes mellitus? A literature review, *Diabetologia* 55(3): 542-551, 2012.

[23] **Cobelli C., Toffolo G., Ferrannini E.**, A model of glucose kinetics and their control by insulin: compartmental and non compartmental approaches, *Math Biosci* 72: 291-315, 1984.

[24] **Cobelli C., Foster D., Toffolo G.M.**, Tracer Kinetics in Biomedical Research: From Data to Model, *Kluwer Academic/Plenum Publishers*, New York, 2000.

[25] **Cobelli C., Carson E.**, Introduction to Modelling in Physiology and Medicine, *Academic Press*, San Diego, 2008.

[26] **Cobelli C., Renard E., Kovatchev B.P.**, Artificial pancreas: past, present, future, *Diabetes* 60(11): 2672-2682, 2011.

[27] **Coggan A.R., Raguso C.A., Williams B.D., Sidossis L.S., Gastaldelli A.**, Glucose kinetics during high-intensity exercise in endurance-trained and untrained humans, *J Appl Physiol* 78: 1203âĂŞ1207, 1995.

[28] **Coggan A.R., Swanson S.C., Mendenhall L.A., Habash D.L., Kien C.L.**, Effect of endurance training on hepatic glycogenolysis and gluconeogenesis during prolonged exercise in men, *Am J Physiol Endocrinol Metab* 78: 1203-1207, 1995.

[29] **Dalla Man C., Caumo A., Cobelli C.**, The oral glucose minimal model: estimation of insulin sensitivity from a meal test, *IEEE Trans Biomed Eng* 49(5): 419-429, 2002.

[30] **Dalla Man C., Caumo A., Basu R., Rizza R., Toffolo G.M., Cobelli C.**, Minimal model estimation of glucose absorption and insulin sensitivity from oral test: validation with a tracer method, *Am J Physiol Endocrinol Metab* 287(4): E637-E643, 2004.

[31] **Dalla Man C., Caumo A., Basu R., Rizza R.A, Toffolo G.M., Cobelli C.**, Measurement of selective effect of insulin on glucose disposal from labeled glucose oral test minimal model, *Am J Physiol Endocrinol Metab* 289(5): E909-E914, 2005.

[32] **Dalla Man C., Yarasheski K.E., Caumo A., Robertson H., Toffolo G.M., Polonsky K.S., Cobelli C.**, Insulin sensitivity by oral glucose minimal models: validation against clamp, *Am J Physiol Endocrinol Metab* 289(6): E954-E959, 2005.

[33] **Dalla Man C., Toffolo G.M., Basu R., Rizza R.A., Cobelli C.**, Use of a labeled oral minimal model to measure hepatic insulin sensitivity, *Am J Physiol Endocrinol Metab* 295: E1152-E1159, 2008.

[34] **Dalla Man C., Breton M.D., Cobelli C.**, Physical activity into the meal-glucose insulin model for type 1 diabetes: in silico studies, *J Diabetes Sci Technol* 3: 56-67, 2009.

[35] **Dalla Man C., Micheletto F., Dayu L., Breton M., Kovatchev B.P., Cobelli C.**, The UVA/Padova type 1 diabetes simulator: new features, *J Diabetes Sci Technol*, 2013 (in press).

[36] **De Nicolao G., Sparacino G., Cobelli C.**, Nonparametric input estimation in physiological systems: problems, methods and cases studies, *Automatica* 33(5): 851-870, 1997.

[37] **DeFronzo R.A., Tobin J.D., Andres R.**, Glucose clamp technique: a method for quantifying insulin secretion and resistance, *Am J Physiol* 237: E214-E223, 1979.

[38] **Derouich M., Boutayeb A.**, The effect of physical exercise on the dynamics of glucose and insulin, *J Biomech* 35: 911-917, 2002.

[39] **Dohm L.**, Invited review: regulation of skeletal muscle GLUT-4 exxpression by exercise, *J App Physiol* 93(2): 782-787, 2002.

[40] **Douen A.G., Ramlal T., Rastogi S., Bilan P.J., Cartee G.D., Vranic M., Holloszy J.O., Klip A.**, Exercise induces recruitment of the "insulin-responsive glucose transporter." Evidence for distinct intracellular insulin- and exercise-recruitable transporter pools in skeletal muscle, *J Biol Chem* 265: 13427-13430, 1990.

[41] **Elleri D., Allen J.M., Kumareswaran K., Leelarathna L., Nodale M., Caldwell K., Cheng P., Kollman C., Haidar A., Murphy H.R., Wilinska M.E., Acerini C.L., Dunger D.B., Hovorka R.**, Closed-loop basal insulin delivery over 36 hours in adolescents with type 1 diabetes: randomized clinical trial, *Diabetes Care* 36(4): 838-844, 2013.

[42] **Feldman M., Nixon J.V.**, Effect of exercise on postprandial gastric secretion and emptying in humans, *J Appl Physiol* 53: 851-854, 1982.

[43] **Felig P., Wahren J.**, Fuel homeostasis in exercise, *N Engl J Med* 293: 1078-1084, 1975.

[44] **Gao J., Gulve E.A., Holloszy J.O.**, Contraction-induced increase in muscle insulin sensitivity: requirement for a serum factor, *Am J Physiol Endocrinol Metab* 266(29): E186-E192, 1994.

[45] **Garetto L.P. Richter E.A., Goodman M.N., Ruderman N.B.**, Enhanced muscle glucose metabolism after exercise in the rat: the two phases, *Am J Physiol Endocrinol Metab* 246: E471-E475, 1984.

[46] **Giacca A., Groenewoud Y., Tsui E., McClean P., Zinman B.**, Glucose production, utilization, and cycling in response to moderate exercise in obese subjects with type 2 diabetes and mild hyperglycemia, *Diabetes* 47: 1763-1770, 1998.

[47] **Goodyear L.J., King P.A., Hirshman M.F., Thompson C.M., Horton E.D., Horton E.S.**, Contractile activity increases plasma membrane glucose transporters in absence of insulin, *Am J Physiol* 258: E667-E672, 1990.

[48] **Goodyear L.J., Hirshman M.F., Horton E.S.**, Exercise-induced translocation of skeletal muscle glucose transporters, *Am J Physiol* 261: E795-E799, 1991.

[49] **Goodyear L.J., Hirshman M.F., Valyou P.M., Horton E.S.**, Glucose transporter number function and subcellular distribution in rat skeletal muscle after exercise training, *Diabetes* 41: 1091-1099, 1992.

[50] **Goodyear L.J., Kahn B.B.**, Exercise, glucose transport and insulin sensitivity, *Annu Rev Med* 49: 235-261, 1998.

[51] **Greiwe J.S., Hickner R.C., Hansen P.A., Racette S.B., Chen M.M. Holloszy J.O.**, Effects of endurance exercise training on muscle glycogen accumulation in humans, *J Appl Physiol* 87: 222-226, 1999.

[52] **Gulve E.A., Cartee G.D., Zierath J.R., Corpus V.M., Holloszy J.O.**, Reversal of enhanced muscle glucose transport after exercise: roles of insulin and glucose, *Am J Physiol Endocrinol Metab* 259: E685-E691, 1990.

[53] **Hamann J.J., Buckwalter J.B., Cliffors P.S., Shoemaker J.K.**, Is the blood flow response to a single contraction determined by work performed?, *J Appl Physiol* 96: 2146-2152, 2004.

[54] **Hamilton J.D.**, Time Series Analysis, *Princeton University Press*, 1994.

[55] **Hansen T., Drivsholm T., Urhammer S.A., Palacios R.T., Vølund A., Borch-Johnsen K., Pedersen O.**, The BIGTT test: a novel test for simultaneous measurement of pancreatic β-cell function, insulin sensitivity, and glucose tolerance, *Diabetes Care* 30: 257-262, 2007.

[56] **Hastie T., Tibshirani R., Friedman J.**, The elements of statistical learning: data mining, inference and prediction (Secon Edition), *Springer Series in Statistics*, 2009.

[57] **Hayashi T., Wojtaszewski J.F.P., Goodyear L.J.**, Exercise regulation of glucose transport in skeletal muscle, *Am J Physiol Endocrinol Metab* 273: E1039-E1051, 1997.

[58] **Henderson G.C., Fattor J.A., Horning M.A., Faghihnia N., Johnson M.L., Luke-Zeitoun M., Brooks G.A.**, Glucoregulation is more precise in women than in men during postexercise recovery, *Am J Clin Nutr* 87: 1686-1694, 2008.

[59] **Henriksen E.J., Bourey R.E., Rodnick K.J., Koranyi L., Permutt M.A., Holloszy J.O.**, Glucose transporter protein content and glucose transport capacity in rat skeletal muscles, *Am J Physiol Endocrinol Metab* 259: E593-E598, 1990.

[60] **Holloszy J.O.**, Exercise-induced increase in muscle insulin sensitivity *J Appl Physiology* 99: 338-343, 2005.

[61] **Horton E.S.**, Role and management of exercise in diabetes mellitus, *Diabetes Care* 11(2): 201-211, 1989.

[62] **Hovorka R., Allen J.M., Elleri D., Chassin L.J., Harris J., Xing D., Kollman C., Hovorka T., Larsen A.M., Nodale M., De Palma A., Wilinska M.E., Acerini C.L., Dunger D.B.**, Manual closed-loop insulin delivery in children and adolescents with type 1 diabetes: a phase 2 randomised crossover trial, *Lancet* 375(9716): 743-751, 2010.

[63] **Iscoe K.E., Riddell M.C.**, Continuous moderate-intensity exercise with or without intermittent high-intensity work: effects on acute and late glycaemia in athletes with type 1 diabetes mellitus, *Diabet Med* 28(7): 824-832, 2011.

[64] **Jenkins A.B., Furler S.M., Chisholm D.J., Kraegen E.W.**, Regulation of hepatic glucose output during exercise by circulating glucose and insulin in humans, *Am J Physiol Regul Integr Comp Physiol* 250: R411-R417, 1986.

[65] **Jeukendrup A.E., Raben A., Gijsen A., Stegen J.H., Brouns F., Saris W.H., Wagenmakers A.J.**, Glucose kinetics during prolonged exercise in highly trained human subjects: effect of glucose ingestion, *J Physiol* 515: 579-589, 1999.

[66] **El-Khatib F.H., Russel S.J., Nathan D.M., Sutherlin R.G., Damiano E.R.**, A bihormonal closed-loop artificial pancreas fro type 1 diabetes, *Sci Transl Med* 2(27): 27ra27, 2010.

[67] **Klip A., Paquet M.R.**, Glucose transport and glucose transporters muscle and their metabolic regulation, *Diabetes Care* 13: 228-242, 1990.

[68] **Koivisto V., Felig P.**, Effects of leg exercise on insulin absorption in diabetic patients, *N Eng J Med* 298: 77-83, 1978.

[69] **Kovatchev B.P., Straume M., Cox D.J., Farhy L.S.**, Risk analysis of blood glucose data: a quantitative approach to optimizing the control of insulin dependent diabetes, *J Theor Med* 3(1): 1-10, 2000.

[70] **Kovatchev B.P., Breton M., Dalla Man C., Cobelli C.**, In silico preclinical trials: a proof of concept in closed-loop control of type 1 diabetes, *J Diabetes Sci Technol* 3(1): 44-55, 2009.

[71] **Kristiansen S., Darakhsna F., Richter E.A., Hundal H.S.**, Fructose transport and GLUT-5 protein in human sarcolemmal vescicles, *Am J Physiol Endocrinol Metab* 273(36): E543-E548, 1997.

[72] **Lakka T.A., Venäläinen J.M., Rauramaa R., Salonen R., Tuomilehto J., Salonen J.T.**, Physical activity/exercise and type 2 diabetes: a consensus statement from the American Diabetes Association, *Diabetes Care* 29(6): 1433-1438, 2006.

[73] **Lampman R.M., Schteingart D.E.**, Effects of exercise training on glucose control, lipid metabolism, and insulin sensitivity in hypertriglyceridemia and noninsulin dependent diabetes mellitus, *Med Sci Sports Exerc* 23: 703-712, 1991.

[74] **Larsen J.J., Dela F., Kjaer M., Galbo H.**, The effect of moderate exercise on postprandial glucose homeostasis in NIDDM patients, *Diabetologia* 40: 447-453, 1997.

[75] **Larsen J.J., Dela F., Madsbad S., Galbo H.**, The effect of intense exercise on postprandial glucose homeostasis in type II diabetic patients, *Diabetologia* 42: 1282-1292, 1999.

[76] **Lawrence R.H.**, The effects of exercise on insulin action in diabetes, *Br Med J* 1: 648-652, 1926.

[77] **Leiper J.B., Nicholas C.W., Ali A., Williams C., Maughan R.J.**, The effect of intermittent high-intensity running on gastric emptying of fluids in man, *Med Sci Sports Exerc* 37: 240-247, 2005.

[78] **Livesey J.H., Wilson P.D.G., Dainty J.R., Brown J.C, Faulks R.M., Roe M.A., Newman T.A., Eagles J., Mellon F.A., Greenwood R.H.**, Simultaneous time-varying systemic appearance of oral and hepatic glucose in adults monitored with stable isotopes, *Am J Physiol Endocrinol Metab* 275: E717-E728, 1998.

[79] **Luijf Y.M., DeVries J.H., Zwinderman K., Leelarathna L., Nodale M., Caldwell K., Kumareswaran K., Elleri D., Allen J., Wilinska M., Evans M., Hovorka H., Doll W., Ellmerer M., Mader J.K., Renard E., Place J., Farret A., Cobelli C., Del Favero S., Dalla Man C., Avogaro A., Bruttomesso D., Filippi A., Scotton R., Magni L., Giornao L., Di Palma F., Soru P., TOffanin C., De Nicolao G., Arnold S., Benesch C., Heinemann L.; AP@home Consortium**, Day and night closed loop control in adults with type 1 diabetes mellitus: a comparison of two closed loop algorithms driving continuous subcutaneous insulin infusion versus patient self management, *Diabetes Care* 36(12): 3882-3887, 2013.

[80] **Lund S., Holman G.D., Schmitz O., Pedersen O.**, Contraction stimulates translocation of glucose transporter GLUT4 in skeletal muscle through mechanism distinct from that of insulin, *Proc Natl Acad Sci USA* 92: 5817-5821, 1995.

[81] **Magni L., Raimondo D.M., Dalla Man C., Breton M., Patek S., De Nicolao G., Cobelli C., Kovatchev B.P.**, Evaluating the efficacy of closed-loop glucose regulation via control-variability grid analysis, *J Diabetes Sci Technol* 2(4): 630-635, 2008.

[82] **Manohar C., Levine J.A., Nandy D.K., Saad A., Dalla Man C., McCrady-Spitzer S.K., Basu R., Cobelli C., Carter R.E., Basu A., Kudva Y.C.**, The effect of walking on postprandial glycemic excursion in patients with type 1 diabetes and healthy people, *Diabetes Care* 35: 2493-2499, 2012.

[83] **Maran A., Pavan P., Bonsembiante B., Brugin E., Ermolao A., Avogaro A., Zaccaria M.**, Continuous glucose monitoring reveals delayed nocturnal hypoglycemia after intermittent high-intensity exercise in nontrained patients with type 1 diabetes, *Diabetes Technol Ther* 12(10): 763-768, 2010.

[84] **Mari A., Wharen J., DeFronzo R., Ferranninni E.**, Glucose absorption and production following oral glucose: comparison of compartmental and arteriovenous-difference methods, *Metabolism* 43: 1419-1425, 1994.

[85] **Matsuda M., DeFronzo R.A.**, Insulin sensitivity indices obtained from oral glucose tolerance testing: comparison with the euglycemic insulin clamp, *Diabetes Care* 22: 1462-1470, 1999.

[86] **Mikines K.J., Sonne B., Farrell P.A., Tronier B., Galbo H.**, Effect of physical exercise on sensitivity and responsiveness to insulin in humans, *Am J Physiol Endocrinol Metab* 254 (17): E248-E259, 1988.

[87] **Minuk H.L., Vranic M., Marliss E.B., Hanna A.K., Albisser A.M., Zinman B.**, Glucoregulatory and metabolic response to exercise in obese non-insulin-dependent diabetes, *Am J Physiol* 240: E458-E464, 1981.

[88] **Nesher R., Karl I.E., Kipnis D.M.**, Dissociation of effects of insulin and contraction on glucose transport in rat epitrochlearis muscle, *Am J Physiol* 249: C226-C231, 1985.

[89] **Patek S.D., Magni L., Dassau E., Hughes-Karvetski C., Toffanin C., De Nicolo G., Del Favero S., Breton M., Dalla Man C., Renard E., Zisser H., Doyle F.J. 3rd, Cobelli C., Kovatchev B.P.; International Artificial Pancreas (iAP) Study Group**, Modular closed-loop control of diabetes, *IEEE Trans Biomed Eng* 59(11): 2986-2999, 2012.

[90] **Pillonetto G., Sparacino G., Cobelli C.**, Reconstructing insulin secretion rate after a glucose stimulus by an improved stochastic deconvolution method, *IEEE Trans Biomed Eng* 48(11): 1352-1354, 2001.

[91] **Ploug T., Galbo H., Richter E.A.**, Increased muscle glucose uptake during contractions: no need for insulin during exercise, *Am J Physiol Endocrinol Metab* 247: E726-E731, 1984.

[92] **Proctor D.N., Shen P.H., Dietz N.M., Eickhoff T.J., Lawler L.A., Ebersold E.J., Loeffler D.L., Joyner M.J.**, Reduced leg blood flow during dynamic exercise in older endurance-trained men *J Appl Physiol* 85(1): 68-75, 1998.

[93] **Radziuk J., Norwich K.H., Vranic M.**, Experimental validation fo measurements of glucose turnover in nonsteady state, *Am J Physiol Endocrinol Metab Gastrointest Physiol* 234: E84-E93, 1978.

[94] **Ramsbottom N., Hunt J.N.**, Effect of exercise on gastric emptying and gastric secretion, *Digestion* 10: 1-8, 1974.

[95] **Ren J.M., Semenkovich C.F., Gulve E.A., Gao J., Holloszy J.O.**, Exercise induces rapid increases in GLUT4 expression, glucose transport capacity, and insulin-stimulated glycogen storage in muscle, *J Biol Chem* 269(20): 14396-14401, 1994.

[96] **Richter E.A., Garetto L.P., Goodman M.N., Ruderman N.B.**, Muscle glucose metabolism following exercise in the rat: increased sensitivity to insulin, *J Clin Invest* 69: 785-793, 1982.

[97] **Richter E.A., Ploug T., Glabo H.**, Increased muscle glucose uptake after exercise: no need for insulin during exercise, *Diabetes* 34: 1041-1048, 1985.

[98] **Richter E.A., Mikines K.J., Galbo H., Kiens B.**, Effect of exercise on insulin action in human skeletal muscle, *J Appl Physiol* 66: 876-885, 1989.

[99] **Richter E.A.**, Handbook of Physiology: Section 12. Exercise: Regulation and Integration of Multiple Systems, *American Physiology Society/Oxford University*, Danville, 1996.

[100] **Riddell M.C., Milliken J.**, Preventing exercise-induced hypoglycemia in type 1 diabetes using real-time continuous glucose monitoring and a new carbohydrate intake algorithm: an observational field study, *Diabetes Technol Ther*, 13(8): 819-825, 2011.

[101] **Ruderman N.B., Balon T. Zorzano A., Goodman M.**, The postexercise state: altered effects of insulin on skeletal muscle and their physiologic relevance, *Diabetes Metab Rev* 1: 425-444, 1986.

[102] **Russell S.J., El-Khatib F.H., Nathan D.M., Magyar K.L., Jiang J., Damiano E.R.**, Blood glucose control in type 1 diabetes with a bihormonal bionic endocrine pancreas, *Diabetes Care* 35(11): 2148-2155, 2012.

[103] **Saad A., Dalla Man C., Nandy D.K., Levine J.A., Bharucha A.E., Rizza R.A., Basu R., Carter R.E., Cobelli C., Kudva Y.C., Basu A.**, Diurnal pattern of insulin secretion and insulin action in healthy individuals, *Diabetes* 61: 2691-2700, 2012.

[104] **Schiavon M., Hinshaw L., Mallad A., Dalla Man C., Sparacino G., Johnson M., Carter R., Basu R., Kudva Y.C., Cobelli C.,**

Basu A., Postprandial glucose fluxes and insulin sensitivity during exercise: a study in healthy individuals, *Am J Physiol Endocrinol Metab* 305: E557-E566, 2013.

[105] **Schiavon M., Dalla Man C., Kudva Y.C., Basu A., Cobelli C.**, In silico optimization of basal insulin infusion rate during exercise: implication for artificial pancreas, *J Diabetes Sci Technol* 7(6): 1461-1469, 2013.

[106] **Sigal R.J., Kenny G.P., Wasserman D.H., Castaned-Sceppa C., White R.D.**, Physical activity/exercise and type 2 diabetes: a consensus statement from the American Diabetes Association, *Diabetes Care* 29(6): 1433-1438, 2006.

[107] **Soru P., De Nicolao G., Toffanin C., Dalla Man C., Cobelli C., Magni L.; AP@home Consortium**, MPC based artificial pancreas: strategies for individualization and meal compensation, *Ann Rev Control* 36(1): 118-128, 2012.

[108] **Steele R., Wall J., DeBodo R., Altszuler N.**, Measurement of size and turnover rate of body glucose pool by isotope diluition method, *Am J Physiol* 187: 15-24, 1956.

[109] **Steele R., Bjerknes C., Rathgeb I., Altszuler N.**, Glucose uptake and production during the oral glucose tolerance test, *Diabetes* 17: 415-421, 1968.

[110] **Steil G.M., Rebrin K., Darwin C., Hariri F., Saad M.F.**, Feasibility of automating insulin delivery for the treatment of type 1 diabetes, *Diabetes*, 55(12): 3344-3350, 2006.

[111] **Stephens J.M., Pilch P.F.**, The metabolic regulation and vesicular transport of GLUT4, the major insulin-responsive glucose transporter, *Endocrine Rev* 16: 529-546, 1995.

[112] **Stumvoll M., Mitrakou A., Pimenta W., Jenssen T., Yki-Jarvinen H., Van Harften T., Renn W., Gerich J.**, Use of the

oral glucose tolerance test to assess insulin release and insulin sensitivity, *Diabetes Care* 23: 295-301, 2000.

[113] **The DECODE Study Group**, Glucose tolerance and mortality: Comparison of WHO and American Diabetes Association diagnostic criteria, *Lancet* 354: 617-621, 1999.

[114] **Thorell A., Hirshman M.F., Nygren J., Jorfeldt L., Wojtaszewski J.F., Dufresne S.D., Horton E.S., Ljungqvist O., Goodyear L.J.** Exercise and insulin cause GLUT-4 translocation in human skeletal muscle, *Am J Physiol*, 277: E733-E741, 1999.

[115] **Toffolo G.M., Cobelli C.**, The hot IVGTT two-compartment minimal model: an improved version, *Am J Physiol Endocrinol Metab* 284: E317-E321, 2003.

[116] **Toffolo G.M., Basu R., Dalla Man C., Rizza R. Cobelli C.**, Assessment of postprandial glucose metabolism: conventional dual- vs. triple-tracer method, *Am J Physiol Endocrinol Metab* 291: E800-E806, 2006.

[117] **Tonoli C., Heyman E., Roelands B., Buyse L., Cheung S.S., Berthoin S., Meeusen R.**, Effects of different types of acute and chronic (training) exercise on glycaemic control in type 1 diabetes mellitus: a meta-analysis, *Sports Med* 42(12): 1059-1080, 2012.

[118] **Treadway J.L., James D.E., Burcel E., Ruderman N.B.**, Effect of exercise on insulin receptor binding and kinase activity in skeletal muscle, *Am J Physiol Endocrinol Metab* 256(19): E138-E144, 1989.

[119] **Verdonk C.A., Rizza R.A., Gerich J.E.**, Effects of plasma glucose concentration on glucose utilization and glucose clearance in normal man, *Diabetes* 30: 525-527, 1981.

[120] **Vicini P., Caumo A., Cobelli C.**, The hot IVGTT two-compartment minimal model: indexes of glucose effectiveness and in-

sulin sensitivity, *Am J Physiol Endocrinol Metab* 273: E1024-E1031, 1997.

[121] **Wahren J., Felig P., Ahlborg G., Jorfeldt L.**, Glucose metabolism during leg exercise in man, *J Clin Invest* 50: 2715-2725, 1971.

[122] **Wallberg-Henriksson H., Gunnarsson R., Henriksson J., DeFronzo R.A., Felig P., Ostman J., Wahren J.**, Increased peripheral insulin sensitivity and muscle mitochondrial enzymes but unchanged blood glucose control in type I diabetics after physical training, *Diabetes* 31(12): 1044-1050, 1982.

[123] **Wallberg-Henriksson H., Holloszy J.O.**, Activation of glucose transport in diabetic muscle: response to contraction and insulin, *Am J Physiol* 249: C233-C237, 1985.

[124] **Wallberg-Henriksson H., Constable S.H., Young D.A., Holloszy J.O.**, Glucose transport into rat skeletal muscle: interaction between exercise and insulin, *J Appl Physiol* 65: 909-913, 1988.

[125] **Wasserman D.H., Williams P.E., Lacy D.B., Green D.R., Cherrington A.D.**, Importance of intrahepatic mechanisms to gluconeogenesis from alanine during exercise and recovery, *Am J Physiol Endocrinol Metab* 254: E518-E525, 1988.

[126] **Wasserman D.H., Geer R.J., Rice D.E., Bracy D., Flakoll P.J., Brown L.L., Hill J.O., Abumrad N.N.**, Interaction of exercise and insulin action in humans, *Am J Physiol* 260: E37-E45, 1991.

[127] **Wasserman D.H., Zinman B.**, Exercise in individuals with IDDM, *Diabetes Care* 17(8): 924-937, 1994.

[128] **Wasserman D.H., Kang L., Ayala J.E., Fueger P.T., Lee-Young R.S.**, The physiological regulation of glucose flux into muscle in vivo, *J Exp Biol* 214: 254-262, 2011.

[129] **Watanabe O., Atobe Y., Akagi M., Nishi K.**, Effects of glucagon on myoelectrical activity of the stomach of conscious and anesthetized dogs, *Eur J Pharmacol* 79: 31-41, 1982.

[130] **Weinzimer S.A., Steil G.M., Swan K.L., Dziura J., Kurtz N., Tamborlane W.V.**, Fully automated closed-loop insulin delivery versus semiautomated hybrid control in pediatric patients with type 1 diabetes using an artificial pancreas, *Diabetes Care* 31(5): 934-939, 2008.

[131] **Wolfe R.R., Nadel E.R., Shaw J.H., Stephenson L.A., Wolfe M.H.**, Role of changes in insulin and glucagon in glucose homeostasis in exercise, *J Clin Invest* 77: 900-907, 1986.

[132] www.diabetes.org

[133] www.easd.org

[134] www.idf.org

[135] **Yardley J.E., Kenny G.P., Perkins B.A., Riddell M.C., Malcolm J., Boulay P., Khandwala F., Sigal R.J.**, Effects of performing resistance exercise before versus after aerobic exercise on glycemia in type 1 diabetes, *Diabetes Care* 35(4): 669-675, 2012.

[136] **Yardley J.E., Iscoe K.E., Sigal R.J., Kenny G.P., Perkins B.A., Riddell M.C.**, Insulin pump therapy is associated with less post-exercise hyperglycemia than multiple daily injections: an observational study of physically active type 1 diabetes patients, *Diabetes Technol Ther* 15(1): 84-88, 2013.

[137] **Yardley J.E., Kenny G.P., Perkins B.A., Riddell M.C., Balaa N., Malcolm J., Boulay P., Khandwala F., Sigal R.J.**, Resistance versus aerobic exercise: acute effects on glycemia in type 1 diabetes, *Diabetes Care* 36(3): 537-542, 2013.

[138] **Zinman B., Murray F.T., Vranic M., Albisser A.M., Leibel B.S.,McClean P.A., Marliss E.B.**, Glucoregulation during moderate exercise in insulin-treated diabetics, *J Clin Endocrinol Metab* 45: 641-652, 1977.

ACKNOWLEDGEMENTS

I want to thank Prof. Claudio Cobelli for his precious and constructive suggestions and giving me the great opportunity to work at the highest level of research in this field.
I would like to express my deep gratitude to my mentor Ing. Chiara Dalla Man for all the time she dedicated to me and the knowledge that she always shared with huge patience and kindness.
I would also like to thank Dr. Ananda Basu, Dr. Yogish Kudva and all Mayo Team for performing the experiments on which this research is based and for the useful debates and the enthusiasm for each new challenge.
I would like to thank all my "travel" mates during these years, old and young, for all the good times we spent together (even the bad ones, which were not so bad with you)!

A very special thanks of course to all my family, my girlfriend Valeria and friends who support and sustain me in everyday life and I know that is not so easy… so thank you!